A Critical Review on Wireless Charging for Electric Vehicles

A Critical Review on Wireless Charging for Electric Vehicles

Philip Machura, Quan Li*

School of Engineering, Institute for Energy Systems, The University of Edinburgh, EH9 3JL UK

*Corresponding author:

Tel.: +44 131 6508562, E-mail address: Quan.Li@ed.ac.uk

Declaration of interest: none

This research did not receive any specific grant from funding agencies in the public, commercial, or not-for-profit sectors.

Abstract

Electric vehicles (EVs) have recently been significantly developed in terms of both performance and drive range. There already are various models commercially available, and the number of EVs on road increases rapidly. Although most existing EVs are charged by electric cables, companies like Tesla, BMW and Nissan have started to develop wireless charged EVs that don't require bulky cables. Rather than physical cable connection, the wireless (inductive) link effectively avoids sparking over plugging/unplugging. Furthermore, wireless charging opens new possibilities for dynamic charging – charging while driving. Once realised, EVs will no longer be limited by their electric drive range and the requirement for battery capacity will be greatly reduced. This has been prioritised and promoted worldwide, particularly in UK, Germany and Korea. This paper presents a thorough literature review on the wireless charging technology for EVs. The key technical components of wireless charging are summarised and compared, such as compensation topologies, coil design and communication. To enhance the charging power, an innovative approach towards the use of superconducting material in coil designs is investigated and their potential impact on wireless charging is discussed. In addition, health and safety concerns about wireless charging are addressed, as well as their relevant standards. Economically, the costs of a wide range of wireless charging systems has also been summarised and compared.

Keywords:

- Wireless Power Transfer (WPT)
- Electric Vehicle (EV)
- Wireless charging of Electric Vehicles

Word count: 17596

List of Abbreviations

A4WP	Alliance for Wireless Power Transfer
AIMD	active implantable medical
BMS	battery management system
CPT	capacitive power transfer
DSRC	designated short-range communication
DWPT	dynamic wireless power transfer
EVs	electric vehicles

FABRIC	Feasibility analysis and development of on-road charging solutions for future electric vehicles
FOD	foreign object detection
FRP	fibre reinforced plastics
G2V	grid to vehicle
GA	ground assembly
H&S	health and safety
HTS	high temperature superconductors
HWFET	Highway Fuel Economy Test
ICE	internal combustion engine
ICNIRP	International Commission on Non-Ionizing Radiation Protection
IGBT	insulated gate bipolar transistors
IPT	inductive power transfer
ISO	International Organization for Standardization
KAIST	Korean Institute of Advanced Technology
LOD	living object detection
MOSFETs	metal-oxide-semiconductor field effect transistors
OLEV	on-line electric vehicle
ORNL	Oak Ridge National Laboratory
PAS	Publicly Available Specification
PFC	power factor correction
REBCO	rare-earth barium copper oxide
RFID	radio-frequency identification
RSU	roadside unit
Rx	receiving coil
SAE	Society of Automotive Engineers
SoC	state of charge
TRL	Technology Readiness Level
Tx	transmitting coil
UDDS	Urban Dynamometer Driving Schedule
UoA	University of Auckland
V2G	vehicle to grid
VA	vehicle assembly
WHO	World Health Organization

WiMAX	Worldwide Interoperability for Microwave Access
WPC	Wireless Power Consortium
WPT	wireless power transfer
ZCS	zero current switching
ZVS	zero voltage switching

Nomenclature

η	efficiency
ω	angular frequency [rad/s]
C	capacitance [F]
I	current [A]
k	coupling coefficient
L	inductance [H]
M	mutual inductance [H]
V	voltage [V]
P	real power [W]
R	resistance [Ω]
Q	quality factor
Z	impedance [Ω]

Subscript

0	resonance
1,2	primary, secondary
ac	alternating current
crit	critical
in	input
L	load
out	output
pc	primary compensation
r	reflected
sc	secondary compensation
tot	total

1 Introduction

The transportation sector is one of the main contributors towards global climate change and CO_2 emissions [1]. With about 60 % of the global oil consumption in transportation in 2017, the need for a clean alternative is urgent [2]. Electric vehicles (EVs) are an important pillar of this transition towards a clean energy society [3]. EVs have recently been significantly developed in terms of both performance and drive range. On the current vehicle market, various models are commercially available. Along with the increasing number of EVs on road, how to charge them effectively and efficiently is still challenging, which has a significant impact on power networks [4], [5]. Electric cables charge almost all of the existing EVs. No matter at home or on a highway, cables need to be physically connected to the EVs for charging. These solid connections could be very dangerous, particularly in bad weather conditions. Besides, they may cause sparking over plugging and unplugging, which significantly limits the application of EVs under certain circumstances, such as near gas stations and in airports. A more flexible and convenient charging method attracted broad attention, which is wireless charging. Several companies, such as Tesla, BMW and Nissan, have already started to develop wirelessly charged EVs that do not require bulky cables. Rather than physical cable connection, the wireless (inductive) link effectively avoids sparking. Furthermore, wireless charging opens new possibilities for dynamic charging – charging while driving.

The idea of wireless power transfer (WPT) can be traced back to the late 19th century, when Nicola Tesla designed the first wireless device, a wireless lightning bulb [6]. Tesla powered the bulb through high-frequency AC potentials between two closely located but separated metal plates. This application initiated new opportunities in wireless charging. However, unsolved technical challenges, such as very limited power density and low transfer efficiencies as the distances increase, made this WPT technology develop very slowly. After two centuries, recent advances in WPT technology enable wireless charging over distances longer than 2 meters by using ‘strongly coupled’ coils [7]. There are two major WPT technologies, inductive power transfer (IPT) and capacitive power transfer (CPT). In the strongly coupled regime, magnetic resonance couples transmitting and receiving coils and realises IPT, while CPT is realised through electric field interaction between coupled capacitors [8]. The coupling capacitance of such capacitors is determined by the available area of the devices [9]. Therefore, CPT is only applicable to low power applications with very short air gaps between 10^{-4} and 10^{-3} metre as shown in Figure 1. IPT can be used for large air gaps around several metres, and its output power is much higher than CPT, which could reach beyond 10 kW.

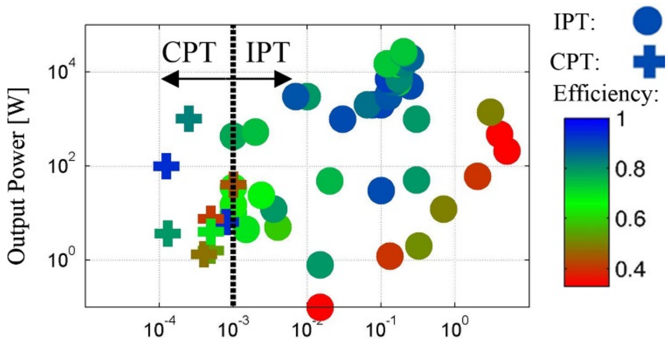

Figure 1 Comparison of output power and air gap length for CPT and IPT [10]

WPT, including both CPT and IPT enable power transfer without solid connections. This advantage ensures inherent safety and convenience due to a clear separation between the subsystems, especially for daily applications such as TVs [11], phone chargers [12], and induction heating [13], [14]. Also in medicine, WPT is used to charge active implantable medical devices (AIMD) [15], i.e. pacemakers [16] and other medical equipment [17]. Additional applications include radio-frequency identification (RFID) [18], [19], Sensors [20], [21], and robotics [22].

Wireless charging for EV is categorised in stationary, semi/quasi-dynamic, and dynamic charging systems. Stationary systems are similar to current plug-in chargers but provide some unique advantages such as "park and charge". An on-board receiving pad and an external charging pad in the pavement substitute the conductive charging system. Quasi-dynamic systems can be installed at bus stops, taxi stops, and traffic lights to provide short term charging in a dynamic environment. Dynamic wireless power transfer (DWPT) systems charge while vehicles are on the move. Hence, DWPT provides energy to the battery and increases the driving range, which consequently overcomes the 'range anxiety' [23]. It has been reported that the required battery capacity can be reduced by up to 20 %, which lowers the initial investment into a new EV [24]. WPT is therefore highly compelling for EVs and can help increase the EV uptake.

Over the past years, multiple reviews on WPT in general and on wireless charging for vehicles in specific have been published, covering a wide range of topics. Vaka and Keshri reported on the fundamentals of WPT for EV charging [25]. Key components such as the coil sub-system and compensation topologies were investigated. However, it lacks current research topics and implementation in a real-world context. Kalwar *et al.* presented a review of stationary charging for EVs focussing on the technical characteristics of the WPT systems and the effects of various parameters on the transfer efficiency [26]. Nevertheless, DWPT and auxiliary topics e.g. health and safety, emerging standards and costs are not covered. Ahmad *et al.* gave an overview of main research areas of WPT, which lacks the latest research work, e.g. control systems, foreign object detection (FOD) and grid impact [27]. Patil *et al.* neatly addressed the design of the coupler structure and compensation networks, but didn't report on the emerging technologies like superconductors [28]. Besides, health and safety of WPT-systems, communication, economics and grid impact is not covered.

Our methodology to review wireless charging for EVs is three-fold: technology, health and safety, and economic impact. All of these aspects will be covered and discussed in great detail. In specific this article aims at filling these gaps and reviews the status of main areas of a wireless charging system for EVs as well as aspects of implementing this technology into our daily lives. It presents recent technical progress in many key areas of WPT, introduces important research centres, evaluates risks associate with WPT and standards put into place, and explores grid impact and cost competitiveness of dynamic wireless charging. The remainder of the article is structured as follows: chapter 2 reviews the key components of a WPT-system including power converter, compensation topology and coils as well as important auxiliary features like foreign object detection and communication. In addition, high temperature superconductors (HTS), an emerging coil material, and related changes to the charging systems in order to accommodate HTS are presented. Chapter 3 presents the leading research institutes and their contributions towards wireless charging of EVs. Chapter 4 addresses arising concerns regarding to safe operation and the impact on the health of operators and bystanders. Evolving standards for WPT systems are summarised in chapter 5. Chapter 6 investigates the impact of the transition from fossil fuelled vehicles to EVs as well as the operation of wireless charging systems in distribution networks. Finally, chapter 7 presents preliminary cost analysis to show the cost incurred by introducing WPT systems, various stretches of road, and potential savings due to battery capacity reduction.

2 Current technology for WPT

By adopting a wireless charging system, the charging process can be simplified and safer. In addition, dynamic charging systems create a unique opportunity to overcome 'range anxiety' while decreasing the upfront costs of EVs. The main components of a WPT system for EV charging are depicted in Figure 2. It consists of two main sub-systems, one of which is located underneath the road surface (ground assembly, GA) and the other one is built into the vehicle underbody (vehicle assembly, VA) [29]. The GA comprises the grid connection, rectifier and high frequency inverter, primary compensation network and the primary/ transmitter coil (Tx). In the VA, the secondary/ receiving coil (Rx) and secondary compensation network forms a resonance circuit that feeds into a high frequency rectifier, a filter network and the battery system. The sub-systems are separated by an air gap. The distance between the two systems depends on the type of vehicle and its ground clearance as well as road conditions such as pavement thickness. Conventionally the air gap is smaller than 0.4 m. In additional, both sub-systems share information via a communication link. A more in-depth discussion of their key features is presented below.

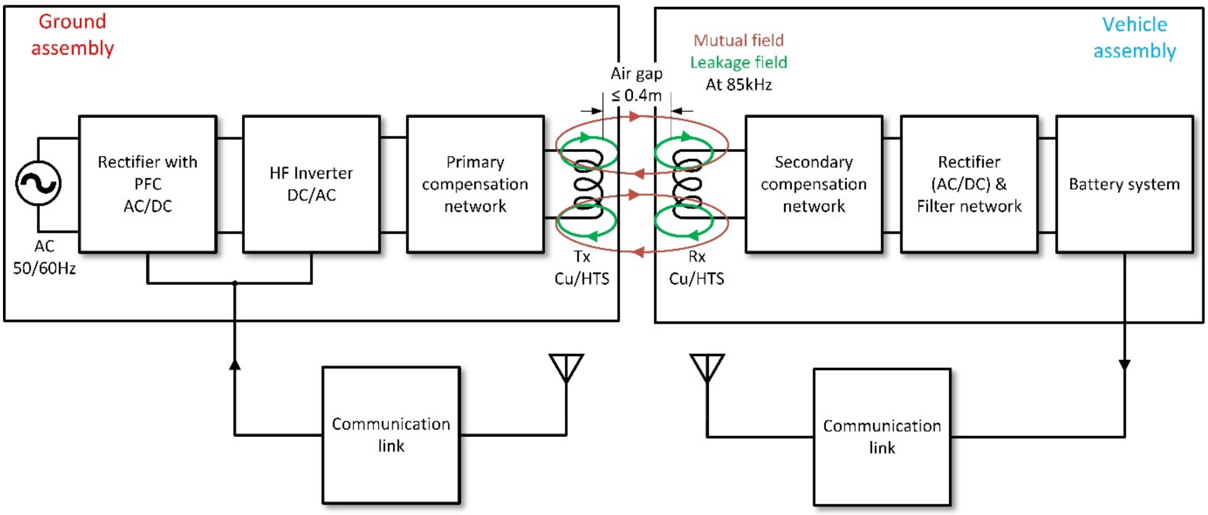

Figure 2 Main components of WPT-systems for EVs

2.1 Power Source and Converter

On the transmitting side, the GA is connected to the distribution network of the electricity grid and it is fed by low-frequency AC power. The supply frequency is too low to link both coils and transfer power. Therefore, the power is converted in either a single step or a two-step process. Even though a direct conversion from low-frequency AC grid power to a high-frequency input into the primary coil is possible, most charging systems employ two-stage AC/DC/AC conversion [30]. At the first stage, a rectifier converts the AC power to DC followed by power factor correction (PFC) to ensure a high-power factor and low harmonic content. It is also possible to use a BUCK converter after the PFC to modify the DC voltage and ensure ‘soft’ starting and stopping of the charger [31], [32]. The high-frequency inverter converts the DC power to high frequency AC and powers the primary pad. On the secondary side, the high-frequency output of the receiving pad is rectified to DC power and filtered to produce a ripple free current that can charge the on-board battery. A diode-bridge rectifier is commonly used [24]. To maximise the power transfer, the load impedance has to be matched to the source impedance. The resonant frequency of the compensation topologies and coils determine the required switching frequency of the inverters. Commonly used resonance frequencies for WPT EV-chargers are within a range of 20 kHz to 100 kHz [33]. At higher frequencies, effects such as increased electromagnetic radiation and higher resistances due to skin and proximity effect occur. Converter losses increase along switching frequency [34]. This is particularly true for switching losses. Zero-voltage/zero-current switching (ZVS/ZCS) reduces switching losses. This means that the switching between *on* and *off* states should occur at either zero voltage or zero current. An additional benefit is reduced voltage stress in the components.

Power converters, especially high-frequency converters, are essential for WPT charging systems and can be categorised into single [35], [36] and three-phase topologies [37]. Power converters commonly comprise multiple devices, such as metal-oxide-semiconductor field effect transistors (MOSFETs) and insulated gate bipolar transistors (IGBTs) connected in parallel to form full or half-bridge configurations. A lot of research is going into the field of high-frequency converters and their key features including circuit simplicity, uncomplicated control strategies, high efficiency at high switching frequency and high power levels, as well as robustness against high voltage and current stress [38]. For the unidirectional power transfer from grid to vehicle (G2V), H-bridge converters are the most commonly used method [39]. A high-power DC/AC converter with a WPT capability of

22 kW has been proposed in [40]. The converter comprises four switches, each of which is connected with an IGBT and SiC-MOSFET in parallel, known as hybrid switch [41]. The system can use soft and hard switching modes and achieves 98 % efficiency at 5 kW. However, experimental results in a DWPT system with loss analysis are not available. Other converter layouts include multi-level converters [42], [43], [44], cascaded multi-level converters [45] [46], [47], and matrix converters [48], [49]. Multi-level converters are particularly interesting for medium and high voltage applications that can reduce the required voltage rating and component stress of single switches by using a modular approach [42]. However, such architectures require complex control schemes and deal with high circulating currents between capacitors. The complexity reduces if the circulating currents can be minimised [50]. A cascaded multilevel converter uses multiple converters (modules) connected in series to increase the power capacity. Therefore, it provides a high degree of scalability and a simpler control scheme [47]. One drawback of such system is the need of multiple power sources and therefore system costs are high, as each converter requires its own power supply. Furthermore, depending on the number of modules, the conduction loss can be larger than that of a conventional H-bridge converter if the same number of switching devices is used [46]. Matrix converter might be employed to reduce the total number of conversion stages, as it is possible to convert the AC grid supply directly into high-frequency AC power, but the power capacity is limited.

A unique approach of DWPT is to use a super-capacitor in tandem with the secondary power rectifier, in order to enable power transfer and energy storage in a single device [51]. Super-capacitors can provide an additional energy buffer before the on-board battery pack in a conventional EV due to their high-power density [52]. Nevertheless, this topology increases the current stress in the secondary converter and introduces harmonics into the voltage waveform. To allow bidirectional power transfer, i.e. G2V and vehicle to grid (V2G), bidirectional converters on transmitting and receiving side are required [53]. With the aid of bidirectional power transfer EVs can act as energy storage with high renewable energy penetration. While renewable energy sources feed into the grid, the energy can be used to charge EV batteries, which reduces the load on the grid [54]. In addition, to prevent intermittency issues within the grid network, EV batteries are discharged to balance the demand [55].

2.2 Compensation topologies

Magnetically coupled coils act like a transformer, but with higher leakage inductance due to a larger air gap between the coils. Hence, the fraction of magnetic coupling that links both coils is much smaller compared to traditional transformers, making them loosely coupled. To be able to transfer sufficient power over long distances, the system operates at resonance frequency with zero phase angle between input current and voltage. In order to achieve a resonant circuit, multiple reactive elements, like inductors and capacitors, are linked together in series and/or parallel. As shown in Figure 2, these compensation networks are located between the high-frequency inverter and the primary coil in the GA, while between the secondary coil and the rectifier in the VA. Capacitors resonate with the transmitting and receiving coils to supply reactive power [56]. The main purpose of the primary compensation network is to reduce the reactive power rating (VAr) of the power supply by cancelling out the reactive component of the primary coil [57]. In addition, the compensation network helps to achieve soft switching in the primary power converter. Compensation networks are also used on the secondary side to improve the power transfer capability of the system by nullifying the receiver inductance [58]. Figure 3 depicts the most basic compensation topologies currently used in WPT systems, each consisting of a single capacitor in either series (S) or parallel (P) to the coil inductance, where SS stands for a series capacitor on the primary side and a series capacitor on the secondary side.

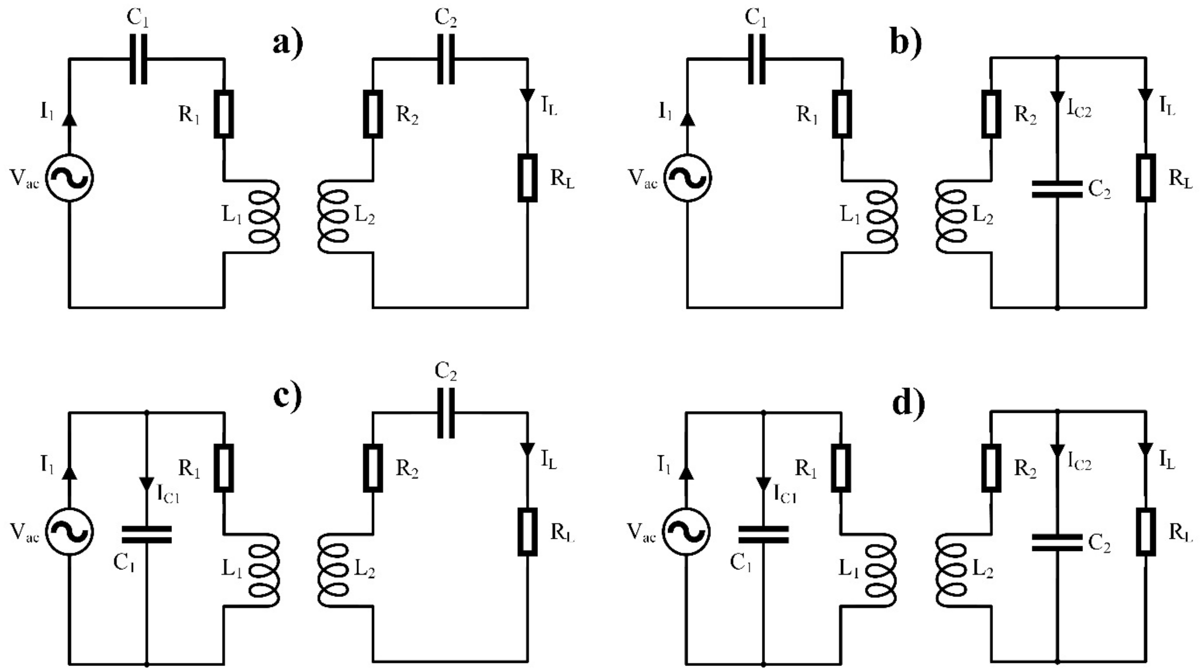

Figure 3 Basic compensation topologies for primary and secondary resonant circuits a) SS b) SP c) PS d) PP

The primary and load current, as well as power transfer efficiency are derived for an SS-compensation topology. Using Kirchhoff's Law, by defining the loop-currents for the circuit shown in Figure 3a) the circuit can be solved using (1).

$$\begin{bmatrix} V_{\mathrm{ac}} \\ 0 \end{bmatrix} = \begin{bmatrix} R_1 + j(L_1 * \omega - \frac{1}{C_1 * \omega}) & -j\omega M \\ -j\omega M & R_2 + R_L + j(L_2 * \omega - \frac{1}{C_2 * \omega}) \end{bmatrix} * \begin{bmatrix} I_1 \\ I_L \end{bmatrix} \tag{1}$$

Equivalent total impedance of the circuit with SS-compensation is the sum of primary circuit impedance and secondary reflected impedance (2). The secondary reflected impedance is the ratio of reflected voltage and primary current.

$$Z_{\mathrm{tot}} = Z_1 + Z_r = \left(R_1 + j\left(L_1 * \omega - \frac{1}{C_1 * \omega}\right)\right) + \frac{(\omega * M)^2}{\left(R_2 + R_{\mathrm{L}} + j\left(L_2 * \omega - \frac{1}{C_2 * \omega}\right)\right)} \tag{2}$$

The current drawn from the power supply can be evaluated with (3).

$$I_1 = \frac{V_{\mathrm{ac}}}{Z_{\mathrm{tot}}} = \frac{V_{\mathrm{ac}} * \left(R_2 + R_{\mathrm{L}} + j\left(L_2 * \omega - \frac{1}{C_2 * \omega}\right)\right)}{\left(R_1 + j\left(L_1 * \omega - \frac{1}{C_1 * \omega}\right)\right) * \left(R_2 + R_{\mathrm{L}} + j\left(L_2 * \omega - \frac{1}{C_2 * \omega}\right)\right) + (\omega * M)^2} \tag{3}$$

According to (1) and (3), the current that supplies the load is:

$$I_{\mathrm{L}} = \frac{-V_{\mathrm{ac}} * j\omega M}{\left(R_1 + j\left(L_1 * \omega - \frac{1}{C_1 * \omega}\right)\right) * \left(R_2 + R_{\mathrm{L}} + j\left(L_2 * \omega - \frac{1}{C_2 * \omega}\right)\right) + (\omega * M)^2}. \tag{4}$$

Input power, output power and efficiency of the power transfer are calculated using (5)-(7). It is assumed that the power is supplied with unity power factor into the primary compensation network.

$$P_{\mathrm{in}} = V_{\mathrm{ac}} * I_1 = \frac{{V_{\mathrm{ac}}}^2 * \left(R_2 + R_{\mathrm{L}} + j\left(L_2 * \omega - \frac{1}{C_2 * \omega}\right)\right)}{\left(R_1 + j\left(L_1 * \omega - \frac{1}{C_1 * \omega}\right)\right) * \left(R_2 + R_{\mathrm{L}} + j\left(L_2 * \omega - \frac{1}{C_2 * \omega}\right)\right) + (\omega * M)^2} \tag{5}$$

$$P_{\mathrm{out}} = R_{\mathrm{L}} * |I_{\mathrm{L}}|^2 = R_{\mathrm{L}} * \left| \frac{-V_{\mathrm{ac}} * j\omega M}{\left(R_1 + j\left(L_1 * \omega - \frac{1}{C_1 * \omega}\right)\right) * \left(R_2 + R_{\mathrm{L}} + j\left(L_2 * \omega - \frac{1}{C_2 * \omega}\right)\right) + (\omega * M)^2} \right|^2 \tag{6}$$

$$\eta = \frac{P_{\mathrm{out}}}{P_{\mathrm{in}}} = \frac{R_{\mathrm{L}}}{\left(R_2 + R_{\mathrm{L}} + j\left(L_2 * \omega - \frac{1}{C_2 * \omega}\right)\right) + \left(R_1 + j\left(L_1 * \omega - \frac{1}{C_1 * \omega}\right)\right) * \left(\frac{R_2 + R_{\mathrm{L}} + j\left(L_2 * \omega - \frac{1}{C_2 * \omega}\right)}{\omega M}\right)^2} \tag{7}$$

At the frequency with a zero phase angle, there is no reactive power flow. To form a resonance circuit with maximum power transfer capability, this frequency must be equal to the resonance frequency ω_0, where the reactive parts in (3)-(7) cancel out. Assuming identical coils in the primary and secondary circuit, the resonance frequency can be calculated using (8).

$$\omega_0 = \sqrt{\frac{1}{L_1 C_1}} = \sqrt{\frac{1}{L_2 C_2}} = \sqrt{\frac{1}{LC}} \tag{8}$$

The efficiency at resonance frequency is expressed by (9) with the quality factors Q for each coil in (10).

$$\eta(\omega_0) = \frac{R_{\mathrm{L}}}{(R_2 + R_{\mathrm{L}}) + R_1 * \left(\frac{R_2 + R_{\mathrm{L}}}{\omega M}\right)^2} = \frac{R_{\mathrm{L}} k^2 Q_1 Q_2}{R_2\left[\left(\frac{R_2 + R_{\mathrm{L}}}{R_2}\right)^2 + \left(\frac{R_2 + R_L}{R_2}\right) * k^2 Q_1 Q_2\right]} \tag{9}$$

$$Q_{1/2} = \frac{\omega_0 * L_{1/2}}{R_{1/2}} \tag{10}$$

The same approach can be used for SP, PS, and PP-compensation networks. Table A-1 in the appendix summarises the total impedance, power transfer efficiency under resonance and the primary capacitance of the basic compensation topologies.

Figure 4 shows the power transfer efficiency and output power characteristics under varying mutual inductance for all four compensation topologies. Under perfectly aligned conditions, the mutual inductance is high and it depends on the length of the air gap. Mutual inductance reduces with increasing air gap length and misalignment. The SS-compensated system reaches high and stable transfer efficiency at low mutual inductances. Furthermore, compared with the other systems, it transmits the highest output power for a fixed input power. A PS-compensated system has the same power transfer efficiency as the SS-compensated system. However, it transfers less power to the load. While the SP-topology transfers slightly less power to the load, the input power required is much higher, resulting in a lower efficiency overall. The lowest power is transferred by a PP-compensated system, making it an unsuitable topology for EV chargers.

Using an SS-compensation network is beneficial for application with variable load conditions, i.e. DWPT charging, as the primary compensation capacitance C_1 is independent of the load. The opposite is true for the remaining topologies, where C_1 changes with varying load and coupling conditions that potentially compromises the resonance frequency and transfer efficiency [59]. As shown in (2), the total impedance of the SS-compensated system drops along with decreasing mutual inductance. This leads to an increase in primary current and therefore to a higher secondary current that supplies the load [60]. While running an EV, it is not always guaranteed to be in perfect alignment with the primary pad or track particularly during DWPT, which causes weak mutual coupling. If the misalignment is pronounced, the switching components experience high current peaks and can be damaged. Using a parallel primary can prevent this behaviour, as the primary current reduces under misalignment.

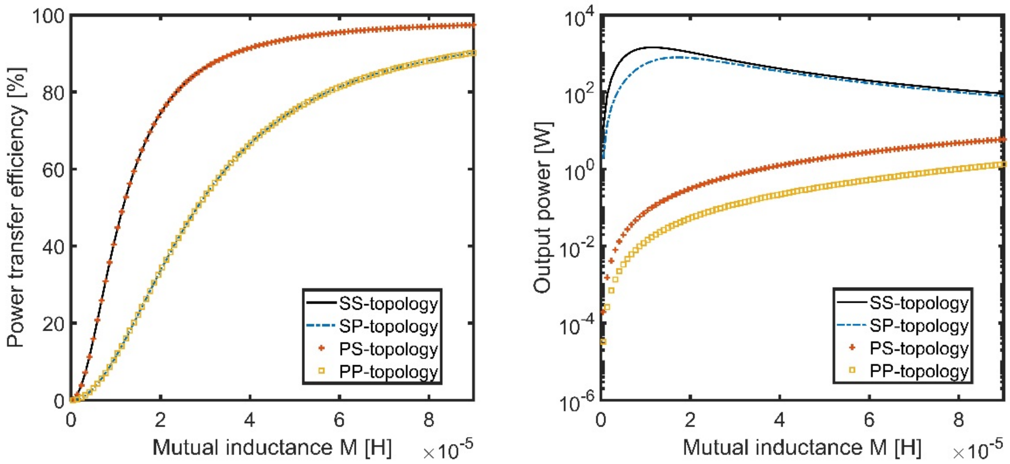

Figure 4 Power transfer efficiency and output power vs varying mutual inductance M for the basic compensation topologies SS, SP, PS, and PP

An optimal selection process of the compensation topology based on the economics of the system is suggested in [61]. It concludes that SS and SP-compensation networks are the most suitable topologies for high-power WPT systems. Additionally, SS compensation requires less copper than the other compensation networks. However, this study does not consider soft switching or bifurcation. Bifurcation or frequency splitting results in multiple frequencies in which a zero-phase angle is possible. It can be avoided by adopting the criteria given in [57]. A specific design guideline for SS-compensated systems is presented in [62].

All basic compensation topologies have disadvantages. It is, therefore, required to investigate other arrangements that alleviate these problems. Proposed extensions to the conventional SS compensation are the so-called S/SP and SP/S topologies. Systems with S/SP topology use an additional parallel capacitance on the secondary side compared to the SS networks [63]. It provides a higher tolerance on varying air gap lengths. Using an SP compensation on the primary side instead and an S network on the secondary side improves the misalignment tolerance of the system, as the additional parallel capacitor allows transition between maximum power and maximum allowable misalignment [60]. However, there is a trade-off between power source rating and achievable misalignment tolerance. To increase the tolerance from 40 % to 75 %, the power source has to supply five times as high as the rated output. Furthermore, load fluctuations, caused by a varying state of charge (SoC) of the battery load, have an impact on the resonant state of the system due to the parallel capacitor. This results in non-zero phase angle operation when the load changes [64].

Samanta & Rathore proposed a WPT system with a CCL-compensated transmitter side and an LC-compensated receiver side [65]. The design uses an additional capacitor connected in series to the conventional parallel-compensated primary and a series compensated secondary side. By using the additional capacitor, the voltage stress on the inverter switches is reduced, which was a major drawback of conventional current-fed systems. One issue with this topology is reduced efficiency in comparison to other compensation networks.

An LCL-compensated receiving coil was developed in [66] and [67]. It uses a parallel capacitor and an additional inductor in series to the receiving coil. By adopting this compensation, the switching loss of the rectifier is reduced. One advantage of LCL-compensated coils is that it produces a constant current output, which is required for supplying multiple receiving coils. If LCL compensation is used on both sides of the WPT system, it enables bidirectional power transfer [68]. However, it requires a complex control scheme with an external coil for synchronous switching [69].

One of the most investigated compensation topologies in more recent years is the LCC compensation shown in Figure 5 [64], [70], [71]. It combines a conventional series-parallel (SP) compensation on one side with a series inductor. This additional inductor can be integrated with the receiving or transmitting coil, hence no additional space is required [72]. By using a bipolar compensation coil, the coupling between main coil and series inductor can be minimised [73], [74]. The resonance frequency is independent on load and coupling conditions, while the current through the primary coil and the output current are constant [75]. Generally, the power transfer efficiency is lower as more components are connected, but the stress on the capacitors and coils is lower [76]. Zhu *et al*. compared the LCC compensation with a conventional SS topology [77]. A critical load resistance $R_{\mathrm{L,crit}}$ is determined to compare the transfer efficiency and mutual inductance characteristics and it is shown in (11).

$$R_{\mathrm{L,crit}} = \sqrt{\frac{L_{\mathrm{sc}}}{C_{\mathrm{sc,2}}}} \tag{11}$$

Secondary compensation inductor and secondary parallel compensation capacitor are denoted by L_{sc} and $C_{\mathrm{sc,2}}$ respectively. If $R_{\mathrm{L,crit}}$ is bigger than $\sqrt{\frac{L_{\mathrm{sc}}}{C_{\mathrm{sc,2}}}}$ then the efficiency of the LCC compensation is more robust to variations in mutual inductance, but with a lower efficiency under perfect alignment. The opposite is also true when $R_{\mathrm{L,crit}}$ is smaller. Under these conditions, the SS compensation is less susceptible to changes in mutual inductance, but it offers lower efficiency under no misalignment. SS and LCC compensations offer the same performance for the condition shown in (11). Due to the parallel capacitance, the total impedance of the LCC system increases similarly to the parallel primary compensation. Thus, it guarantees safe operation under high misalignment. Furthermore, LCC compensation offers lower magnetic field radiation [70].

LCL and LCC topologies can also be combined, where LCL is used on the primary side and LCC on the secondary [78].

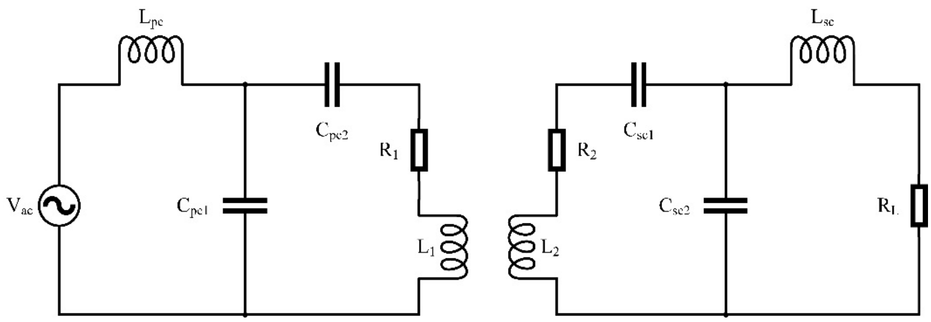

Figure 5 LCC-compensation network on primary and secondary side of a WPT-system, not showing primary side inverter and secondary side rectifier and filter

2.3 Coil designs

The main components of the WPT system are two coupled coils that allow power transfer via magnetic field. Electric current flows through the primary coil and generates a time-varying magnetic field around it. In the vicinity of the primary coil, the secondary coil intercepts the magnetic field, which induces a voltage. The amount of induced voltage depends on the air gap length between these coils, the number of turns and the derivative of the magnetic field over time. Due to this voltage, an induced current flows in the secondary coil. The set of coils forms a loosely coupled transformer linked by the main flux path including leakage that does not contribute towards the power transfer. By connecting each coil to the compensation network, the current flowing in the coils is maximised due to resonance. The main parameters that should be maximised during the design process of the primary and secondary pads are coil quality factor Q and the coupling coefficient k with a high tolerance for increasing air gap lengths and lateral/longitudinal displacements.

In order to strengthen the coupling between coils, ferromagnetic materials, so called cores, can be used to guide magnetic flux. Prevalent losses within the coil system arise from the core losses of the ferrite material and ohmic losses of the coils, including proximity and skin effect losses. Skin effect losses are reduced by using Litz wire, whereas core losses depend on the core material. To reduce core losses the flux density should be below the saturation flux density of the material. However, the available design options are limited by both power and space requirements. After reduction of the potential losses, the efficiency of the power transfer can be improved by three design parameters, which ultimately affect the product kQ [79], [80]. As shown in (9), these parameters include the mutual inductance M or coupling coefficient k, the self-inductance of the coils L and the frequency ω. A rise in frequency will increase the induced voltage in the secondary coil, while also increase frequency-dependent losses such as switching losses, joule losses in the coil, and core losses. Besides, high frequency inverters are more expensive than ‘slower’ power electronics [79]. It is therefore important to choose the design frequency carefully. The self-inductance of coils increases with increasing coil dimensions and number of turns. In practice, the maximum size of the coil is limited by the size of the underbody of the vehicle. Increasing the number of turns is possible but constrained by the available space. In addition, the area enclosed by the windings is important, as it affects the coupling efficiency. The larger the area enclosed by the winding becomes, the higher the coupling is [81]. Another way to increase the coupling is to decrease the air gap length or increase the coil dimension. Again, the air gap length is pre-determined by the application i.e. EV-charging and the size of the coils is limited. The coupling can be maximised by using equally sized coils as shown in Figure 6. Having equally sized coils also reduces eddy currents induced in the vehicle chassis and leakage magnetic field surrounding the coils [80]. Reducing the size of the receiving coil is convenient, as it would be easier to incorporate in the vehicle. However, it would weaken the magnetic coupling and reduce efficiency, as less magnetic flux is intercepted by the receiving coil.

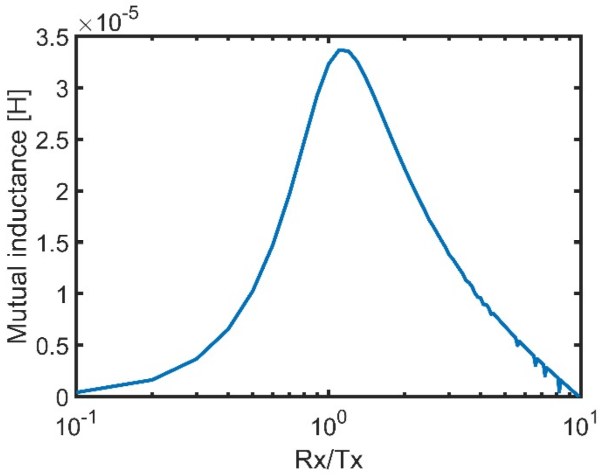

Figure 6 Mutual inductance vs ratio of receiving Rx and transmitting Tx coil radius at an air gap length of 0.1 m

With these dependencies in mind, the coils can be designed appropriately. At the beginning, circular coil designs were popular due to their simplicity. This design originated from pot cores, where the magnetic field is guided within a small volume as the core material encloses the coil [82], [83], [84]. As the secondary circuit must be installed on vehicles, a reduction in size and weight is advantageous. In addition, using less ferrite reduces the price of each pad. Therefore, pot structures were converted to plates, disks or rods that are evenly spaced out above the coil [85]. A pad structure designed by Budhia *et al.*, shown in Figure 7, minimizes the amount of ferrite, while maintaining a critical coupling between the primary and the secondary circuits [86].

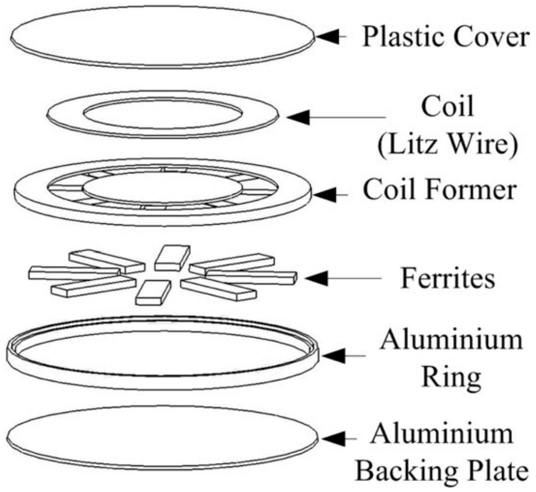

Figure 7 Circular primary/secondary pad design using minimal amount of ferrite to achieve critical coupling [86]

The magnetic field produced by circular coils reaches its maximum at the centre of the coil. It drops significantly with offset, resulting in a low non-directional misalignment tolerance. At a lateral offset of circa 40 % of the diameter, circular pads have a null in their power distribution, as equal amounts of magnetic flux enter the coil from either side. Consequently, this makes a circular coil unsuitable for DWPT. Another disadvantage of circular coils is the limited achievable flux height. The coupling height depends on the diameter of the coil and is within one quarter of the diameter limited. Nevertheless, circular coils exhibit the highest magnetic coupling amongst similar sized coil geometries like square and rectangular designs [81]. Therefore, circular coils are still popular for stationary WPT-systems where the coil performance is maximised using multi-objective optimisation algorithms. These algorithms range from parametric sweeps [87] to genetic [88] and evolutionary algorithms [89]. In contrast, rectangular pads are the most common design for DWPT due to their high tolerance against longitudinal misalignment and efficient use of space on the vehicle [90], [91]. According to [92], rectangular pads are the most cost-effective option in comparison to circular and hexagonal design. This means that rectangular pads transfer the highest power over a specific area with a given material allowance.

To increase the flux path produced by the transmitting pad and the misalignment tolerance, a new design approach was proposed as shown in Figure 8. By winding the coil around a ferrite bar, a so-called flux pipe, flat solenoid or H-core pad is created [93], [94], [95]. Due to the increased flux path, the coupling between transmitter and receiver side is higher. In comparison to the circular design, the flux pipe has a better lateral misalignment tolerance. The windings must be carefully designed, to reduce the overall amount of material used. Budhia *et al*. split the windings and used two separate coils connected in series per pad [93]. Whereas [94] used split cores to reduce the weight and cost of the pads. One major problem of these designs is the double-sided nature of the magnetic flux. Because the windings are on both sides, a leakage flux is produced on the backside of the pad, which lowers the coupling and reduces the transfer efficiency. It is possible to use an aluminium shield on the backside. However, there will be losses associated with the eddy currents produced in the shield and the interactions between the shield and coil.

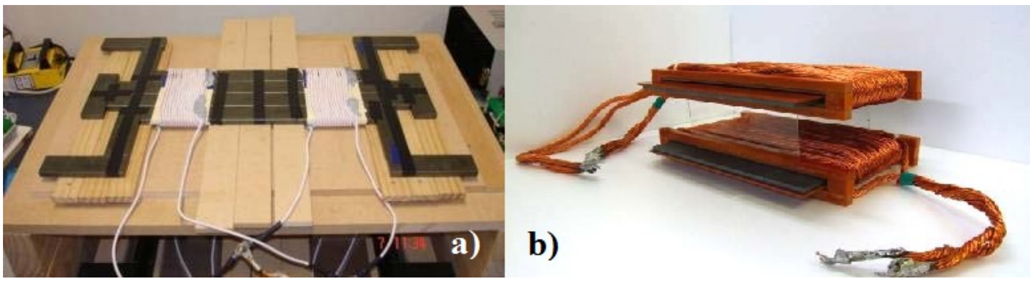

Figure 8 Flux pipe/ flat solenoid coil configuration a) flux pipe by [93] b) flat solenoid by [94]

As shown, the tolerance against lateral misalignment is a key factor in designing the coil structures in WPT systems. Commonly there is a null in the power distribution as the lateral offset increases regardless of the coil design. Elliott *et al.* designed a multiphase pickup coil (quadrature coil) that uses two windings, combining a horizontal winding and a vertical winding, wound on top of each other around a ferrite E-core [96], [97]. Using these two windings, one is compensating the power null of the other and vice versa, alleviating the problem, while achieving similar power levels as conventional coil structures. However, it uses twice the amount of copper wires.

The feature of producing a single sided flux sparked new research on advanced coil structures. Popular examples are the DD and DDQ pads [98], [99], the bipolar pad [100], [101], tripolar pad [102], [103], and a novel design called ZigZag [104]. A DD-pad uses a similar approach as the flux pipe design, but instead of winding the coil around the core material, it is wound like a circular spiral coil on top of the core material, which channels the magnetic flux and re-directs it to the front. Therefore, this design does not produce flux on the coil backside. As shown in Figure 9 a) the flux that links the transmitting and receiving pad is produced by the coupling between both coils in one pad. In order to maximise the coupling effect, the ‘flux pipe’ length has to be optimised. One drawback of the DD design is that it only couples the horizontal flux. By adding the quadrature coil designed in [96], the vertical components can be utilised and a DDQ structure is created as shown in Figure 9 b). The DDQ pad uses more wires as it combines two windings and creates twice the flux height of a circular coil. Bosshard *et al.* compared the performance of rectangular and DD charging systems [105]. A rectangular WPT system has a slightly higher mass and surface area related power density than the DD system, but the DD pads create a lower magnetic leakage field. Recently, new adaptations of the DD pads have emerged including an overlapped DD array [106] and a crossed DD coil [107]. The crossed DD coil setup uses two rectangular coils next to each other similar to the conventional DD coil. In contrast, one of the coils is shifted by half a coil length in longitudinal direction. The system improves misalignment tolerance if multiple coils are placed next to each other. To guarantee minimal changes in mutual inductance two coil pairs have to be excited at the same time. As multiple coils are energised, the magnetic field of the uncovered coils needs to be shielded. An overlapped DD array uses multiple stacks of DD coils on top of each other with an offset between the different layers [106]. It optimises the transfer efficiency and aims at very low-speed dynamic power transfer.

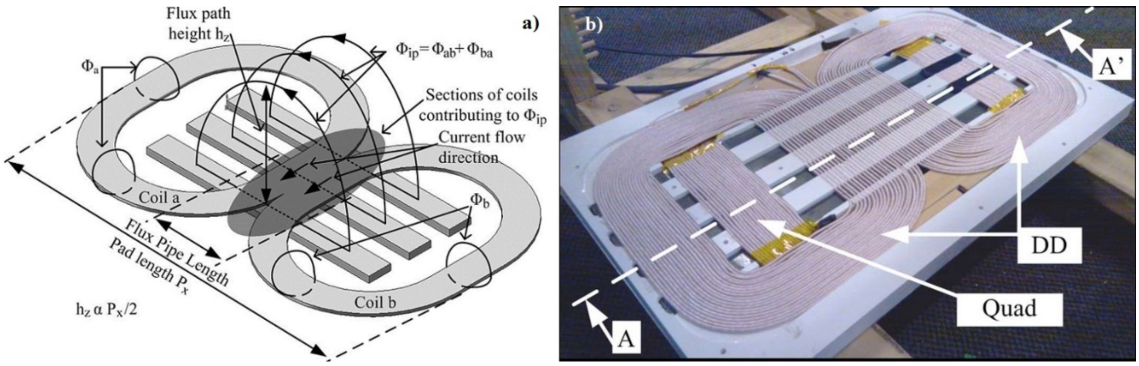

Figure 9 Single-sided flux coil designs a) DD- and b) DDQ-pad [99]

The bipolar pad design is similar to the DD pad, but the individual coils overlap. It has similar power transfer capabilities but uses approximately 25 % less wire material [101]. Furthermore, both coils require an independent converter, which are synchronised [106].

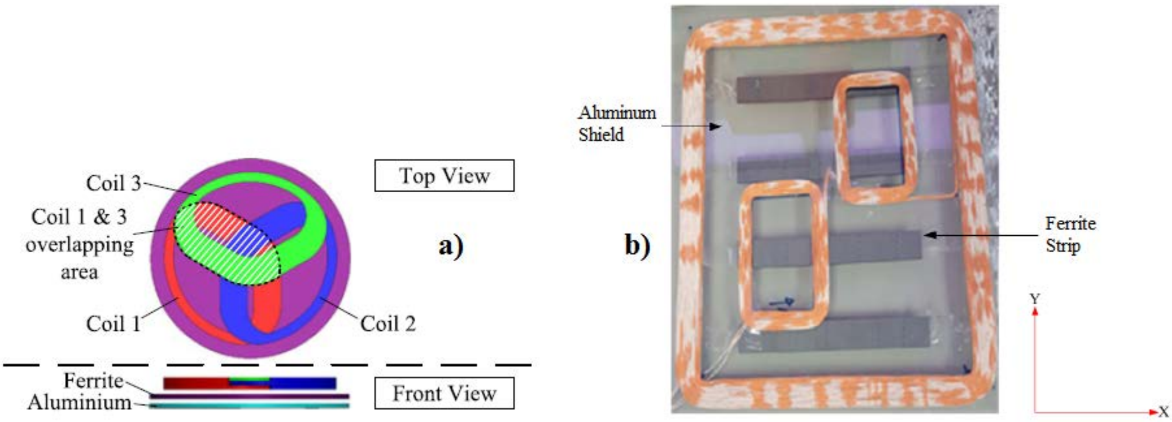

Figure 10 Three-coil design pads a) circular-shaped tripolar pad [103] b) ZigZag pad [104]

In contrast to the two coils used in a DD pad, the tripolar design uses three coils similar to the DDQ coil [102]. The three oval-shaped coils are decoupled from each other and overlap at the centre of the coil as shown in Figure 10 a). Decoupling is achieved by adjusting the overlapping area to minimise the induced field in the adjacent coils [109]. By adopting multiple coils, the pad provides a high non-directional misalignment tolerance and therefore a larger effective area to transfer rated power [110]. In addition, the leakage field is significantly reduced in comparison to a circular pad. One disadvantage is the complex control scheme required. Furthermore, each coil is driven independently by an individual inverter, leading to increased costs. Figure 10 b) shows another design that uses three coils per pad, one large coil wound as a rectangle enclosing two smaller rectangular coils [104]. It has a uniform magnetic flux distribution in the smaller coils. The output power provided to the load changes only slightly over a wide range of misalignment. Again, a large amount of wire material is used. It is also possible to use intermediate coils between the main transmitting and receiving coils to further increase the transmission distance [111]. However, intermediate coils were not addressed in this review. Table 1 summarises the differences in achievable misalignment tolerance and if the design is subject to a null in the power distribution, as well as flux path height for different coil designs.

Table 1 Comparison of different coil design approaches

Coil design	Misalignment tolerance	Flux path height	Reference
Circular	Null at 40 % of diameter	¼ of coil diameter	[86]
Flux pipe/ flat solenoid	Good tolerance in one direction	½ of coil length	[93], [94]
DD	Null at 34 % of length of pad (in x-direction)	½ of coil length	[99]
DDQ	Null at ca. 95 % of length (in x-direction)	Twice of circular	[99], [101]
Bipolar	Null at ca. 95 % of length (in x-direction)	Twice of circular	[101]
Tripolar	Non-symmetric tolerance	N/A	[110]
Zigzag	No null	1/(2.5) of coil length	[104]

2.3.1 High temperature superconductors (HTS) as coil material

So far, coils have been conventionally made of copper wire as it has high conductivity, while still low in cost and easy to manufacture. To reduce the impact of proximity and skin effects at higher frequencies, Litz copper wires are used. While copper has a good balance between performance and cost/availability, new materials emerge to improve the system performance of WPT systems. One of these new materials is high temperature superconductor (HTS) [112]. Even though HTS is more expensive than copper, it has already been used as coil material, e.g. for power generators of wind turbines [113], [114] and fault current limiters [115], [116]. But HTS is not as prevalent in WPT. In addition, HTS capacitors for WPT are proposed [117]. HTS provides virtually no resistance and high current densities in critical state. Incorporating HTS in a WPT system can increase the system efficiency due to smaller resistance. Furthermore, higher current densities lead to smaller dimensions of the system, while maintaining the power level. Another positive effect is the increase in possible transmission distance as the magnetic field density is higher. The critical state is dictated by the temperature, current density and magnetic field. All these critical values depend on the type of HTS used. Beyond this critical state, HTS 'quenches' and converts back to a normal conductor. Additionally, HTS lose their superconductivity if bent too far [118], [119].

One requirement of HTS material is an additional cooling system that cools the coils below their critical temperatures. The coolant depends on their critical temperatures. Conventionally, rare-earth barium copper oxide (REBCO) superconductors are used, which are cooled with liquid nitrogen to 77 K. An additional component increases the size and cost of the system and handling cryogenic material can cause safety concerns. This is particularly true for HTS in receiving coils mounted underneath a vehicle. If HTS is used in transmitting coils, special training is required for the installation of the transmitting pads/ rails.

Compared to conventional copper, HTS material has interesting AC loss characteristics [120], [121], [122]. Operating at higher frequencies causes increased AC losses in HTS, which has direct influence on the power transfer efficiency. AC losses in HTS contain transport losses, hysteresis losses, and eddy-current losses [123]. It is important to quantify and minimise these losses, as heat is dissipated proportionally to the losses, which puts an additional burden onto the cooling system. Because of the lower resistance, HTS coils have a higher Q-value compared to conventional copper coils and therefore support higher transfer efficiency. Like a typical coil system, HTS-WPT systems require resonance to achieve maximum power transfer efficiency. Therefore, bifurcation can occur as well and must be considered by the controller [123].

In general, using HTS as coil material on both sides can increase the power transfer capabilities as shown in Figure 11 a). The transfer efficiency for conventional copper systems increases when the coils are cooled, as the resistance decreases [124]. HTS coils on both sides require cooling, which might not be possible due to space constraints and cost. Chung *et al*. and Kim *et al*. stated that a receiver coil with high Q-values and low impedance is advantageous over a transmitting coil with high Q-values [124], [125]. Conversely, as shown in Figure 11b), the influence of using HTS in the transmitting coil is greater than for HTS in the receiving coil.

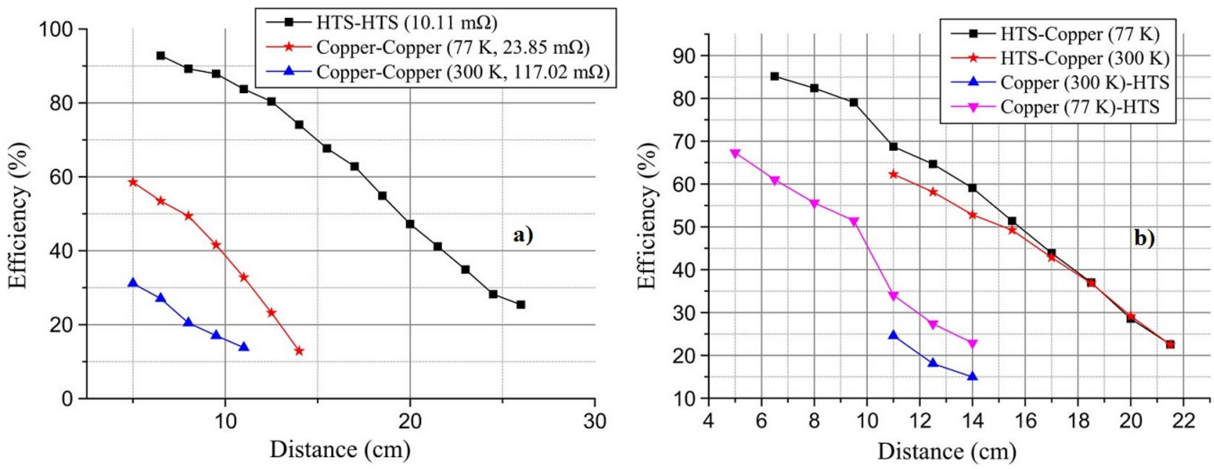

Figure 11 Power transfer efficiency for different coil materials at a resonance frequency of 3 kHz a) same material is used for receiving and transmitting coil b) different materials for receiving and transmitting coil [123]

Traditional WPT-charging systems use single coil sub-systems. Some DWPT systems, particularly the chargers using power supply rails, can supply multiple receiving coils with a single transmitting coil. Multi-coil systems are investigated, where one copper coil is substituted with an HTS-coil [126]. Kim *et al*. proposed a system with four coils, two of which were made from HTS [127]. It has a power coil connected to the power supply and a transmitting coil, which is coupled to the power coil, on the transmitting side. Both made of copper wire and operated at room temperature. The receiving system contains an HTS receiving coil and an HTS load coil that is connected to the load. Power and load coil have one turn and have an air gap length of 3 cm to the transmitting and receiving coil, respectively. At an air gap length of 0.3 m, a current transfer efficiency of 50 % was achieved. A key aspect of the experiments was the impedance matching between the load and the transmitting coil pair. The experiments conducted in this study used a resonance frequency of 13.56 MHz, which is not viable for charging EV. However, it shows a general principle of using multiple HTS and copper coils within one system

Chung *et al*. suggested to use a resonator coil between transmitting and receiving coil [128]. Three different arrangements were tested and are shown in Figure 12. At the frequency of 370 kHz, the system using two HTS coils in the transmitting sub-system had the highest transfer efficiency of 79 % compared to 67 % achieved by the three-coil system with cooled coils. A total of 4 litres of liquid nitrogen per hour during testing is consumed by the copper coil system, whereas just under 2 litres were consumed by the HTS system while supplying 400 W to the transmitting coil. This consumption can be reduced by adopting and optimising different cooling systems, instead of using a batch approach without covering the cooling vessel. One issue of using an additional resonator coil is the varying air gap length between resonator and receiving coil. As the gap length varies, the resonance coupling between the coils changes, which introduces power losses and therefore thermal losses to be compensated by the cooling system. An higher transfer efficiency, when using HTS resonator coils compared to copper coils, was reported in [129].

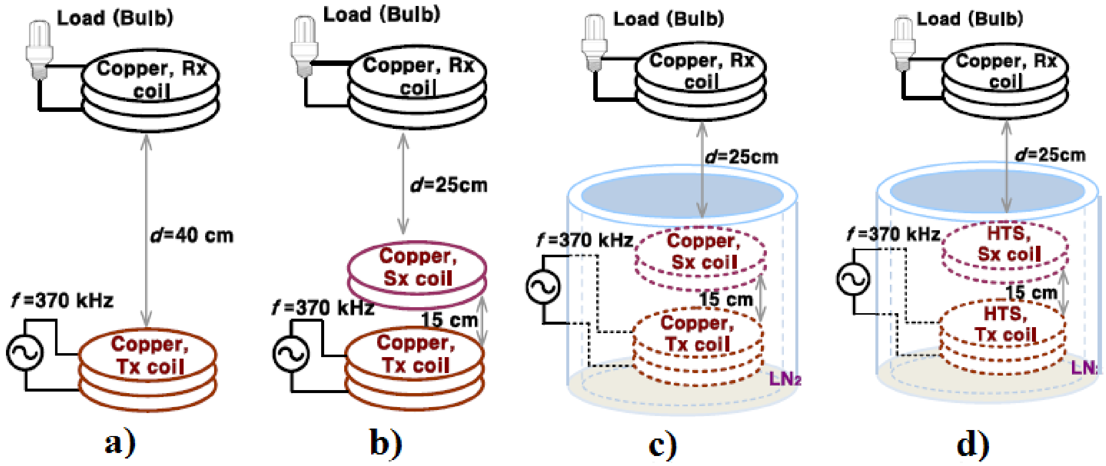

Figure 12 Different coil arrangements for a three coil WPT-systems incorporating HTS a) conventional system with copper coils at room temperature, b) copper coil resonator in conventional system, c) three-coil system with cooled transmitting and resonator coil (77 K), d) HTS-three-coil system with HTS transmitting and resonator coil cooled to 77 K [128]

A study conducted by Inoue *et al*. investigated the impact of low-frequency operation on the power transfer efficiency [130]. It has been shown that at low resonance frequencies, the HTS-system has much higher transfer efficiency due to the higher quality factor of HTS coils compared to traditional copper systems. Furthermore, the HTS system presents a higher robustness against frequency variation compared to copper systems. This allows more leeway in the frequency control. A summary of experiments conducted with HTS systems is presented in Table 2.

While losses in the pavement material are negligible [131], the material of the cooling vessel has great impact on the coil-to-coil efficiency. Jeong *et al*. compared multiple vessel materials under various air gap lengths [132]. The system comprised copper source, load coils and two YBCO coils (Yttrium barium copper oxide) in the transmitting sub-system. The tested vessel materials were fibre reinforced plastics (FRP), Bakelite, polystyrene, aluminium, and iron. While FRP, Bakelite and other plastics have high wave penetration characteristics, aluminium and iron have high electrical conductivity and are used as shielding and core materials. While the air gap length increases, the reflection parameter was measured and compared. The plastic materials have only minor impact on power transfer, with FRP achieving the highest unaffected transmission distance of 2 m. Hence, FRP is the most favourable cooling vessel material amongst the tested ones. Instead of absorbing or reflecting incident magnetic waves, it does not affect them. In addition, its durability is very high, and it has a very low thermal conductivity of 0.5 W/(m*°C) [133]. On the other hand, iron and aluminium are the least favourable materials as they absorb magnetic flux and cause losses. Other investigated plastics have good properties regarding to power transfer efficiency, but the exhibit low durability and therefore are not suitable for WPT systems. Kang *et al*. investigated the effect of steel and Styrofoam material as cooling vessel material for the HTS receiving coil [134]. Styrofoam has a similar magnetic permeability to air and liquid nitrogen, and therefore does not affect the magnetic field. Whereas steel channels the magnetic field inside the cooling vessel and lowers the incident magnetic field on the HTS coil. Hence, metallic materials should not be used as cooling vessel materials for WPT systems, as they severely affect the magnetic field and cause losses. While experiments investigated the effect of vessel materials on the power transfer, they did not outline practical solutions for real world systems and did not consider safety regulations. The effect of rain or water between the charging pads was investigated in [135]. Different containers, surrounding the coils, were filled with fresh water or salt water with a salinity of 3.4 %. The results show that fresh water reduces the transmission efficiency by up to 5 %, even when only one coil is surrounded. If salt water is used, the efficiency decreases significantly with a maximum efficiency decrease of 30 % when both containers are filled. This is due to the shielding effect of the salt element in the water.

Table 2 Summary of experiments using HTS coils

Power level [W]	Separation distance [m]	Frequency [kHz]	Coil specifications, diameter [m]	Reference
500	0.3	370	HTS Tx: 0.3m Copper Rx: 0.3m	[124]
200	0.5-1.5	13560	Copper Tx: 0.28m HTS Rx: 0.28m	[125]
11	0.05-0.22	3	HTS Tx: 0.29m Copper Rx 0.29m	[123]
N/A	0.03-0.18	63.1	HTS Tx: 0.3m Copper Rx: 0.2-0.3m	[118]
<10	0.02	10	HTS-system: 0.09m Copper-system: 0.09m	[130]
N/A	0.3	370	Copper Tx: 0.3m HTS Rx: 0.3m	[134]
60	0.4	370	HTS Tx: 0.3m Copper Rx: 0.3m	[136]

2.3.2 Track layout

Not only has the geometry of the charging pads impact on the system performance but also the system layout, particularly on the primary side. While the layout for stationary system is straight forward, there are different options available for DWPT mostly related to the dynamic nature of the charging process. A main challenge associated with DWPT is the short time period in which the transmitting and receiving pad can interact with each other and transfer power. As vehicles approach transmitting pads and move across them, magnetic flux is intercepted by receiving coils and therefore magnetic coupling changes. This causes power and transfer efficiency fluctuation and increases stress on the power electronic devices. To reduce the impact on the charging system and grid connection, charging pads must have a high degree of misalignment tolerance. Depending on the layout of the transmitting coil and power supply, two designs can be distinguished and are shown in Figure 13.

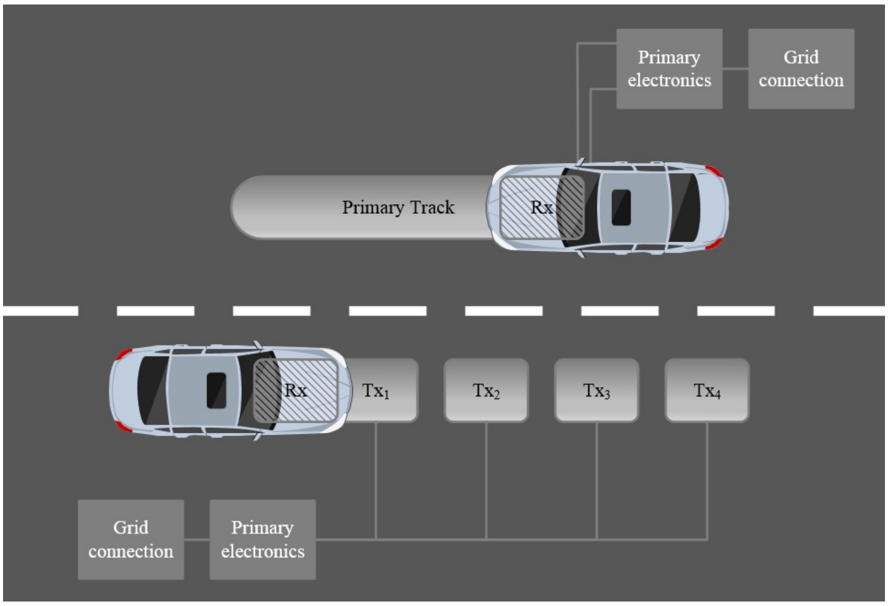

Figure 13 Different track layout options for DWPT

While stationary charging uses a single power supply to power one or multiple separate transmitting pads, another option is considered for DWPT charging. Instead of using multiple segmented transmitting pads for DWPT, a long transmitter rail is widely used [137], [138]. Both designs have advantages over the other approaches, while having their own disadvantages. Using a long transmitter track minimises the amount of system components and reduces control complexity, as it produces a constant power output and current once the receiving pad is located above the track. However, it increases the ratings of all components supplied by a single power source. And if a fault occurs, the whole system must be switched off, decreasing the system reliability. In addition, the efficiency is low during part load operation, as the whole track needs to be energised at all times. And coupling is low as well, as the receiving coil is small. The electromagnetic field produced by the parts that are not in use must be supressed to reduce harmful radiation. Furthermore, the consumption of coolant is higher if HTS coils are used [139]. On the other hand, if the transmitting sub-system contains multiple segmented pads [140], [141], it requires a multitude of components like power sources and high-frequency inverters, as every pad has to be connected separately. By using multiple inverter-pad sub-systems, the reliability of the system increases through redundancy. The charging system is still functional, when faults occur within one segment. It is also possible to connect multiple pads together instead of using several inverters, with one high power inverter connected via switches to the transmitter pads [142]. Each of the pads switches off as soon as a vehicle passes over it, reducing the electromagnetic field radiation and alleviating the reduced coupling. In addition, each transmitter pad has a compact low weight structure, which simplifies deployment. Disadvantages of this layout are increased cost and control complexity to increase efficiency and lower its grid impact due to power fluctuations. The inter-pad spacing needs to be optimised as it affects the system performance [143], [144]. If the pads are too close, coupling between transmitting pads will occur, which produces negative current stress and increases the number of pads per given length. The coupling between the transmitting coils can be reduced by placing them farther apart, but this will eventually result in discontinuous power transfer and has negative effects on the grid network.

2.4 Control methods

For controlling the power throughput and output of the system, multiple control methods can be used. The most fundamental methods are primary side control [145], [146], secondary side control [147], [148] and both combined [24], [149]. A primary control method cannot be used for power supply with multiple pickup coils. It is necessary that one supply is connected to only one receiver [150]. The primary current and the frequency are controlled to regulate the power output on the secondary side. This strategy provides higher efficiencies at lower loads compared to the secondary control [151]. One requirement for primary control strategies is a communication link between transmitting and receiving pad. The battery management system (BMS) is transmitting information about the battery, e.g. SoC etc., to the primary pad. By controlling the transmitting pad, the secondary electronics can be simplified, thus reducing complexity and cost.

Two important strategies are considered for inverter control, namely phase shift control and frequency control. When phase shift control is used, the phase difference at constant switching frequency between inverter legs varies [152]. While varying the phase shift, the pulse width of the voltage output signal changes. This causes the amplitude of the voltage fundamental to change accordingly and controls the power output. However, it compromises soft switching as bifurcation during operation close to resonance can occur, which can lead to non-inductive conditions and high switching and conduction losses. Phase shift control does not require any communication link between transmitting and receiving pad, but it is only usable for full-bridge inverter [153]. During frequency control, the phase shift between inverter legs is constant and the switching frequency varies [154]. This affects the DC output voltage feeding into the battery on the receiver side. The controller constantly monitors the switching conditions and updates the inverter frequency and switching signals. A range of possible switching conditions needs to be pre-defined so that the controller can limit the frequency to achieve ZVS. To reduce losses, the WPT system has to operate under inductive conditions and the actual resonance frequency must be measured in real time.

Secondary side controllers keep the supply current and the frequency constant and each receiving system adjusts the power it draws according to their load [155]. If multiple receiving pads are connected to the primary, an active rectifier in each secondary system is required. The power drawn by the secondary system can be controlled by varying the Q-value. As the whole supply rail must be powered, efficiency under part load is low. A combination of control methods on both sides can vary current and power demand according to load on the secondary side. Hence, it requires the same power electronics as the primary and the secondary control. Highest efficiency is achieved by controlling current and Q-values, to match primary side losses and secondary side losses [156]. Advantages of primary and secondary side control can be combined. Diekhans & De Doncker proposed a dual-side controlled WPT system with a full-bridge inverter on the primary side and an active rectifier on the secondary side [157]. The lower half of the rectifier consists of switches instead of diodes. By varying the pulse width of the secondary voltage, the fundamental output voltage to the battery can be adjusted. At the same time, the inverter is phase shift controlled. The primary current is controlled by the secondary rectifier pulse width, while the primary inverter pulse width affects the secondary current. A control strategy is developed that uses this additional degree of freedom to maximise the overall efficiency by adjusting the point of operation. While the frequency is limited to 35 kHz, it is not clear to what extend the system behaviour changes when a higher switching frequency of 85 kHz is used. A bidirectional frequency control is proposed in [149]. It uses the system frequency to control the supplied power. A new controller is demonstrated in [158], which uses active and reactive power, measured at the resonant circuit of the secondary side, to regulate the bi-directional power flow. The new controller does not require a dedicated communication link between primary and secondary side. However, the system has lower efficiency in the part load regime.

2.5 Communication in WPT-systems

Equally important to the power transfer system is the communication link between GA and VA. This also includes the communication to the GA grid connection to manage demand upon grid status. Communication between sub-systems is required throughout the charging process in a stationary environment as well as under dynamic charging conditions. VA needs to detect and request charging from GA. At the same time, GA must approve or deny the request. In addition, GA must detect any foreign objects on the road, which might affect the charging process. Once a charging request has been approved, VA transmits its charging requirements. These include SoC, power level, misalignment and ground clearance. To ensure optimal charging conditions, VA has an alignment assistance to maximise transfer efficiency. During the charging process, SoC and position of the vehicle are monitored [159]. After the charging process, the method of payment must be communicated between the parties. Wireless communication for stationary charging systems is possible, particularly for smart charging purposes [160], [161]. Key technologies for communication systems under review for stationary WPT include Zigbee, Wi-Fi, Bluetooth and cellular [162]. However, conventional off-the-shelf communication systems, i.e. Wi-Fi or Bluetooth, are not well suited for wireless communication in WPT systems, as one of the key requirements is a two-way link with simultaneous data transfer (duplex) [163].

For DWPT there are additional requirements caused by the speed of the vehicle and the potential to charge multiple vehicle at the same time. Problems like priority charging and queuing, as well as the potential of speed limitations on the stretch of road arise. Therefore, commonly used technologies in stationary wireless charging cannot be used for DWPT systems. Special requirements for the dynamic system include low latency to ensure stable real-time communication at higher velocities, an increased communication range to reduce roaming between charging zones and the potential to support multiple vehicles [164]. The SAE J2954 guideline outlines Wi-Fi, Dedicated Short Range Communication (DSRC) or RFID as potential communication technology for WPT systems. RFID communication is suitable for stationary charging, but not usable under dynamic conditions due to latency issues. Furthermore, the signal strength after propagating through concrete to reach the transmitting coil might not be sufficient enough [165]. A study conducted by Gil, *et al.* compared DSRC, radio communication, cellular communication, satellite communication and WiMAX [164]. It concluded that DSRC and cellular communication are the most favourable options. DSRC has a very low latency while maintaining a reasonable high data rate. However, the effective maximum coverage is limited to around 300 m, which might not be enough depending on the length of the charging lane. Cellular communication has a very high coverage area, in which it can transfer with high data rates but with higher latency than DSRC. An additional benefit of DSRC is its current utilisation in safety applications, hence providing a secure communication link [166].

Echols, *et al.* proposed a hybrid communication system based on wireless and wired communication [167]. The infrastructure uses a wireless communication link (cellular and DSRC) between VA and GA to process the detection of the approaching vehicle, and the charging request. After the charging request has been approved the information are transmitted to a roadside unit (RSU) and the vehicle is tracked by GPS. The communication between RSU and GA is realised via optical cables to provide low latency, real-time exchange of information. So far, the communication with a single EV has been tested but the impact of multiple vehicles charging at the same time has not been investigated. Another hybrid system based on two different wireless communication links is suggested in [168]. It uses DSRC for the communication between VA and GA, providing a low latency and low jitter link. A Fog management system manages and supervises the DSRC-system. Information gathered during the VA-GA communication are stored in a cloud network and can be accessed by users without disturbing time-sensitive communication. Hybrid systems provide a valuable alternative to single technology communication. However, increased complexity of the communication link could raise additional problems like user accessibility. Another technology that might be viable for future wireless communication in DWPT is 5G, as it provides fast data transfer between multiple parties with low latency [169], [170]. Currently, 5G technology is still in the early stage of deployment [171].

2.6 Foreign object detection and EV detection

Foreign object detection (FOD) is a key auxiliary system required to enable widespread application of wireless charging. It covers the detection of living objects (LOD) and non-living objects, e.g. conductive objects and approaching EVs. If the system detects objects between the charging pads, it immediately shuts down and prevents any power transfer. By doing so, it prevents heating of conductive objects, which can cause safety hazards. Furthermore, it prevents living matter, e.g. people and animals, subject to magnetic and electric fields. On the technical side, it also prevents system losses and switches off power transfer when receiving coils are not near transmitting pads.

Multiple methods are known to date that mostly rely on sensors, i.e. inductive or capacitive, optical, and mechanical [172]. A simple and low cost way is the comparison of power losses with and without the presence of a conductive object between the pads [173]. Unfortunately, as WPT systems transfer high power, the losses generated are small and difficult to detect [172]. Another approach is to use the quality factor Q of the secondary pad [174]. This method is viable for stationary systems that include alignment mechanisms. If pads are misaligned, quality factor of the receiving system changes disguising the change due to an object. It is also true for DWPT systems as the receiving coils are constantly moving, causing a changing quality factor. Jang *et al.* proposed an FOD-system based on the change of the magnetic field [175]. It uses multiple non-overlapping coils in the transmitting pad to detect an object and the voltage difference in the sensing coils across the pad area. The detection of living objects uses similar technologies. By using the capacitive coupling between the transmitting pad and the ground, an approaching living object can be detected [176]. The presence of the living object alters the coupling, but changes are minimal and require careful tuning of the sensors.

Vehicle detection is a special form of metal object detection and is mainly used for switching the transmitting pad on and off depending on the presence of the receiving pads. It is possible to incorporate the vehicle detection into the FOD-system [177]. Figure 14 shows the detection coils of a combined system for stationary charging. It comprises two sets of coils, one for lateral direction and the other one for longitudinal direction. The system uses the difference in induced voltage in each of the detection coils to locate an object, while the impact on the power loss characteristic is widely minimised. Due to the additional coils, the material usage of the system is high.

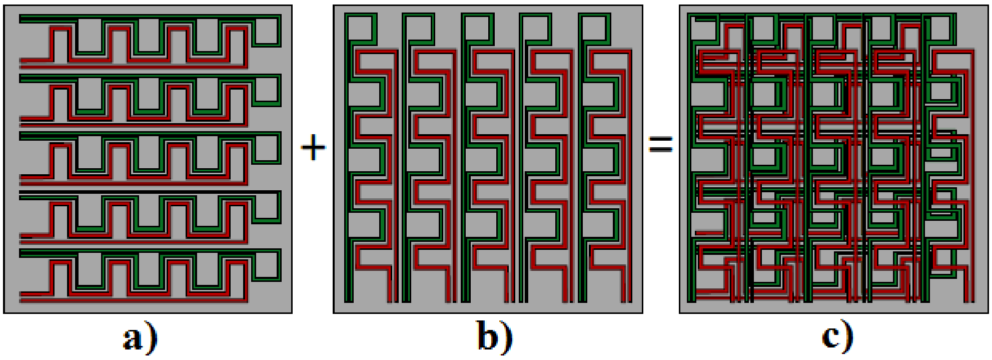

Figure 14 Detection coils for a) longitudinal direction b) lateral direction and c) combined [177]

Vehicle detection for DWPT systems is a main research area within wireless charging systems. A wide range of detection systems exist. A multi-coil system is used in [165].The transmitting pad includes two coils with an offset in the direction of travel, and a single detection coil is incorporated in the receiving pad. The detection coil in the receiving coil is energised, which induces a voltage in the detection coil in the transmitting pad as EVs approach the charger. Due to the longitudinal offset of the coils, the voltage profile is different, and the phase difference can be used to detect vehicles. One drawback of this method is that only vehicles approaching along the direction of travel are detected. In general, neighbouring transmitting pads should be decoupled to reduce the negative impact on the transfer efficiency. However, there is a small and almost negligible coupling between the pads depending on the pad spacing. Here, this coupling is used to detect approaching vehicles [178]. As EVs approach the transmitting pads, the ferrite in the receiving coils affects the coupling and allows a voltage to be induced in the latter transmitting coil. If the primary pad resonates with its tuning capacitor, a current flows that is measured and utilised to detect the vehicles. While the current sensor is already part of the transmitting pad, the system is only applicable to segmented DWPT systems that use closely spaced transmitters. Other approaches include phase differences between voltage and current in transmitting pads [179] or RFID [180]. These systems are limited to a single vehicle per pad and by vehicle speed.

3 Research on WPT for EV

Research in the field of WPT has increased over the past decade and early research has been conducted in the following research institutes. Based on the fundamental concept proven by these institutes, large-scale research projects are funded and realised in collaboration between academia and industry. The aim of this chapter is not to provide a complete list of research institutes, projects and consortia, rather, we summarise the work done by key institutes and recent projects.

3.1 Korean Institute of Advanced Technology (KAIST)

Since 2009, KAIST has been researching on WPT, with their focus on DWPT. Over the years, multiple systems, called "generations" of the On-Line Electric Vehicle (OLEV), based on the improvements of the previous designs, have been proposed. OLEV is the first commercialised DWPT system for electric busses. It started with a small golf cart (1st Generation) that was powered by an E-type supply rail instead of multiple charging pads [181]. Over an air gap of 1 cm, 3 kW could be transferred, achieving a system efficiency of 80 % while operating at a frequency of 10 kHz. The vehicle was mechanically aligned to ensure a maximum lateral misalignment of 3 mm.

Later that year, KAIST announced their 2nd Generation based on an E-Bus. Main improvement to the first generation was an increase in air gap length to a maximum of 17 cm [182]. To power the bus, ten I-type pickup coils were installed underneath the bus. Each of these pickup coils could receive 6 kW. The maximum efficiency of the system was 72 % while transferring 60 kW. Instead of using an E-type supply rail, the design was reworked, and a U-type rail was used. Another key improvement was the increase in lateral misalignment tolerance to 23 cm, while achieving 70 % of the maximum power output. In addition, the operating frequency was increased to 20 kHz.

Just two months later, in August 2009, an SUV was fitted with the wireless charging system, forming the 3rd Generation [183]. The power supply rail design was changed to a W-type structure and the pickup coils consisted of overlapping E-type windings to reduce the produced magnetic field. Due to the reduction in magnetic field, no shielding was required, while the system was still satisfying the guidelines on magnetic field emissions. The system transferred 17 kW per pickup coil over an air gap of 17 cm with an efficiency of 71 % [184]. After revision of these results, smaller changes to the system improved the efficiency to 80 % with an air gap length of 20 cm. The width of the supply rail was halved, which reduced the manufacture and deployment costs of the system. In addition, a bone structure was patented that can reduce the mechanical stress onto the rail [185].

In 2010, a new charging system (4th generation) was developed to charge both buses and EVs. It is based on an I-type supply rail with a width of 10 cm [186]. With an air gap length of 20 cm and a lateral tolerance of 24 cm, the system has similar properties to the 3rd generation. The maximum output power is 27 kW for a double pickup coil at 74 % efficiency [186]. To reduce the voltage stress in the rail structure an SS compensation network was used. By using a constant-current source inverter, the output voltage of the charging system can be held constant and independent from the load, providing an inherent robustness against load changes [187]. Like previous systems, the magnetic field emissions fulfilled the ICNIRP guidelines. In addition to the system design, the cost for the infrastructure was stated with $0.4m/km for a one-way lane including inverters.

Further improvements were made in the past few years, leading to a new S-type power supply rail. With only 4 cm in width, it has been the smallest supply rail structure so far [188]. Due to the small width, the construction cost of the coils as well as the installation time was reduced. Even though the width was reduced significantly, the tolerance to lateral offset between the GA and VA was further increased to 30 cm over an air gap length of 20 cm. The maximum efficiency (without power inverter) of 91 % was achieved at 9.5 kW, whereas the maximum power of 22 kW was transferred with an efficiency of 71 % [189]. One downside of the new rail design was the increase in self-inductance, which causes higher voltage stresses in the rails [190].

The latest design, the 6th Generation, includes a power supply rail with similar shape to the W-type rail used in the 3rd Generation, but without a core plate in the rail [190]. The system is designed to not only supply driving vehicles, but also stationary EVs. In previous designs, the operating frequency was limited due to voltage stress in the components. By adopting the new coreless design, the inductance in the power supply rail is reduced, lowering the voltage stresses. Therefore, the operating frequency can be increased to the recommended 85 kHz [191].

3.2 Oak Ridge National Laboratory (ORNL)

ORNL, based in the USA, started researching on WPT in 2011. Instead of using a long supply rail, their research focusses on multiple segmented coils for transmitting power to moving vehicles [192]. Due to their simplicity, circular coils were used for transmitting and receiving. To enable continuous power transfer to a moving vehicle, multiple coils were placed behind each other. As the tolerance of circular coils against lateral misalignment is low, the separation distance between the coils was small. The research conducted by ORNL focusses on coil and pad design, vehicle integration, power flow control, and the interaction between grid and charging system [193], [194], [195], [146], [196]. In 2013, a VA of a stationary charging system (6 kW) was integrated into a Toyota Prius [197]. As part of this, the effect of concrete and asphalt material onto the power transfer was investigated. Three years later, a similar system with a capacity of 12 kW was installed in a Toyota RAV4 [198]. It achieved a DC-to-DC efficiency of 95 % over an air gap length of 16 cm. Later, wireless charging for heavy-duty vehicles was investigated as well [199]. The system fitted onto the Toyota RAV4 was further improved and is now able to transfer 20 kW at 95 % efficiency [200]

3.3 University of Auckland (UoA)

Research on WPT started in the early 1990s with its main aim to provide charging for material handling via EVs [201]. Since then, a multitude of systems has been designed, that initially adopted circular coils, with ferrite bars to guide magnetic flux and reduce electromagnetic radiation [86]. Due to their lack of lateral misalignment tolerance, the overall coil structure was revised. In 2010, a so-called flux pipe was proposed that provided the system with an increased tolerance against lateral offset between receiving and transmitting coils and a focussed magnetic flux in the air gap [93]. One key aspect in designing coil structures is the limitation or guiding of magnetic flux in a way that it only exits the transmitting coil on one side. These designs are referred to as single sided polarised coils and are part of the research conducted at UoA [202], [100], [98], [101]. Furthermore, UoA is investigating DWPT and possible layouts for future charging systems and their control [203], [204], [205].

3.4 Commercial and Non-commercial WPT projects

Consortia of universities, vehicle manufacturers and energy operators conducted multiple projects on wireless power transfer for EVs around the world. One early adopter was PATH (Partners for Advanced Transit and Highways). It is a programme founded in 1986 and led by the University of California, Berkeley. One research project run by PATH focussed on dynamic charging for EVs. In 1994, it developed the first prototype of such system [206]. It transferred 60 kW over a two inch air gap and achieved 60 % transfer efficiency [207]. The project showed that a practical approach towards commercialisation is achievable. However, it was terminated, as it was impossible to design an economically feasible system at that time.

Two recent European projects were FABRIC and UNPLUGGED. FABRIC (Feasibility analysis and development of on-road charging solutions for future EVs) is a project that started in 2014 and ran until the end of 2017. It was mostly funded by the European Commission and comprised 24 members [208]. Its main objective was to investigate the feasibility of DWPT technologies for EV range extension as well as efficiency of DWPT. Deliveries include analysis of existing solutions for DWPT and their technical feasibility [209], [210], [211]. DWPT systems of Qualcomm Halo and PoliTo as well as Seat were tested in three different test sites, France, Italy and Sweden [212].

The second project called UNPLUGGED, ran from 2012 until 2015. It examined the impact of WPT of EVs on customers in urban areas and the feasibility of DWPT for range extension [213]. As the FABRIC project, it was funded by the European Commission and was conducted by a consortium of 17 partners [214]. Technical and economic feasibility analysis of the DWPT project have been published in 2013 and 2015 [215], [216]. As part of the project two prototypes of a wireless charging system were built.

In tandem with international projects, national governments and highway operator investigate the possibility to adopt WPT. For example, Highways England performed a feasibility study on DWPT on major English roads in 2015 [217]. Main aims of the study were the identification of key technologies, their technology readiness level (TRL), important stakeholders and early adopters, and system requirement and economic feasibility. After the study, off-road trials were scheduled but were delayed until “at least 2018” [218].

Besides consortia-run projects, there are also a wide range of companies using WPT. The majority are using this technology for low-power appliances. However, a few companies offer products for EVs. The main companies include WiTricity and HaloIPT. Both companies are based on research conducted at universities and were later formed by researching staff of Massachusetts Institute of Technology (MIT) and UoA, respectively. WiTricity is focussing its production on stationary charging system of EV. It offers a wide range of different power levels up to 11 kW with efficiencies of up to 94 % [219]. HaloIPT was acquired by Qualcomm in 2011 and is now part of the wireless charging solution offered by Qualcomm. Qualcomm Halo offers stationary charging pads in power levels of 3.3 kW, 6.6 kW, and 7 kW with efficiencies higher than 90 % [220].

4 Health and Safety concerns

The use of time-varying currents and voltages, particularly at higher power levels, brings certain risks and concerns to health and safety (H&S). However, these risks are well known due to their usage in other fields and can therefore be addressed. They include electromagnetic field exposure, electrical shock, and fire hazards [221]. Hence, the bigger challenge with H&S in WPT is the public perception of the safe employment rather than any actual challenge for the system [222]. The high-frequency currents in the system produce varying magnetic and electric fields. Due to the low coupling between coils, the share of leakage field is high. It causes undesirable electromagnetic interference and field exposure, which not only lowers the system efficiency, but also leads to safety risks. To limit the impact of magnetic and electric fields on employees and for the public in general, the International Commission on Non-Ionizing Radiation Protection (ICNIRP) proposed a guideline for field limitations [223], [224]. The reference levels of electric and magnetic fields for public and occupational exposure are shown in Figure 15.

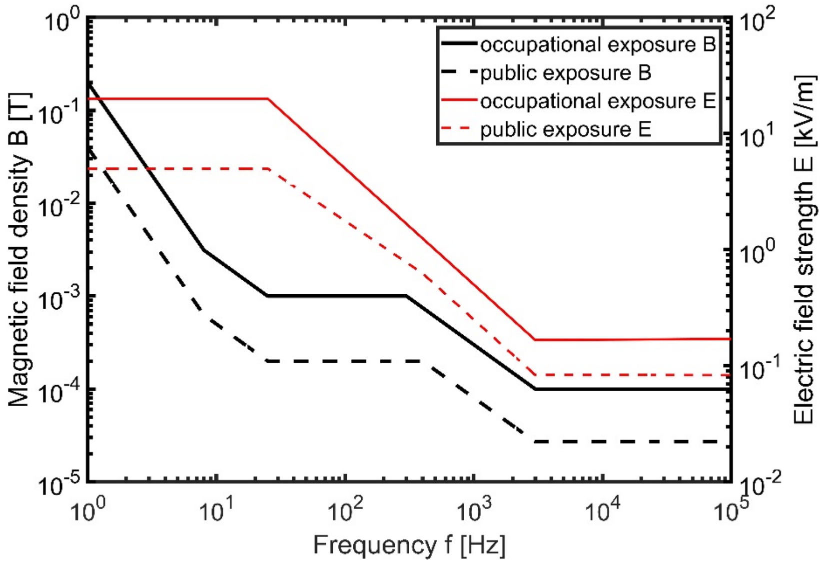

Figure 15 ICNIRP reference levels on magnetic and electric fields for occupational and public exposure [223]

In the late 2000s, the World Health Organization (WHO) presented a report that stated there was a lack of scientific evidence for health risks caused by fields with a frequency below 100 kHz [225]. Since then, the amount of research on low-frequency magnetic and electric fields has increased but it is difficult to study the long-term effects of magnetic radiation. Short-term effects and biological response can be studied by using experiments on animals, mainly mice [226]. A study conducted by Nishimura, *et al*. could not observe any changes in reproductive organs of rats during and after magnetic field exposure with frequencies of 20 kHz and 60 kHz [227]. The investigated magnetic fields had a higher field intensity but a lower frequency than currently present in WPT. It is therefore difficult to gauge possible impacts on the human body.

With the aid of anatomical models of humans, it is possible to assess the impact of external magnetic field exposure on humans [228], [229], [230]. These models are based on MRI-scanned human bodies and include properties of multiple different tissues, organs, and body fluids [31]. By coupling the anatomical model and the magnetic field generated by the WPT system, a tool is obtained to investigate the impact of magnetic field exposure. A person can interact with the wireless charging system and its most delicate areas in multiple ways. Due to the proximity to the transmitting coil, the area underneath the vehicle has the highest magnetic field strengths and is most likely to exceed the reference levels of the guidelines [232]. Other areas that need further investigation include the space surrounding and inside vehicles. The inside is particularly important for future DWPT systems.

A study conducted by Shimamoto, *et al*. investigated the effect of a 7 kW WPT system operated at 85 kHz on a human body [233]. The magnetic field distribution around the vehicle, generated by a two-coil system under misalignment (0.2 m later and 0.1 m front-to-back), is modelled using ANSYS HFSS. To mimic the field incident to the human MRI-model, the results are extracted and the magnetic vector potential that would yield the same magnetic field is calculated. This is done to ensure that the resolution of the incident field distribution is equal to the MRI-model. After that, four cases are investigated. A kneeling person touching the vehicle chassis, a person lying next to the vehicle with his right arm stretched towards the coils, a person standing on the transmitting coil (neglecting receiving coil) and a person sitting on the driver's seat were simulated. The induced electric field distribution for the person sitting on the driver's seat is shown in Figure 16.

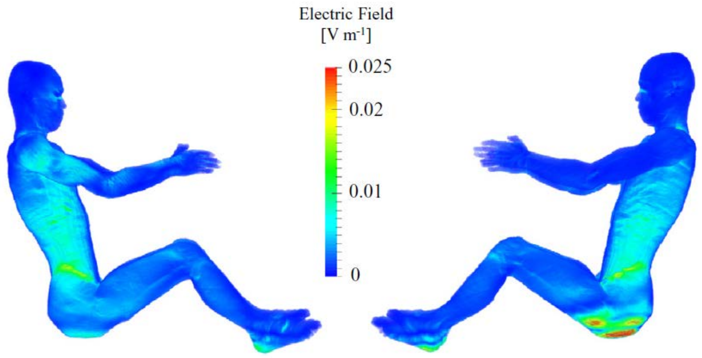

Figure 16 Induced electric field distribution of the human model sitting on driver's seat [233]

The maximum induced electric field for all scenarios are shown in Table 3. The highest values are obtained when the person is lying on the ground, next to the vehicle where the magnetic field is the strongest. ICNIRP limits the maximum internal electric field in the frequency range of 3 kHz-10 MHz to 1.35*f*10^{-4}, which limits the electric field to 11.39 V/m at 85 kHz [223]. All the investigated scenarios are within the guideline. It has been shown that the system complies with current guidelines even under misaligned conditions. However, only a single pair of primary and receiving pad is investigated, neglecting the effect of supply rails and the increased magnetic field due to lower coupling and greater area coverage. In addition, power during the absence of the receiving pad was reduced to 5 W, ignoring the cases when rated power is transferred during open circuit operation.

Table 3 Maximum induced electric fields for each scenario after [233]

Posture and position	99.9th percentile *in-situ* E-field (V/m)	Site of maximum E-Field	Tissue types of the highest E-field
Stand next to the vehicle	0.4	Ankle	Fat (71 %), bone (26 %), other (3 %)
Crouch toward the vehicle	0.92	Thigh	Fat (78 %), bone (21 %), other (1 %)
Lie on the ground	2.3	Chest	Fat (67 %), bone (26 %), muscle (7 %)
Lie on the ground (arm stretched)	5.95	Hand/forearm	Fat (41 %), bone (21 %), muscle (38 %)
Sit on driver's seat	0.024	Buttocks	Fat (90 %), bone (8 %), other (2 %)
Stand on transmitting coil	0.55	Foot	Fat (76 %), bone (12 %), muscle (12 %)

Park used a 3.3 kW WPT system that operates at 85 kHz, to evaluate the electromagnetic exposure [234]. A two-stage process to solve the bio-electromagnetic problem in human model proposed in [235] was used. The equivalent currents radiated by the WPT system are resolved . With the known incident fields, the internal electric fields in the human body are calculated by the quasistatic finite-difference time-domain method. Three different positions of the human model relative to the WPT system were considered. A person standing next to the WPT system (case 3 foot), one lying in front of it with the head pointing towards the system (case 3 head), and the WPT system is positioned at half the height of the human model (case 3). In addition, the system is covered with a 1.5 m x 1.5 m x 1 mm metal plate to mimic the vehicle floor panel, while a person is standing next to it (case 3 metal). The lateral distance between the system and the human was constantly 0.1 m. As the magnetic field changes with the relative position of the coils to each other, the perfectly aligned case as well as the misaligned one were investigated. Figure 17 shows the normalised results for the misaligned case, which is the worst-case scenario. By simulating the vehicle chassis, the induced field is much smaller than in the other case. The induced current in the head is the largest, as the conductivity of the tissue was the largest. Nonetheless, all results were below the ICNIRP guidelines. The cases at rated output during absence of the receiving coil, as well as a receiving pad supplied by a power rail were not investigated. Similar models were built with human models of children and the induced electric field was smaller, due to the smaller cross-sectional area of the body [231].

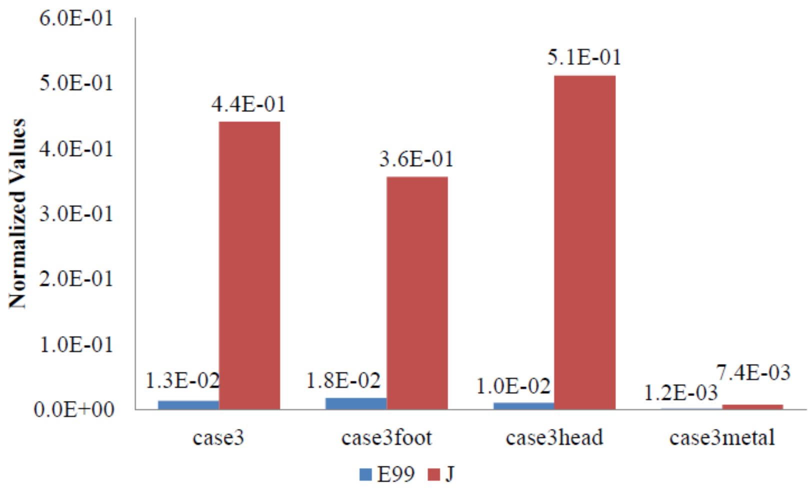

Figure 17 Internal electric field normalised to basic restrictions from ICNIRP guidelines of 1998 (J) and 2010 (E99) for the cases where the WPT-system is placed in the middle of the human model (case 3), next to the feet (case 3 foot), next to the head (case 3 head) and covered by metal plate (case 3 metal) [234]

Campi *et al.* investigated the magnetic field produced by a 22 kW WPT system operated at 85 kHz [236]. 3D FEA-modelling was used to calculate the magnetic flux inside a vehicle and its surroundings. The WPT system was compliant with ICNIRP reference levels for the fully aligned cases. However, under large misalignments small areas around the vehicle were reported in which the magnetic field exceeded the limits. Passengers located within the vehicle were not subject to increased magnetic fields.

These studies were conducted for light-duty EVs and their power requirements. In contrast to the research conducted for light-duty vehicles, the early adopters for WPT also include electric buses for public or freight transport [237]. This is particularly true for DWPT [217]. Research on higher power systems for charging buses is limited. Tell *et al*. measured the magnetic and electric field emitted by a WPT system designed for charging buses with 60 kW at 20 kHz [238]. With a maximum magnetic field of 7.98 µT and maximum electric field of 1.17 V/m inside the bus, the exposure levels were similar to the magnetic field generated by a video display terminal. Again, the ICNIRP guidelines were not exceeded.

In general, the use of pacemakers and other AIMDs is not considered in these studies. The leakage field can interfere with the medical equipment of the operator or people nearby and negatively affect its operation. In addition, implants can contain metallic parts and wires, which are affected by induced currents and can form local temperature ‘hot spots’ [239], [240]. To make WPT systems accessible to everybody, including people using AIMDs, the system must be in accordance with the ISO 14117:2012 standard that limits fields even further [241]. These limits are used in the standards regarding to WPT for vehicle charging purposes to limit the fields inside vehicles and above the ground clearance.

In recent research, only stationary charging was investigated. Due to the constant change in coupling and the higher power levels of DWPT systems, magnetic leakage field can be significantly high. The influence of dynamic behaviour needs to be investigated to allow safe operation of such systems. Nevertheless, there is no immediate threat to the health of the persons operating or using a WPT system based on the electromagnetic emission. Nevertheless, conducting objects, i.e. cans, between the coils can be a safety concern due to the increase in temperature caused by eddy currents [242]. Consequently, such charging systems require foreign object detection as presented in Chapter 2.6 to interrupt power transfer immediately in the event of a foreign object entering into the space between the charging pads.

To reduce the radiated fields and losses, shielding and magnetic field cancellation methods can be employed [243], [244]. Such shielding systems can be categorised into passive and active methods [245]. In passive shielding, ferromagnetic materials are used to guide the magnetic flux. By redirecting the magnetic flux, the systems performance can be improved while the leakage field is limited. However, there are limits depending on the material used, as hysteresis losses occur with increasing frequency. Ferrites with high permeability should be employed to reduce the negative impact on the system performance. Passive shielding is an effective way to reduce leakage field [246], [247]. Passive cancellation methods use conducting materials like aluminium sheets to establish a magnetic field that opposes the original field. The incident magnetic field induces eddy currents within the material, which produce magnetic fields in opposite directions. These fields cancel incoming fields and reduce the net magnetic field overall. Furthermore, active methods for field cancellation have been introduced in the past years. These rely on the same principles as passive methods, as they create a magnetic field with opposite direction but provide a more effective way to reduce the leakage field. At higher power levels, an additional power source for the cancellation coil is required, which increases the weight, size, and overall complexity of the sub-system [248]. Kim *et al*. and Moon *et al.* designed a reactive resonant current loop that generates an opposing magnetic field from the original magnetic field [249], [250]. The resonant circuit consists of a capacitor in series with a shield coil. By adjusting the capacitor, the coil current can be tuned to generate a magnetic field that is equal in magnitude but opposite in direction to the incident field, which hence reduces the overall leakage field [251]. The impact of the cancellation coil on the transfer efficiency depends on the coupling between the shielding coil and the receiving coil. With increasing coupling, the transfer efficiency decreases, so the shielding coil has to be decoupled from the transfer system. Zhu *et al.* proposed a similar shielding mechanism relying on the null in the mutual inductance profile of two coupled coils [252]. By shifting the shielding coil in the transmitting pad to the null position of the receiving coil, it is uncoupled from the receiving coil. Therefore, it can shield the transmitting pad's leakage field. One advantage is the applicability of this approach as it can be used in both pads. The adverse effect on the transfer efficiency is reduced, compared to that of an aluminium shield.

A different approach is used in [253], where a handheld stationary charging system is proposed. It uses the same approach as plug-in chargers, but it has two separated sub-systems. The transmitting coil is inserted into the receiving coil. Therefore, it supports a safe way of operation in any weather conditions and lower magnetic field exposure. However, this approach is only applicable to stationary charging.

5 Standards for EV WPT

Since the first appearance of WPT for charging purposes, there was a need for standardization. Low-power appliances like mobile phones, toothbrushes and laptops were at the forefront of the adoption of WPT, and standardization of these power ranges emerged first. Currently there is a multitude of standards for these applications, mainly formed through consortia between industrial partners. The QI standard was defined by the Wireless Power Consortium (WPC) for applications in the power range of 5-15 W [254]. It limits the maximum air gap length for power delivery to 4 cm and the operating frequency range to 87-205 kHz. Another standard is the Rezence standard designed by the Alliance 4 Wireless Power Transfer (A4WP) [255]. It is designed for power delivery of up to 50 W at a frequency of 6.78MHz.

As the power transfer, levels required for vehicular applications are much higher than for small scale applications, and therefore these standards cannot be used. However, consumers and manufacturers require standards for a commercialisation and rapid market uptake. Until 2016, there was no standard for wireless charging of EVs. This hindered large-scale deployment of WPT technology within the automobile industry, as vehicle manufacturers saw it as risks to invest into non-market-ready technologies. Standards ensure a minimum quality of the charging system, safe operational conditions and allow comparison between multiple systems from different manufacturers. With the introduction of the SAE J2954-2016 'Wireless Power Transfer for Light-Duty Plug-In/ Electric Vehicles and Alignment Methodology' guideline in May 2016, a first attempt was made towards standardisation of WPT for EVs [29]. The usage of this guideline is not mandatory but provides a thorough overview of possible targets in a wide range of properties. Criteria mentioned in the guideline include interoperability, electromagnetic compatibility, minimum requirements on performance and safety, communication, as well as testing of charging systems for light-duty EVs.

Currently the guideline is limited to stationary charging systems within the three power levels of 3.3 kVA, 7.7 kVA, and 11.1 kVA. DWPT and stationary WPT with higher power levels for heavy-duty vehicles and buses will be part of future guidelines. It classifies multiple ground clearances between 100 and 250 mm as well as maximum misalignment tolerances a proposed system should comply with. The maximum lateral offset a system can transfer rated power at is ±100 mm, whereas the allowable longitudinal offset is ±75 mm. Additional performance parameters are shown in Table 4. Electromagnetic compatibility and EMI levels are defined as in the ICNIRP guideline presented in chapter 4. Furthermore, it outlines interoperability between different modules. The efficient coupling between any type of transmitting and receiving system, regardless of manufacturer and home/office applications, within a certain power class and ground clearance must be guaranteed. In addition, systems must be able to charge various battery systems for a whole range of EVs. On one hand, private systems, i.e. home chargers and garage chargers, can be surface mounted. On the other hand, publicly available systems and DWPT systems should be embedded in the road surface to allow safe operation and protect the systems from mechanical impacts. A feature that is not covered by the guideline is the bi-directional power transfer between EVs and grids.

Table 4 Proposed power classes and system performances [29]

Power Classes	Maximum input [kVA]	Minimum transfer efficiency [%]	Minimum transfer efficiency with offset [%]	Frequency [kHz]
WPT1	3.7	>85	>80	Nominal 85 Within range 81.38-90
WPT2	7.7	>85	>80	
WPT3	11.1	>85	>80	
WPT4	22	TBA	TBA	

At the beginning of 2017, the International Organization for Standardization (ISO) has published a Publicly Available Specification (PAS) in response to the increasing interest in WPT for EVs. ISO/PAS 19363:2017 'Electrically propelled road vehicles – Magnetic field wireless power transfer – Safety and interoperability requirements' defines criteria for safety requirements and initial classification of charging systems for light-duty vehicles and passenger vehicles [256]. It is structured in the same way as the SAE guideline. But due to the nature of the PAS, it is less detailed. Once technical experience with WPT for EV is acquired, the PAS will be converted into a fully operational and binding ISO standard. A list of key standards applicable for WPT systems for EV charging is summarised in Table 5.

Table 5 Important standards for WPT-systems

Standard	Description	Ref.
SAE J2954	Wireless Power Transfer for Light-Duty Plug-In/ Electric Vehicles and Alignment Methodology	[29]
SAE J2894/1	Power Quality Requirements for Plug-In Electric Vehicle Chargers	[257]
SAE J2847/6	Communication between Wireless Charged Vehicles and Wireless EV Chargers	[258]
SAE J2931/6	Signaling Communication for Wirelessly Charged Electric Vehicles	[259]
ICNIRP 2010	ICNIRP Guidelines for limiting exposure to time-varying electric and magnetic fields (1 Hz-100 kHz)	[223]
ISO 14117:2012	Active implantable medical devices – Electromagnetic compatibility – EMC test protocols for implantable cardiac pacemakers, implantable cardioverter defibrillators and cardiac resynchronization devices	[241]
ISO/PAS 19363:2017	Electrically propelled road vehicles – Magnetic field wireless power transfer – Safety and interoperability requirements	[256]
ISO 15118	Road vehicles – Vehicle to grid communication interface	[260]
IEC 61980-1	Electric vehicle wireless power transfer (WPT) systems – Part 1: General requirements	[261]

6 Grid impact of WPT

With the potential large-scale deployment of EVs, a new way to introduce renewable energy sources into our daily lives is possible. However, the change from conventional ICE relying on fossil fuels to EVs that use electricity as ‘fuel’ puts additional burden on the electricity networks. Due to the increasing number of EVs and the current lack of public charging infrastructure, most EV-user will charge their vehicles at home. EVs are active loads that, once connected to the grid, increase the demand on the grids. An increase in demand load influences the line voltage, network frequency, harmonic content, and losses of the distribution grids. By increasing the demand on a particular line, the network approaches its maximum load capability, which causes voltage drops and can ultimately lead to failures within the network. The same is true for the frequency and its effect on the network. Network operators coordinate the power distribution from large power stations towards consumers and try to mitigate negative impacts on the network. Even though, the additional load due to EV charging is somewhat deterministic. It is difficult to predict as the decision to charge an EV is based on the driving pattern of individual users, initial charge of the vehicle, and potential short-term charging. The mode of charging has an additional impact on the grid. Slow charging processes have a small impact on the grid as a small current is used to charge the vehicle. On the other hand, fast chargers use high currents, and have a bigger impact on the grid [262]. Conventionally, home systems use plug-in chargers, but stationary WPT systems are commercially available. Stationary WPT systems provide safer charging with the same grid impact compared to conventional plug-in chargers if they use the same charging power level. Most EV-users charge their vehicles at home, usually after work. This increases the already high demand during the evening peak. Current distribution networks are not capable of allowing large numbers of EV-chargers to draw power at the same time, especially during the peak hours [263]. Smart charging methods can reduce or prevent such impacts [264]. Shifting the charging process from evening to night can help reducing the impact by a significant margin, as the base demand during night-hours is very low, compared to peak hours. Therefore, the load on the grid network still follows the conventional two-peak curve, but the trough in the early morning hours is increased and the loading on each line is kept below the maximum loading [265]. Zhang *et al.* used the IEEE radial distribution network with 13 nodes and investigated the impact of shifting the charging process to the night-hours [266]. At 30 % EV penetration, the grid losses were reduced from 3.7 % to 3.1 %. Additionally, EVs provide frequency control and help regulating the network frequency [267]. The impact analysis shows positive results for a small network but relies on the installation of smart meters and the possibility to control the EVs directly. While smart meters gain popularity, a widespread deployment is yet to be achieved.

In comparison to conventional stationary (wireless) charging, DWPT systems introduce highly variable load profiles. Due to the nature of charging that depends on the vehicle speeds, the charging process consists of a series of very short (in the range of few to several milliseconds), high power charging pulses. This characteristic directly transfers to the electricity network, if no intermediate power storage is used. Currently there is a high demand for information on the grid impact of these systems, driving research in recent years [268], [269]. The impact of DWPT and fast stationary chargers on the distribution network in a Greek city has been investigated [270]. Two approaches for stationary charging were used: a conventional home charger at power levels of 3.6 kW or 11 kW, and a fast-inductive charger with a power level of 30 kW. Using real data from implemented fast chargers, the probability distribution of a charging event occurring within a one-hour period and its charging time was calculated. DWPT systems were used for emergency charging during the day, and the possibility of a charging event occurring on a DWPT system depends on the amount of EVs on the street and the probability of a charging event. A total of four scenarios were investigated and are outlined in Table 6.

Table 6 Scenarios for grid network impact analysis in [270]

Scenario	Charging at home	EVs using fast chargers	DWPT
A	0	0	No
B	1000	0	No
C-I	1000	100	No
C-II	1000	300	No
D-I	1000	100	Yes
D-II	1000	300	Yes

In scenario C-I, 6 additional fast chargers are required, whereas in C-II 19 chargers are used. The same number of stationary chargers is required for D-I and D-II, with an additional 68 and 61 dynamic chargers. The maximum number of operating chargers is determined based on the likelihood of a charging event and the number of vehicles currently on the roads. Figure 18 a) shows the power demand profiles of these different scenarios. An increase of approximately 28 % in evening peak demand is caused by the home charging of 1000 EVs. This additional demand is present in the rest of the scenarios. Using fast chargers increases the demand in the morning and mid-day hours, causing an increase of 10 % when 300 vehicles use the chargers. However, the impact of fast chargers on the evening peak is minor compared to the increase of the morning peak demand. Figure 18 b) depicts the demand increase due to DWPT systems. DWPT introduces high demands over the course of the day and creates an additional peak before the evening peak in scenario B, as these systems are used more frequently during the evening rush hours. This rush hour peak coincides with the beginning of home charging and both combined cause an increase of 44 % in a very short period of time between 18:45 and 19:00. While investigating the additional demand, the impact of the EV usage on the network frequency and voltage was not included.

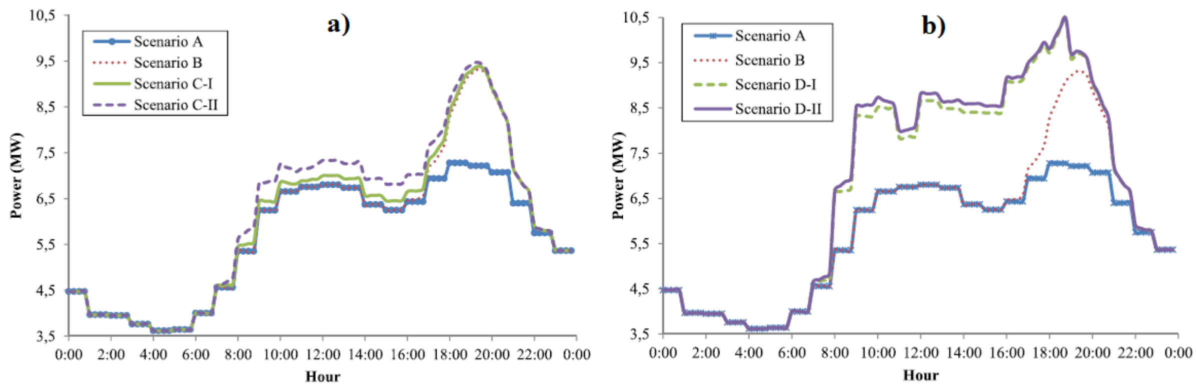

Figure 18 Demand power curves for different cases of EV penetration a) scenarios C-I and C-II, b) D-I and D-II [270]

Garcia-Vazquez *et al.* examined the effect of DWPT systems in Spain. Real traffic data from an 11.3 km long stretch along a highway with a speed limit of 100 km/h, a 75.3 km long motorway with a speed limit of 120 km/h and an urban road with a length of 2.4 km and a speed limit of 50 km/h were used [271]. The DWPT system comprised multiple transmitter pads of 8 m length and 5 m inter-pad spacing. Three transmitter pads are connected to one power source and form one segment of the DWPT system. Each segment can transfer up to 40 kW to a single EV. A Nissan Leaf is used with a 24 kWh Li-Ion battery. The vehicle uses regenerative braking and uses air conditioning (AC) for 94 % of the time its driving. It is assumed that 25 % of the vehicles driving on these roads are EVs. While driving at 100 km/h on the highway, the SoC of the battery increases by 1 %. Whereas, the SoC would decrease by up to 10 % without DWPT charging. The load profile shows morning and evening peaks depending on the direction the vehicles are travelling as illustrated in Figure 19 a). On the motorway, the DWPT system cannot increase the SoC of the battery, but still has a positive effect on the maximum driving distance. The annual average power drawn from the grid is shown in Figure 19 b). While driving in the urban area, the highest increase in SoC is realised with up to 12.7 %. This is due to the reduced speed of the vehicle and the longer charging times per pad. Without the DWPT system, the SoC would decrease by approximately 2 %. As shown in the previous study and Figure 19 c), the power demand profile within a city follows the daily demand curve.

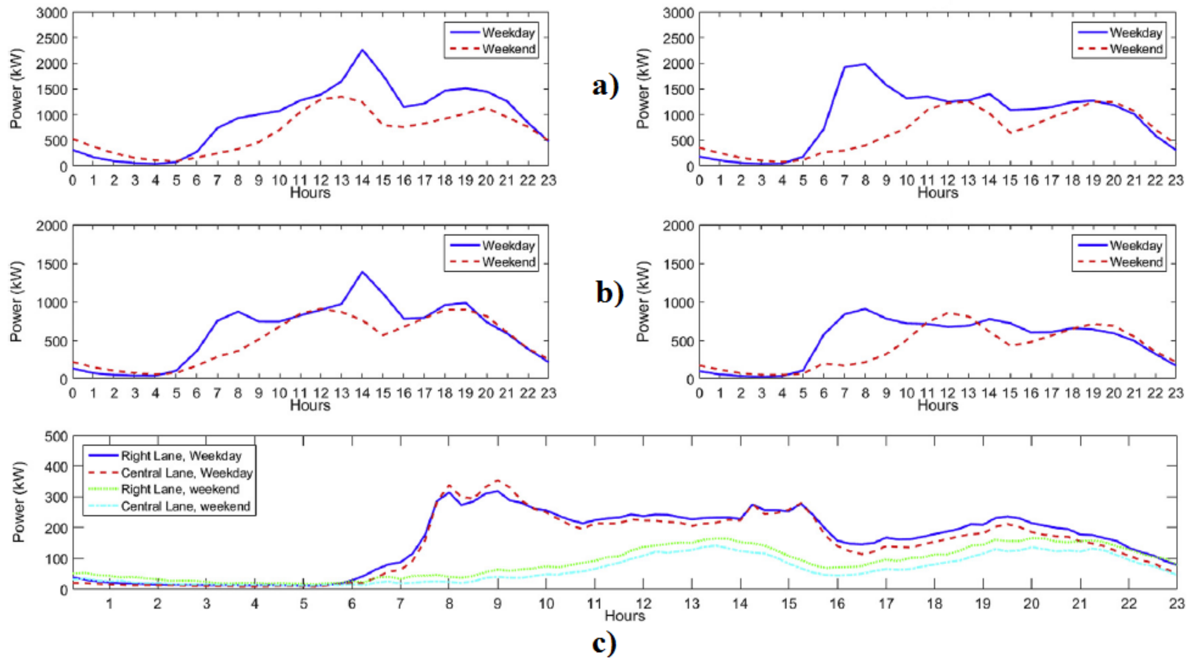

Figure 19 Annual average load profiles on DWPT-system during weekdays/ weekends for a) highways: right: from Cadiz, left: from San Fernando b) motorways: right: from Las Cabezas de San Juan, left: from Jerez and c) urban road [271]

It has been shown that any form of WPT-system puts an additional burden onto the electricity network. While stationary charging can be controlled in such a manner that there is no increase in peak demand, DWPT-system will most likely follow the daily demand curve.

7 Costs of WPT

As presented in chapter 3.4, commercial solutions are available for stationary WPT systems. Stationary wireless chargers are more expensive than conventional conductive chargers, as they include the cost of charging pads and inverters to produce the high-frequency coupling between transmitting and receiving coils. However, due to the novelty of dynamic wireless charging technology, the economic feasibility has not been fully investigated and the literature is scarce. Available literature and cost analysis mainly comes from research projects. Currently EVs are more expensive than conventional ICE-vehicles due to the large on-board battery packs. While using stationary wireless charging, the conventional plug-in charging system is substituted with a charging pad installed in the ground. Compared to a conventional charging system, this means that the vehicle battery pack must have the same size and capacity. One advantage of DWPT is that the vehicle can be charged while it is driving. Hence, the change in SoC of the battery pack while driving is reduced, and the total on-board battery capacity can be reduced [272], [273]. This leads to a significant reduction in initial cost of EVs [274], [275]. On the other hand, to support the reduced storage capacity DWPT systems need to be deployed at a large scale. However, construction and maintenance of the transmitter structure result in high capital costs. Recent global trends show that a large portion of driven mileage is located on a small number of roads, i.e. highways and motorways. For example, between 2016 and 2017, 65 % (212 billion miles) of the driven miles in the UK were located on 13 % (~32,000 miles) of the road length [276]. This means that much of the daily driven mileage can be covered by installing DWPT on these key roads. In general, the economic feasibility of a DWPT system depends on road coverage, power level, EV penetration rate, and battery size [277].

From the few DWPT systems built and tested so far, costs of some system components can be estimated. The third generation OLEV used a W-type transmitter rail to transmit 100 kW, and the system cost were 1.069M$/km [182]. In the following fourth generation (I-type rail), the total costs were reduced by about 21 % to 0.85M$/km. Shin *et al.* estimated the cost of the power supply system to be 0.235M$/km [278]. Based on these costs, multiple case studies have investigated the economic feasibility of DWPT. Shekhar *et al.* used a set of linear equations to estimate the SoC of an on-board battery pack depending on the mass, frontal area, auxiliary power demand of a vehicle, and road coverage and charging power level of a DWPT-system [279]. With the aid of this model, a case study based on a bus service in North Holland was investigated. The bus service included 25 buses, five of which were kept as redundancy. Each bus was equipped with a 500 kWh battery pack and was expected to drive 400 km/day, split into ten 40 km long services with six minute breaks. Along the service, there were 24 stops of 20 s each. The Urban Dynamometer Driving Schedule (UDDS) standard driving cycle was utilised and a climate model predicted the auxiliary power consumption of each bus to be 25 kW. Under these conditions the SoC dropped to 68.66 % after the first 40 km. The required SoC of the on-board battery to achieve a total of 400 km was calculated to be 87 %. A combination of stationary charging and dynamic charging was used to remove the discrepancy between actual and required SoC. Figure 20 depicts the variation in the final SoC and achievable driving range of the bus depending on the stationary charging power on each stop. The SoC can be increased to 77.7 % when a 200 kW stationary system is used. As this is still below the required SoC, an additional DWPT system must be deployed.

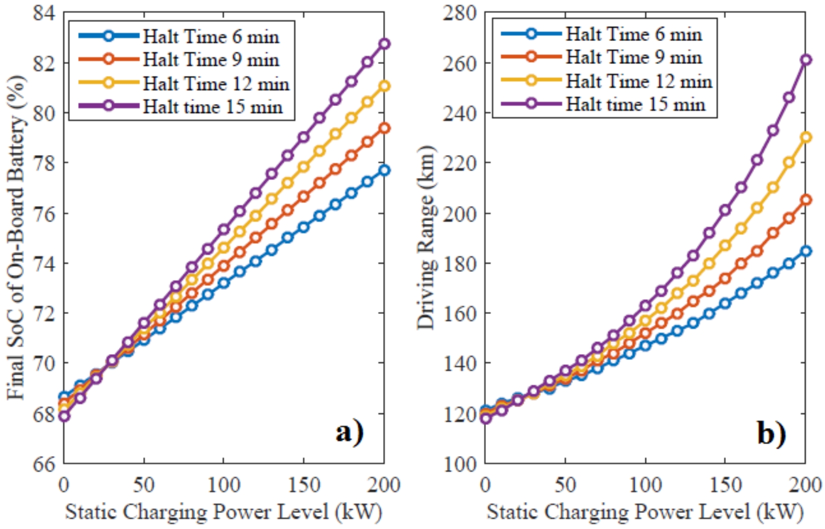

Figure 20 a) SoC and b) achievable driving range variation depending on stationary wireless charging power [279]

The required length of transmitter coils and therefore the cost of the DWPT system depends on the charging power level of the system. As shown in Figure 21, the required road coverage decreases with increasing power level. This is because a higher amount of power can be transferred in a shorter time period, which therefore means that less road needs to be covered by the charging system. On one hand, the system cost of the charger increases with increasing power level. On the other hand, as the construction and infrastructure cost are very high, a reduction in road coverage can lower the total cost. An urban environment with low vehicle speeds and frequent stops was assumed for this study. The effect of other driving cycles e.g. Highway Fuel Economy Test (HWFET) or hybrid cycles with higher speeds intermitted by stops was not investigated.

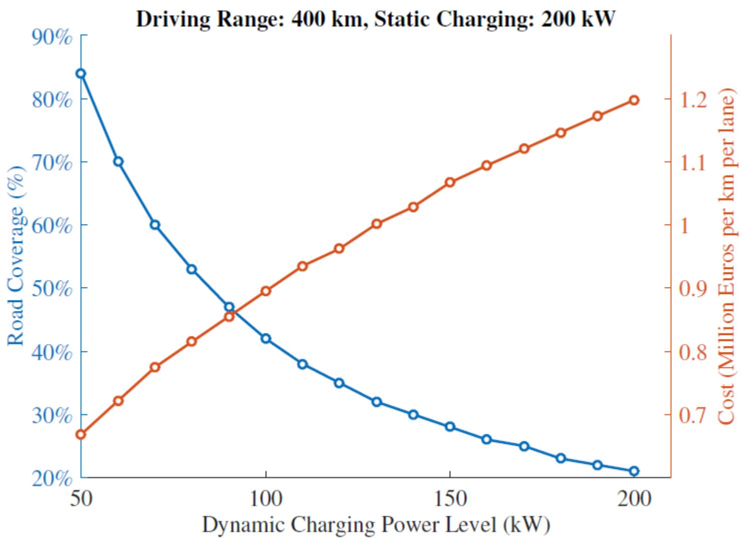

Figure 21 Cost estimates and road coverage for various DWPT power levels [279]

Currently there are two OLEV buses in use within the public transport system of Gumi City. The buses are powered via DWPT and travel about 34.5 km per service. To date the buses use a 100 kWh battery pack and the authors in [280] have investigated the economic impact of DWPT compared to stationary charging in terms of how much the battery capacity can be reduced, when DWPT is used. An economic model is built, based on the SoC of the battery pack and the real driving cycle of the buses. The model evaluates the cost of the charging system when 18 buses with 50 kWh battery packs are running on the route. It would require seven charging pads with a maximum length of 372 m and a charging power level of 80 kW to maintain a SoC above 50 %. Figure 22 shows the total cost of the

DWPT system over a ten-year period. The total cost of the DWPT system is approximately 20 % lower than the system cost of a stationary charging system. Due to the lack of charging possibilities for the stationary charging system a higher on-board battery capacity is required. In this case study, the battery capacity is assumed to be 100 kWh. After the battery has reached the end of its life, it must be replaced. By employing DWPT and reducing the battery capacity, the life of the battery can be extended as the depth of discharge is limited and shallow charge-discharge cycles are used [281]. In future research, the authors will focus on including a stochastic approach to the driving cycle including traffic and driving uncertainties. Bi *et al.* conducted a life cycle cost assessment between ICE-, plug-in, hybrid, and wirelessly charged busses [282]. The wireless system has the lowest cumulative cost over its lifetime, confirming previous findings. Key uncertainties influencing the total cost of wireless charging are battery price, price of electricity and installation cost of charging pads.

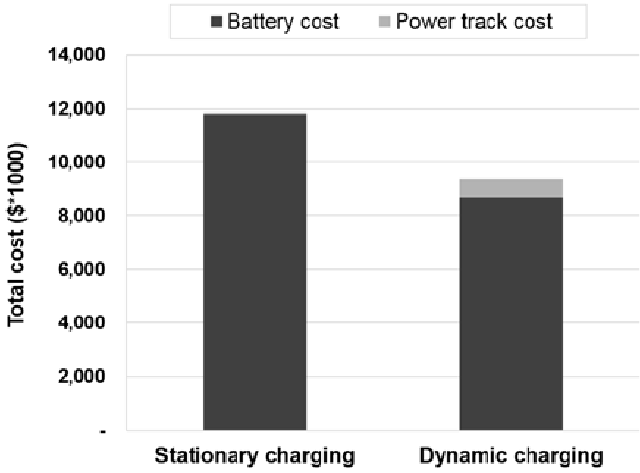

Figure 22 Total cost comparison over 10 years between stationary and dynamic charging systems [280]

Battery swapping and DWPT targets a similar market, i.e. electric taxis [283]. Chen *et al.* conducted a cost-competitiveness analysis of dynamic charging lanes, charging stations and battery swapping stations [284]. An empirical analysis using real world data from a bus rapid transit corridor in Los Angeles, USA was used to evaluate the total cost of each infrastructure. The transit corridor is 35.2 miles long, with a service frequency of 16 busses per hour and an average vehicle speed of 19.9 mph. Battery swapping stations are the most cost competitive, followed by the dynamic charging lane. DWPT has the highest infrastructure cost but the lowest fleet cost. As there is no recharging delay for DWPT, busses do not experience any downtime and less busses are required. In comparison, battery swapping has better balanced costs. While additional batteries are required, the infrastructure cost is lower due to smaller construction space. Furthermore, swapping batteries only introduces little downtime to the service. The same design model is used for a large number of transit corridors from all over the world and the majority of the proposed infrastructures are DWPT systems. Driving distance, vehicle speed and service frequency are the key factors determining the cost competitiveness. High service frequency and low vehicle speeds favour DWPT due to reduced specific infrastructure cost. While high vehicle speeds, medium driving distance, and service frequency aid battery swapping stations.

Another important factor that affects the feasibility of DWPT systems is the EV fleet penetration. Limb *et al.* and Quinn *et al.* investigated the societal payback time for two different DWPT systems and their large-scale deployment on primary and secondary roads in the USA [285], [286], [287]. Societal payback time is the time required for savings associated with WPT-EV usage to break even with the initial deployment cost of the charging infrastructure. Vehicles drive following the Highway Fuel Economy Test (HWFET) when they use motorways and UDDS for urban roadways. As a large portion of total mileage is being driven on a fraction of the roads, a total of 83.5 % of the motorways and 2.6 % of the urban roadways need to be covered with 25 kW charging pads to maintain the SoC. Figure 23 depicts the societal payback time for a deployment cost of 2.4 M$/(mile*lane) and an electricity price of 0.127 \$/kWh. Battery replacement cost is not considered, and the maintenance cost of DWPT system is assumed to be similar to conventional road maintenance cost.

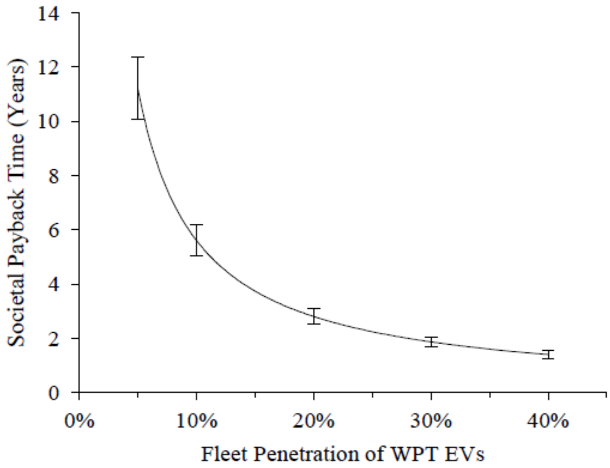

Figure 23 Societal payback time for different fleet penetrations [286]

Fuller *et al.* estimated the cost for installing 626 miles of roadways in California with 40 kW DWPT system to be \$2.5 billion [288]. This would be sufficient to allow a 200-mile EV to reach destinations within California on a single battery charge. Aiming at a payback time of 20 years, with a total number of EVs of 300,000, the costs per vehicle and year would be \$512. An increase to 1 million EVs would further reduce the costs to \$168 a year per vehicle. Moreover, DWPT would still be more cost effective for extending driving range than increasing the battery capacity even at very competitive battery prices of \$100 per kWh. It has been demonstrated that WPT and particularly DWPT systems require a large upfront investment due to high construction and instalment costs. However, the costs across the society are comparably small and can be further reduced by a higher adoption of EVs. The cost-effectiveness of DWPT depends greatly on multiple factors and therefore has significant uncertainties associated with it. However, the fast development and recent improvements can drastically reduce these. Furthermore, conductive chargers have been in mass production for an extended period, whereas WPT is at the beginning of its market readiness. Mass production will positively affect the cost of WPT-technology.

8 Conclusion

This paper presents an in-depth review of the key topics related to WPT systems for EV charging. It gives an overview of the components used in WPT systems and the major research interests and findings within each component. The coil structure and compensation topology are the most studied parts within a wireless charging system and research focusses on transfer efficiency, misalignment tolerance, and component stress. While copper is conventionally used as coil material, new materials like HTS with advantageous properties are proposed. However, HTS coils introduce additional design criteria for cooling below its critical temperature. Auxiliary topics such as communication and foreign object detection are reviewed. While stationary charging can draw on communication technologies from conventional plug-in chargers, DWPT systems cannot employ these technologies. DSRC communication is a viable way of allowing wireless communication between GA and VA in a dynamic environment. A summary of key research institutes and their contributions towards commercial WPT for EV applications is given. KAIST is driving research on DWPT and OLEV buses are currently operating under real world conditions. As EVs are a key pillar of the transition towards a clean and low-carbon society, it is necessary to present that WPT charging has no negative impact on its users and surroundings. All currently used WPT systems have electromagnetic emissions below the limits determined by ICNIRP. Tougher limits have been introduced for vehicular applications to protect AIMD user. Since 2016, a voluntary guideline for design and testing of EV WPT chargers has been in circulation and a PAC has formed the beginning of a binding standard for stationary chargers. Further standards covering dynamic wireless charging will be added. While shifting towards electricity 'fuelled' vehicles brings the advantage of reducing the CO_2 emissions at the application, its effect on the distribution network needs to be addressed. Stationary wireless chargers have a similar impact on the network as conventional conductive chargers, with demand peaks in the evening. They also provide the option to shift demand to avoid peak hours. On the other hand, the demand of dynamic chargers follows the conventional daily load profile. Wireless charging requires substantial upfront investment into the infrastructure. However, due to the novelty of the technology, the economic feasibility of such a system is difficult to evaluate and is mostly based on KAIST's commercial site. Research on WPT for EVs is becoming increasingly popular, resulting in a rapidly growing community of academia and industry. To achieve market readiness, several challenges have to be overcome, while exploring potential prospects. Table 7 summarises challenges and opportunities of WPT-charging for EVs.

Table 7 Summary of challenges and opportunities of WPT-technology for EV charging

Challenges	Opportunities
Misalignment tolerance of the charger	Application for HTS and other new materials
Timing of power transfer at high speed	Range and battery life extension of current EVs
Charging multiple vehicles per transmitter	Driverless vehicles
Lifespan of charger, durability under real conditions	Energy storage for renewable energy sources
Grid impact	Frequency control at grid connection
Expensive infrastructure & large-scale deployment	Cost reduction of EVs
Interoperability between multiple manufacturers	Environmental benefits if electricity is renewable
Policies for WPT introduction	
Fast charging	
Universal standards	

Appendix A

Table A-1: Total impedance, power transfer efficiency, primary and secondary capacitance of SS, SP, PS, PP topology [54], [56], [57], [58]

Comp. topology	Total impedance Z_{tot}	Power transfer efficiency at resonance η	Primary Capacitance C_1
SS	$R_1 + j\left(L_1\omega - \frac{1}{C_1\omega}\right) + \frac{(\omega M)^2}{\left(R_2 + R_{\mathrm{L}} + j\left(L_2\omega - \frac{1}{C_2\omega}\right)\right)}$	$\frac{R_{\mathrm{L}}}{R_2 + R_{\mathrm{L}} + R_1\left(\frac{R_2 + R_{\mathrm{L}}}{\omega M}\right)^2}$	$\frac{L_2 C_2}{L_1}$
SP	$R_1 + j\left(L_1\omega + \frac{1}{C_1\omega}\right) + \frac{(\omega M)^2}{\left(R_2 + jL_2\omega + \frac{R_{\mathrm{L}}}{1 + jR_{\mathrm{L}}C_2\omega}\right)}$	$\frac{R_{\mathrm{L}}}{R_2 + R_{\mathrm{L}} + \frac{R_2 {R_{\mathrm{L}}}^2}{(\omega L_2)^2} + \frac{R_1 {R_2}^2}{(\omega M)^2} + \frac{R_1\left(L_2\omega^2 + \frac{R_{\mathrm{L}}R_2}{\omega^2 L_2}\right)^2}{(\omega M)^2}}$	$\frac{{L_2}^2 C_2}{L_1 L_2 - M^2}$
PS	$\frac{1}{R_1 + j\omega(L_1 + C_1) + \frac{(\omega M)^2}{\left(R_2 + R_{\mathrm{L}} + j\left(L_2\omega - \frac{1}{C_2\omega}\right)\right)}}$	$\frac{R_{\mathrm{L}}}{R_2 + R_{\mathrm{L}} + R_1\left(\frac{R_2 + R_{\mathrm{L}}}{\omega M}\right)^2}$	$\frac{L_1 (C_2 L_2 R_L)^2}{M^4 + L_1 L_2 {R_L}^2}$
PP	$\frac{1}{\frac{1}{R_1 + jL_1\omega + \frac{(\omega M)^2(1 + jR_{\mathrm{L}}C_2\omega)}{\left(R_{\mathrm{L}} + (R_2 + jL_2\omega)(1 + jR_{\mathrm{L}}C_2\omega)\right)}} + jC_1\omega}$	$\frac{R_{\mathrm{L}}}{R_2 + R_{\mathrm{L}} + \frac{R_2 {R_{\mathrm{L}}}^2}{(\omega L_2)^2} + \frac{R_1 {R_2}^2}{(\omega M)^2} + \frac{R_1\left(L_2\omega^2 + \frac{R_{\mathrm{L}}R_2}{\omega^2 L_2}\right)^2}{(\omega M)^2}}$	$\frac{{L_2}^2 (L_1 L_2 - M^2) C_2}{(L_1 L_2 - M^2)^2 + M^4 {R_L}^2 L_2 C_2}$

Bibliography

[1] International Energy Agency (IEA), "Global Energy & CO2 Status Report 2017," IEA, 2018.

[2] BP, "BP Energy Outlook 2017," 2017. [Online]. Available: https://www.bp.com/content/dam/bp/pdf/energy-economics/energy-outlook-2017/bp-energy-outlook-2017.pdf. [Accessed 14 March 2018].

[3] N. Adnan, S. M. Nordin, I. Rahman, P. Vasant and M. A. Noor, “An overview of electric vehicle technology: a vision towards sustainable transportation”, Intelligent Transportation and Planning: Breakthroughs in Research and Practice, 2018.

[4] S. Sachan and N. Adnan, “Stochastic charging of electric vehicles in smart power distribution grids”, Sustainable Cities and Society, Vol. 40, pp. 91-100, 2018.

[5] N. Adnan, S. M. Nordin and O. Althawadi, “Barriers towards widespread adoption of V2G technology in smart grid environment: from laboratories to commercialization”, Sustainable Interdependent Networks, pp. 121-134, 2018.

[6] N. Tesla, "Apparatus for Transmitting Electrical Energy". New York, USA Patent 1119732, 1914.

[7] A. Kurs, A. Karalis, R. Moffatt, J. Joannopoulos, P. Fisher and M. Soljacic, "Wireless Power Transfer via Strongly Coupled Magnetic Resonances," *Science*, vol. 317, no. 5834, pp. 83-86, 2007.

[8] B. Regensburger, S. sinha, A. Kumar, J. Vance, Z. Popovic and K. K. Afridi, "Kilowatt-Scale Large Air-Gap Multi-Modular Capacitive Wireless Power Transfer System for Electric Vehicle Charging," in *IEEE Applied Power Electronics Conference and Exposition (APEC)*, San Antonio, USA, 2018.

[9] M. Kline, I. Izyumin, B. Boser and S. Sanders, "Capacitive Power Transfer for Contactless Charging," in *Twenty-Sixth Annual IEEE Applied Power Electronics Conference and Exposition (APEC)*, Forth Worth, USA, 2011.

[10] J. Dai and D. C. Ludois, "A Survey of Wireless Power Transfer and a Critical Comparison of Inductive and Capacitive Coupling for Small Gap Application," *IEEE Transactions on Power Electronics*, vol. 30, no. 11, pp. 6017-6029, 2015.

[11] J. Kim, H.-c. Son, D.-h. Kim and Y.-j. Park, "Optimal Design of a Wireless Power Transfer System with Multiple Self-Resonators for an LED TV," *IEEE Transactions on Consumer Electronics*, vol. 58, no. 3, pp. 775-780, 2012.

[12] J. Moon, H. Hwang, B. Jo, C.-K. Kwon, T.-G. Kim and S.-W. Kim, "Design and Implementation of a high-efficiency 6.78MHz resonant wireless power transfer system with a 5W fully integrated power receiver," *IET Power Electronics*, vol. 10, no. 5, pp. 577-578, 2017.

[13] V. Esteve, J. Jordán, E. Sanchis-Kilders, E. J. Dede, E. Maset, J. B. Ejea and A. Ferreres, "Comparative Study of a Single Inverter Bridge for Dual-Frequency Induction Heating Using Si and SiC MOSFETs," *IEEE Transactions on Industrial Electronics*, vol. 62, no. 3, pp. 1440-1450, 2015.

[14] J. Martis and P. Vorel, "Apparatus for Induction Heating 2.5kW Using a Series Resonant Circuit," in *Proceedings of the 16th International Conference on Mechatronics - Mechatronika*, Brno, Czech Republic, 2014.

[15] K. Agrawal, R. Jegadeesan, Y.-X. Guo and N. V. Thakor, "Wireless Power Transfer Strategies for Implantable Bioelectronics: Methodological Review," *IEEE Reviews in Biomedical Engineering*, vol. 10, pp. 1-28, 2017.

[16] V. B. Gore and D. H. Gawali, "Wireless Power Transfer Technology for Medical Applications," in *Conference on Advances in Signal Processing (CASP)*, Pune, India, 2016.

[17] T. Sun, X. Xie and Z. Wang, Wireless Power Transfer for Medical Microsystems, First ed.,

New York, USA: Springer, 2013.

[18] D.-B. Lin, T.-H. Wang and F.-J. Chen, "Wireless Power Transfer via RFID Technology for Wearable Device Applications," in *International Microwave Workshop Series on RF and Wireless Technologies for Biomedical and Healthcare Applications (IMWS-BIO)*, Taipei, Taiwan, 2015.

[19] K. Finkenzeller, RFID Handbook - Fundamentals and Applications in Contactless Smart Cards, Radio Frequency Identification and Near-Field Communication, Third ed., Chichester, United Kingdom: Wiley, 2010.

[20] R. W. Porto, V. J. Brusamarello, I. Müller, F. L. Cabrera Riaño and F. R. De Sousa, "Wireless Power Transfer for Contactless Instrumentation and Measurement," *IEEE Instrumentation & Measurement Magazine*, vol. 20, no. 4, pp. 49-54, 2017.

[21] R. Trevisan and A. Costanzo, "A UHF Near-Field Link for Passive Sensing in Industrial Wireless Power Transfer Systems," *IEEE Transactions on Microwave Theory and Techniques*, vol. 64, no. 5, pp. 1634-1643, 2016.

[22] M. Sugino and T. Masamura, "The wireless power transfer systems using the Class E push-pull inverter for industrial robots," in *IEEE Wireless Power Transfer Conference (WPTC)*, Taipei, Taiwan, 2017.

[23] S. Chopra and P. Bauer, "Driving Range Extension of EV With On-Road Contactless Power Transfer-A Case Study," *IEEE Transactions on Industrial Electronics*, vol. 60, no. 1, pp. 329-338, 2013.

[24] S. Li and C. C. Mi, "Wireless Power Transfer for Electric Vehicle Applications," *Journal of Emerging and Selected Topics in Power Electronics*, vol. 3, no. 1, pp. 4-17, 2015.

[25] R. Vaka and R. K. Keshri, "Review on Contactless Power Transfer for Electric Vehicle Charging," *Energies*, vol. 10, no. 636, 2017.

[26] K. A. Kalwar, M. Aamir and S. Mekhilef, "Inductively coupled power transfer (ICPT) for electric vehicle charging - A review," *Renewable and Sustainable Energy Reviews*, vol. 47, pp. 462-475, 2015.

[27] A. Ahmad, M. S. Alam and R. Chabaan, "A Comprehensive Review of Wireless Charging Technologies for Electric Vehicles," *IEEE Transactions on Transportation Electrification*, vol. 4, no. 1, pp. 38-63, 2018.

[28] D. Patil, M. K. Mcdonough, J. M. Miller, B. Fahimi and P. T. Balsara, "Wireless Power Transfer for Vehicular Applications: Overview and Challenges," *IEEE Transactions on Transportation Electrification*, vol. 4, no. 1, pp. 3-37, 2018.

[29] Society of Automotive Engineers (SAE), "J2954 - Wireless Power Transfer for Light-Duty Plug-In/ Electric Vehicles and Alignment Methodology," SAE international, Warrendale, USA, 2016.

[30] H. L. Li, P. A. Hu and G. Covic, "A High Frequency AC-AC Converter for Inductive Power Transfer (IPT) Applications," in *Wireless Power Transfer - Principles and Engineering Explorations*, K. Y. Kim, Ed., InTech, 2012, pp. 253-272.

[31] M. Petersen and F. W. Fuchs, "Development of a 5 kW Inductive Power Transfer System Including Control Strategy for Electric Vehicles," in *International Exhibition and Conference for Power Electronics, Intelligent Motion, Renewable Energy and Energy Management*, Nuremberg, Germany, 2014.

[32] A. Pevere, R. Petrella, C. C. Mi and S. Zhou, "Design of a high efficiency 22 kW wireless power transfer system for EVs fast contactless charging stations," in *IEEE International Electric Vehicle Conference (IEVC)*, Florence, Italy, 2014.

[33] D. Vilathgamuwa and J. Sampath, "Wireless Power Transfer (WPT) for Electric Vehicles (EVs) - Present and Future Trends," in *Plug In Electric Vehicles in Smart Grids - Integration Techniques*, S. Rajakaruna, A. Gosh and F. Shahnia, Eds., Singapore, Springer Science+Business Media Singapore, 2015, pp. 33-61.

[34] A. Triviño, J. González-González and J. Aguado, "Evaluation of Losses in a Bidrectional Wireless Power Transfer System for Electric Vehicles," in *IEEE International Conference on Environment and Electrical Engineering and IEEE Industrial and Commercial Power Systems Europe (EEEIC / I&CPS Europe)*, Milan, Italy, 2017.

[35] B. Singh, B. N. Singh, A. Chandra, K. Al-Haddad, A. Pandey and D. P. Kothari, "A Review of Single-Phase Improved Power Quality AC-DC Converter," *IEEE Transactions on Industrial Electronics*, vol. 50, no. 5, pp. 962-981, 2003.

[36] E. Ciprioano dos Santos, C. Brandao Jacobina, E. R. Cabral da Silva and N. Rocha, "Single-Phase to Three-Phase Power Converters: State of the Art," *IEEE Transactions on Power Electronics*, vol. 27, no. 5, pp. 2437-2452, 2012.

[37] B. Singh, B. N. Singh, A. Chandra, K. Al-Haddad, A. Pandey and D. P. Kothari, "A Review of Three-Phase Improved Power QUality AC-DC Converter," *IEEE Transactions on Industrial Electronics*, vol. 51, no. 3, pp. 641-660, 2004.

[38] P. Raval, D. Kacprzak and A. P. Hu, "Technology Overview and Concept of Wireless Charging Systems," in *Wireless Power Transfer*, J. I. Agbinya, A. Jamalipour, M. Ruggeri and H. Nikookar, Eds., Aalborg, Denmark, River Publishers, 2016, pp. 347-384.

[39] P. Ning, J. M. Miller, O. C. Onar and C. P. White, “A Compact Wireless Charging System for Electric Vehicles,” in *IEEE Energy Conversion Congress and Exposition*, Denver, USA, 2013.

[40] S. Rosu, M. Khallian, V. Cirimele and P. Guglielmi, "A Dynamic Wireless Charging System for Electric Vehicles Based on DC/AC Converters with SiC MOSFET-IGBT Switches and Resonant Gate-Drive," in *Annual Conference of the IEEE Industrial Electronics Society (IECON)*, Florence, Italy, 2016.

[41] K. F. Hoffmann and J. P. Kärst, "High Frequency Power Switch - Improved Performance by MOSFETs and IGBTs Connected in Parallel," in *European Conference on Power Electronics and Applications*, Dresden, Germany, 2005.

[42] S. Zhang, U. K. Madawala, D. J. Thrimawithana and B. S. Riar, "A Model for a Three-phase Modular Multi-level Converter based on Inductive Power Transfer Technology (M2LC-IPT)," in *IEEE 2nd International Future Energy Electronics Conference (IFEEC)*, Taipei, Taiwan, 2015.

[43] D. Baros, K. Bampouras, P. Apostolidou, E. Ioannou and N. Papanikolaou, "Multilevel Inverters for Motor Drives and Wireless Power Transfer Applications," in *Panhellenic Conference on Electronics and Telecommunications (PACET)*, Xanthi, Greece, 2017.

[44] E. Asa, K. Colak, M. Bojarski and D. Czarkowski, "A Novel Multi-Level Phase-Controlled Resonant Inverter with Common Mode Capacitor for Wireless EV Chargers," in *IEEE Transportation Electrification Conference and Expo (ITEC)*, Dearborn, USA, 2015.

[45] M. Malinowski, K. Gopakumar, J. Rodriguez and M. A. Perez, "A Survey on Cascaded Multilevel Inverters," *IEEE Transactions on Industrial Electronics*, vol. 57, no. 7, pp. 2197-2206, 2010.

[46] B. X. Nguyen, D. Vilathgamuwa, G. Foo, A. Ong, P. K. Sampath and U. K. Madawala, "Cascaded Multilevel Converter based Bidirectional Inductive Power Transfer (BIPT) System," in *International Power Electronics Conference*, Hiroshima, Japan, 2014.

[47] B. X. Nguyen, D. M. Vilathgamuwa, G. Foo, P. Wang and A. Ong, "A Modified Cascaded Multilevel Converter Topology for High Power Bidirectional Inductive Power Transfer Systems With The Reduction Of Switching Devices and Power Losses," in *IEEE 11th International Conference on Power Electronics and Drive Systems*, Sydney, Australia, 2015.

[48] X. B. Nguyen, D. M. Vilathgamuwa and U. K. Madawala, "A SiC-Based Matrix Converter Topology for Inductive Power Transfer System," *IEEE Transactions on Power Electronics*, vol. 29, no. 8, pp. 4029-4038, 2014.

[49] A. Ecklebe and A. Lindemann, "Bi-directional Switch Commutation for a Resonant Matrix Converter supplying a Contactless Energy Transmission System," in *Power Conversion Conference*, Nagoya, Japan, 2007.

[50] B. S. Riar, U. K. Madawala and D. J. Thrimawithana, "Analysis and Control of a Three-Phase Modular Multi-level Converter based on Inductive Power Transfer Technology (M2LC-IPT)," in *IEEE International Conference on Industrial Technology (ICIT)*, Cape Town, South Africa, 2013.

[51] S. Ruddell, U. K. Madawala, D. J. Thrimawithana and M. Neuburger, "A Novel Wireless Converter Topology for Dynamic EV Charging," in *IEEE Transportation Electrification Conference and Expo (ITEC)*, Dearborn, USA, 2016.

[52] S. M. Lukic, J. Cao, R. C. Bansal, F. Rodriguez and A. Emadi, "Energy Storage Systems for Automotive Applications," *IEEE Transactions on Industrial Electronics,* vol. 55, no. 6, pp. 2258-2267, 2008.

[53] M. Moghaddami and A. I. Sarwat, "Single-Phase Soft-Switched AC-AC Matrix Converter With Power Controller for Bidirectional Inductive Power Transfer Systems," *IEEE Transactions on Industry Applications,* vol. 54, no. 4, pp. 3760-3770, 2018.

[54] H. N. Nguyen, C. Zhang and J. Zhang, "Dynamic Demand Control of Electric Vehicles to Support Power Grid With High Penetration Level of Renewable Energy," *IEEE Transactions on Transportation Electrification,* vol. 2, no. 1, pp. 66-75, 2016.

[55] H. N. Nguyen, C. Zhang and M. A. Mahmud, "Optimal Coordination of G2V and V2G to Support Power Grids With High Penetration of Renewable Energy," *IEEE Transactions on Transportation Electrification,* vol. 1, no. 2, pp. 188-195, 2015.

[56] W. Zhang and C. C. Mi, "Compensation Topologies of High-Power Wireless Power Transfer Systems," *IEEE Transactions on Vehicular Technology,* vol. 65, no. 6, pp. 4768-4778, 2016.

[57] C.-S. Wang, G. A. Covic and O. H. Stielau, "Power Transfer Capability and Bifurcation Phenomena of Loosely Coupled Inductive Power Transfer Systems," *IEEE Transactions on Industrial Electronics,* vol. 51, no. 1, pp. 148-157, 2004.

[58] C.-S. Wang, O. H. Stielau and G. A. Covic, "Design Considerations for a Contactless Electric Vehicle Battery Charger," *IEEE Transactions on Industrial Electronics,* vol. 52, no. 5, pp. 1308-1314, 2005.

[59] S. Chopra and P. Bauer, "Analysis and Design Considerations for a Contactless Power Transfer System," in *IEEE 33rd International Telecommunications Energy Conference (INTELEC),* Amsterdam, Netherlands, 2011.

[60] J. L. Villa, J. Sallan, J. F. S. Osorio and A. Llombart , "High-Misalignment Tolerant Compensation Topology For ICPT System," *IEEE Transactions on Industrial Electronics,* vol. 59, no. 2, pp. 945-951, 2012.

[61] J. Sallán, J. L. Villa, A. Llombart and J. F. Sanz, "Optimal Design of ICPT Systems Applied to Electric Vehicle Battery Charge," *IEEE Transactions on Industrial Electronics,* vol. 56, no. 6, pp. 2140-2149, 2009.

[62] K. Aditya and S. S. Williamson, "Design Guidelines to Avoid Bifurcation in a Series-Series Compensated Inductive Power Transfer System," *IEEE Transactions on Industrial Electronics,* 2018.

[63] J. Hou, Q. Chen, S.-C. Wong, C. K. Tse and X. Ruan, "Analysis and Control of Series/Series-Parallel Compensated Resonant Converter for Contactless Power Transfer," *IEEE Journal of Emerging and Selected Topics in Power Electronics,* vol. 3, no. 1, pp. 124-136, 2015.

[64] W. Li, H. Zhao, S. Li, J. Deng, T. Kan and C. C. Mi, "Integrated LCC Compensation Topology for Wireless Charger in Electric and Plug-in Electric Vehicles," *IEEE Transactions on Industrial Electronics,* vol. 62, no. 7, pp. 4215-4225, 2015.

[65] S. Samanta and A. K. Rathore, "A New Current-Fed CLC Transmitter and LC Receiver Topology for Inductively Wireless Power Transfer Application: Analysis, Design, and Experimental Results," *IEEE Transactions on Transportation Electrification,* vol. 1, no. 4, pp. 357-368, 2015.

[66] N. A. Keeling, G. A. Covic and J. T. Boys, "A Unity-Power-Factor IPT Pickup for High-Power Applications," *IEEE Transactions on Industrial Electronics,* vol. 57, no. 2, pp. 744-751, 2010.

[67] C.-Y. Huang, J. T. Boys and G. A. Covic, "LCL Pickup Circulating Current Controller for Inductive Power Transfer Systems," *IEEE Transactions on Power Electronics*, vol. 28, no. 4, pp. 2081-2093, 2013.

[68] U. K. Madalawa and D. J. Thrimawithana, “A Bidirectional Inductive Power Interface for Electric Vehicles in V2G Systems,” *IEEE Transactions on Industrial Electronics,* vol. 58, no. 10, pp. 4789-4796, 2011.

[69] D. J. Thrimawithana, U. K. Madawala and M. Neath, "A Synchronization Technique for Bidirectional IPT Systems," *IEEE Transactions on Industrial Electronics,* vol. 60, no. 1, pp. 301-309, 2013.

[70] T. Campi, S. Criciani, F. Maradei and M. Feliziani, "Near-Field Reduction in a Wireless Power Transfer System Using LCC Compensation," *IEEE Transactions on Electromagnetic Compatibility,* vol. 59, no. 2, pp. 686-694, 2017.

[71] S. Li, W. Li, J. Deng, T. D. Nguyen and C. C. Mi, "A Double-Sided LCC Compensation Network and Its Tuning Method for Wireless Power Transfer," *IEEE Transactions on Vehicular Technology,* vol. 64, no. 6, pp. 2261-2273, 2015.

[72] T. Kan, T.-D. Nguyen, J. C. White, R. K. Malhan and C. C. Mi, "A New Integration Method for an Electric Vehicle Wireless Charging System Using LCC Compensation Topology: Analysis and Design," *IEEE Transactions on Power Electronics,* vol. 32, no. 2, pp. 1638-1650, 2017.

[73] T. Kan, F. Lu, T.-D. Nguyen, P. P. Mercier and C. C. Mi, "Integrated Coil Design for EV Wireless Charging Systems Using LCC Compensation Topology," *IEEE Transactions on Power Electronics,* vol. 33, no. 11, pp. 9231-9241, 2018.

[74] J. Deng, B. Pang, W. Shi and Z. Wang, "A new integration method with minized extra coupling effects using inductor and capacitor series-parallel compensation for wireless EV charger," *Applied Energy,* vol. 207, pp. 405-416, 2017.

[75] H. Feng, T. Cai, S. Duan, J. Zhao, X. Zhang and C. Chen, "An LCC-Compensated Resonant Converter Optimized for Robust Reaction to Large Coupling Variation in Dynamic Wireless Power Transfer," *IEEE Transactions on Industrial Electronics,* vol. 63, no. 10, pp. 6591-6601, 2016.

[76] W. Li, H. Zhao, J. Deng, S. Li and C. C. Mi, "Comparison Study on SS and Double-Sided LCC Compensation Topologies for EV/PHEV Wireless Chargers," *IEEE Transactions on Vehicular Technology,* vol. 65, no. 6, pp. 4429-4439, 2016.

[77] G. Zhu, D. Gao, S. Wang and S. Chen, "Misalignment Tolerance Improvement in Wireless Power Transfer Using LCC Compensation Topology," in *IEEE PELS Workshop on Emerging Technologies: Wireless Power Transfer (WoW),* Chongqing, China, 2017.

[78] C. Xia, R. Chen, Y. Liu, G. Chen and X. Wu, "LCL/LCC resonant topology of WPT system for constant current, stable frequency and high-quality power transmission," in *IEEE PELS Workshop on Emerging Technologies: Wireless Power Transfer (WoW),* Knoxville, USA, 2016.

[79] B. R. Long, J. M. Miller, A. Daga, P. C. Schrafel and J. Wolgemuth, "Which Way for Wireless Power: High Q or High K," in *IEEE PELS Workshop on Emerging Technologies: Wireless Power Transfer (WoW),* Knoxville, USA, 2016.

[80] J. M. Miller, P. C. Schrafel, B. R. Long and A. Daga, “The WPT dilemma - High k or high Q?,” in *IEEE PELS Workshop on Emerging Technologies: Wireless Power Transfer (WoW),* Knoxville, USA, 2016.

[81] R. Bosshard, J. Muehlethaler, J. Kolar and I. Stevanovic, “Optimized Magnetic Design for Inductive Power Transfer Coils,” in *Twenty-Eighth Annual IEEE Applied Power Electronics Conference and Exposition (APEC),* Long Beach, USA, 2013.

[82] R. Laouamer, M. Brunello, J. P. Ferieux, O. Normand and N. Buchheit, “A Multi-Resonant Converter for Non-Contact Charging with Electromagnetic Coupling,” in *23rd International Conference on Industrial Electronics, Control and Instrumentation (IECON),* New Orleans, USA, 1997.

[83] A. J. Moradewicz and M. P. Kazmierkowski, "Contactless Energy Transfer System With

FPGA-Controlled Resonant Converter," *IEEE Transactions on Industrial Electronics,* vol. 57, no. 9, pp. 3181-3190, 2010.

[84] J. Hirai, T.-W. Kim and A. Kawamura, "Study on Intelligent Battery Charging Using Inductive Transmission of Power and Information," *IEEE Transactions on Power Electronics,* vol. 15, no. 2, pp. 335-345, 2000.

[85] F. Nakao, Y. Matsuo, M. Kitaoka and H. Sakamoto, "Ferrite Core Couplers for Inductive Chargers," in *Proceedings of the Power Conversion Conference-Osaka 2002* , Osaka, Japan, 2002.

[86] M. Budhia, G. A. Covic and J. T. Boys, "Design and Optimization of Circular Magnetic Strucutres for Lumped Inductive Power Transfer Systems," *IEEE Transactions on Power Electronics,* vol. 26, no. 11, pp. 3096-3108, 2011.

[87] R. Bosshard, J. W. Kolar, J. Mühlethaler, I. Stevanovic, B. Wunsch and F. Canales, "Modeling and η-α-Pareto Optimization of Inductive Power Transfer Coils for Electric Vehicles," *IEEE Journal of Emerging and Selected Topics in Power Electronics,* vol. 3, no. 1, pp. 50-64, 2015.

[88] J. Han, Y. D. Kim and N.-H. Myung, "Efficient performance optimisation of wireless power transmission using genetic algorithm," *Electronics Letters,* vol. 50, no. 6, pp. 462-464, 2014.

[89] T. Yilmaz, N. Hasan, R. Zane and Z. Pantic, "Multi-Objective Optimization of Circular Magnetic Couplers for Wireless Power Transfer Applications," *IEEE Transactions on Magnetics,* vol. 53, no. 8, 2017.

[90] R. Bosshard and J. W. Kolar, "Multi-Objective Optimization of 50 kW/85 kHz IPT System for Public Transport," *IEEE Journal of Emerging and Selected Topics in Power Electronics,* vol. 4, no. 4, pp. 1370-1382, 2016.

[91] Z. Luo and X. Wei, "Analysis of Square and Circular Planar Spiral Coils in Wireless Power Transfer System for Electrical Vehicles," *IEEE Transactions on Industrial Electronics,* vol. 65, no. 1, pp. 331-341, 2018.

[92] W. Chen, C. Liu, C. H. Lee and Z. Shan, "Cost-Effectiveness Comparison of Coupler Designs of Wireless Power Transfer for Electric Vehicle Dynamic Charging," *Energies,* vol. 9, no. 906, 2016.

[93] M. Budhia, G. Covic and J. Boys, "A New IPT Magnetic Coupler for Electric Vehicle Charging Systems," in *36th Annual Conference on IEEE Industrial Electronics Society,* Glendale, USA, 2010.

[94] Y. Nagatsuka, N. Ehara, Y. Kaneko, S. Abe and T. Yasuda, "Compact Contactless Power Transfer System for Electric Vehicles," in *International Power Electronics Conference - ECCE ASIA* -, Hokkaido, Japan, 2010.

[95] M. Chigira, Y. Nagatsuka, Y. Kaneko, S. Abe, T. Yasuda and A. Suzuki, "Small-Size Light-Weight Transformer with New Core Structure for Contactless Electric Vehicle Power Transfer System," in *IEEE Energy Conversion Congress and Exposition,* Phoenix, USA, 2011.

[96] G. A. J. Elliott, S. Raabe, G. A. Covic and J. T. Boys, "Multiphase Pickups for Large Lateral Tolerance Contactless Power-Transfer Systems," *IEEE Transactions on Industrial Electronics,* vol. 57, no. 5, pp. 1590-1598, 2010.

[97] S. Raabe and G. A. Covic, "Practical Design Considerations for Contactless Power Transfer Quadrature Pick-Ups," *IEEE Transactions on Industrial Electronics,* vol. 60, no. 1, pp. 400-409, 2013.

[98] M. Budhia, G. A. Covic, J. T. Boys and C.-Y. Huang, "Development and evaluation of single sided flux couplers for contactless electric vehicle charging," in *IEEE Energy Conversion Congress and Exposition,* Phoenix, USA, 2011.

[99] M. Budhia, J. T. Boys, G. A. Covic and C.-Y. Huang, "Development of a Single-Sided Flux Magnetic Coupler for Electric Vehicle IPT Charging Systems," *IEEE Transactions on Industrial Electronics,* vol. 60, no. 1, pp. 318-328, 2013.

[100] G. A. Covic, M. L. G. Kissin, D. Kacprzak, N. Clausen and H. Hao, "A Bipolar Primary Pad

Topology for EV Stationary Charging and Highway Power by Inductive Coupling," in *IEEE Energy Conversion Congress and Exposition*, Phoenix, USA, 2011.

[101] A. Zaheer, D. Kacprzak and G. A. Covic, "A Bipolar Receiver Pad in a Lumped IPT System for Electric Vehicle Charging Applications," in *IEEE Energy Conversion Congress and Exposition (ECCE)*, Raleigh, USA, 2012.

[102] S. Kim, G. A. Covic and J. T. Boys, "Analysis on Tripolar Pad for Inductive Power Transfer Systems," in *IEEE PELS Workshop on Emerging Technologies: Wireless Power Transfer (WoW)*, Knoxville, USA, 2016.

[103] S. Kim, G. A. Covic and J. T. Boys, "Tripolar Pad for Inductive Power Transfer Systems for EV Charging," *IEEE Transactions on Power Electronics,* vol. 32, no. 7, pp. 5045-5057, 2017.

[104] M. M. Alam, S. Mekhilef, M. Seyedmahmoudian and B. Horan, “Dynamic Charging of Electric Vehicle with Negligible Power Transfer Fluctuation,” *Energies*, vol. 10, no. 701, 2017.

[105] R. Bosshard, U. Iruretagoyena and J. W. Kolar, "Comprehensive Evaluation of Rectangular and Double-D Coil Geometry for 50 kW/85kHz IPT System," *IEEE Journal of Emerging and Selected Topics in Power Electronics,* vol. 4, no. 4, pp. 1406-1415, 2016.

[106] Y. Liu, R. Mai, D. Liu, Y. Li and Z. He, "Efficiency Optimization for Wireless Dynamic Charging System With Overlapped DD Coil Arrays," *IEEE Transactions on Power Electronics,* vol. 33, no. 4, pp. 2832-2846, 2018.

[107] L. Xiang, X. Li, J. Tian and Y. Tian, "A Crossed DD Geometry and Its Double-Coil Excitation Method for Electric Vehicle Dynamic Wireless Charging Systems," *IEEE Access,* vol. 6, pp. 45120-45128, 2018.

[108] A. Zaheer, H. Hao, G. A. Covic and D. Kacprzak, "Investigation of Multiple Decoupled Coil Primary Pad Topologies in Lumped IPT Systems for Interoperable Electric Vehicle Charging," *IEEE Transactions on Power Electronics,* vol. 30, no. 4, pp. 1937-1955, 2015.

[109] S. Kim, A. Zaheer, G. Covic and J. Boys, "Tripolar Pad for Inductive Power Transfer System," in *40th Annual Conference of the IEEE Industrial Electronics Society,* Dallas, USA, 2014.

[110] S. Kim, G. A. Covic and J. T. Boys , "Comparison of Tripolar and Circular Pads for IPT Charging Systems," *IEEE Transactions on Power Electronics,* vol. 33, no. 7, pp. 6093-6103, 2018.

[111] D. H. Tran, V. B. Vu and W. Choi, "Design of a High-Efficiency Wireless Power Transfer System WIth Intermediate Coils for the On-Board Chargers of Electric Vehicles," *IEEE Transactions on Power Electronics,* vol. 33, no. 1, pp. 175-187, 2018.

[112] R. J. Sedwick, "Long range inductive power transfer with superconducting oscillators," *Annals of Physics,* vol. 325, no. 2, pp. 287-299, 2010.

[113] K. Kails, Q. Li and M. Mueller, “Novel model of stator design to reduce the mass of superconductor generators”, Superconductor Science and Technology, Vol. 31, 055009, 2018.

[114] T. Nishimura, T. Nakamura, Q. Li, N. Amemiya, and Y. Itoh, “Potential for Torque Density Maximization of HTS Induction/Synchronous Motor by Use of Superconducting Reluctance Torque”, *IEEE Transactions on Applied Superconductivity*, Vol. 24, No. 3, 5200504, 2014.

[115] D. Lee, H.-C. Jo and S.-K. Joo, "Economic Evaluation Method for Fault Current Limiting Superconducting Cables Considering Network Congestion in a Power System," *IEEE Transactions on Applied Superconductivity*, vol. 26, no. 4, 2016.

[116] Z. Wei, Y. Xin, J. Jin and Q. Li, “Optimized Design of Coil and Iron Cores for a Saturated Iron Core Superconducting Fault current Limiter”, *IEEE Transactions on Applied Superconductivity*, Vol. 26, No. 7, 5603904, 2016.

[117] Y. He, Y. Wang, X. Nie, W. Chen and Z. Yan, "High-Temperature Superconducting Capacitor and Its Application to a Superconducting Wireless Power Transfer System," *IEEE Transactions on Applied Superconductivity,* vol. 29, no. 1, 2019.

[118] I.-S. Jeong, H.-S. Choi and M.-S. Kang, “Application of the Superconductor Coil for the Improvement of Wireless Power Transmission Using Magnetic Resonance,” *Journal of Superconductivity and Novel Magnetism,* vol. 28, pp. 639-644, 2015.

[119] B. Yoo, J.-B. Song, J. C. Kim, Y.-G. Kim, J. Kim, K. Sim, I. Shin, D. Y. Hwang and H. Lee, "Superconducting Properties of Reacted Mono- and Multifilament MgB2 Wires With Respect to Bending Diameters Using a Custom-Made Bending Test Probe," *IEEE Transactions on Applied Superconductivity,* vol. 28, no. 3, 2018.

[120] Q. Li, M. Yao, Z. Jiang, C. Bumby and N. Amemiya, “Numerical modelling of dynamic loss in HTS coated conductors under perpendicular magnetic field”, IEEE Transactions on Applied Superconductivity, Vol. 28, No. 2, 6600106, 2018.

[121] Q. Li, N. Amemiya, K. Takeuchi, T. Nakamura and N. Fujiwara, “Effects of Unevenly Distributed Critical Currents and Damaged Coated Conductors to AC losses of Superconducting Power Transmission Cables”, IEEE Transactions on Applied Superconductivity, Vol. 21, No. 3, 2011.

[122] Q. Li, Y. Xin and S. Wang, “Dependance of AC Loss on Structural Compactness of Superconducting Power Cables with Narrow Coated Conductors”, IEEE Transactions on Applied Superconductivity, Vol. 26, No. 7, 5900705, 2016.

[123] G. Zhang, H. Yu, L. Jing, J. Li, Q. Liu and X. Feng, “Wireless Power Transfer Using High Temperature Superconducting Pancake Coils,” *IEEE Transactions on Applied Superconductivity,* vol. 24, no. 3, 2014.

[124] Y. D. Chung, C. Y. Lee, H. K. Kang and Y. G. Park, "Desing Consideration and Efficiency Comparison of Wireless Power Transfer With HTS and Cooled Copper Antennas for Electric Vehicle," *IEEE Transactions on Applied Superconductivity,* vol. 25, no. 3, 2015.

[125] D. W. Kim, Y. D. Chung, H. K. Kang, Y. S. Yoon and T. K. Ko, "Characteristics of Contactless Power Transfer for HTS Coil Based on Electromagnetic Resonance Coupling," *IEEE Transactions on Applied Superconductivity,* vol. 22, no. 3, 2012.

[126] H. Yu, G. Zhang, G. Liu, L. Jing and Q. Liu, "Asymmetry in Wireless Power Transfer Between a Superconducting Coil and a Copper Coil," *IEEE Transactions on Applied Superconductivity,* vol. 28, no. 3, 2018.

[127] D. W. Kim, Y. D. Chung, K. Khang, C. Y. Lee, H. M. Kim, H. C. Jo, Y. J. Hwang, J. Y. Jang and Y. S. Yoon, “Effects and Properties of Contactless Power Transfer for HTS Receivers With Four-Separate Resonance Coils,” *IEEE Transactions on Applied Superconductivity,* vol. 23, no. 3, 2013.

[128] Y. D. Chung, C. Y. Lee, H. Kang and Y. G. Park, “Design Considerations of Superconducting Wireless Power Transfer for Electric Vehicle at Different Inserted Resonators,” *IEEE Transactions on Applied Superconductivity,* vol. 26, no. 4, 2016.

[129] X. Wang, X. Nie, Y. Liang, F. Lu, Z. Yan and Y. Wang, “Analysis and experimental study of wireless power transfer with HTS coil and copper coil as the intermediate resonators system,” *Physica C: Superconductivity and its applications,* vol. 532, pp. 6-12, 2017.

[130] R. Inoue, D. Miyagi, M. Tsuda and H. Matsuki, “High-Efficiency Transmission of a Wireless Power Transmission System for Low-Frequency Using REBCO Double-Pancake Coils,” *IEEE Transactions on Applied Superconductivity,* vol. 27, no. 1, 2017.

[131] F. Chen, N. Taylor, R. Balieu and N. Kringos, "Dynamic application of the Inductive Power Transfer (IPT) systems in an electrified road: Dielectric power loss due to pavement materials," *Construction and Building Materials,* vol. 147, pp. 9-16, 2017.

[132] I.-S. Jeong, Y.-K. Lee and H.-S. Choi, “Characteristics analysis on a superconductor resonance coil WPT system according to cooling vessel materials in different distances,” *Physica C: Superconductivity and its applications,* vol. 530, pp. 123-132, 2016.

[133] U. Berardi and N. Dembsey, "Thermal and Fire Characteristics of FRP Composites for Architectural Applications," *Polymers,* vol. 7, pp. 2276-2289, 2015.

[134] H. K. Kang, Y. D. Chung and S. W. Yim, “Conceptual design of contactless power transfer into HTS receiver coil using normal conducting resonance antenna,” *Cryogenics,* vol. 63, pp. 209-214, 2014.

[135] Y. D. Chung, E. Y. Park, W. S. Lee and J. Y. Lee, "Impact Investigations and Characteristics by

Strong Electromagentic Field of Wireless Power Charging System for Electric Vehicdle Under Air and Water Exposure Indexes," *IEEE Transactions on Applied Superconductivity*, vol. 28, no. 3, 2018.

[136] Y. D. Chung, C. Y. Lee, H. C. Jo, Y. G. Park and S. W. Yim, “Operating characteristics of contactless power transfer for electric vehicle from HTS antenna to normal conducting receiver,” *Physica C,* vol. 504, pp. 115-119, 2014.

[137] M. Yilmaz, V. T. Buyukdegirmenci and P. T. Krein, "General Design Requirements and Analysis of Roadbed Inductive Power Transfer System for Dynamic Electric Vehicle Charging," in *IEEE Transportation Electrification Conference and Expo (ITEC)*, Dearborn, USA, 2012.

[138] M. L. Kissin, J. T. Boys and G. A. Covic, "Interphase Mutual Inductance in Polyphase Inductive Power Transfer Systems," *IEEE Transactions on Industrial Electronics,* vol. 56, no. 7, pp. 2393-2400, 2009.

[139] Y. D. Chung, C. Y. Lee and H. R. Jeon, "Operating characteristics and cooling cost evaluation for HTS receiver arrays of wireless power charging system in superconducting MAGLEV train," *Cryogenics*, vol. 94, pp. 79-83, 2018.

[140] G. R. Nagendra, G. A. Covic and J. T. Boys, "Sizing of Inductive Power Pads for Dynamic Charging of EVs on IPT Highways," *IEEE Transactions on Transportation Electrification,* vol. 3, no. 2, pp. 405-417, 2017.

[141] T. Fujita, T. Yasuda and H. Akagi, "A Dynamic Wireless Power Transfer System Applicable to a Stationary System," *IEEE Transactions on Industry Applications,* vol. 53, no. 4, pp. 3748-3757, 2017.

[142] L. Chen, G. R. Nagendra, J. T. Boys and G. A. Covic, "Double-Coupled Systems for IPT Roadway Applications," *IEEE Journal of Emerging and Selected Topics in Power Electronics,* vol. 3, no. 1, pp. 37-49, 2015.

[143] W. Zhang, S.-C. Wong, C. K. Tse and Q. Chen, "An Optimized Track Length in Roadway Inductive Power Transfer Systems," *IEEE Journal of Emerging and Selected Topics in Power Electronics,* vol. 2, no. 3, pp. 598-608, 2014.

[144] G. Buja, M. Bertoluzza and H. K. Dashora, "Lumped Track Layout Design for Dynamic Wireless Charging of Electric Vehicles," *IEEE Transactions on Industrial Electronics,* vol. 63, no. 10, pp. 6631-6640, 2016.

[145] H. L. Li, A. P. Hu, G. A. Covic and C. Tang, "A New Primary Power Regulation Method for Contactless Power Transfer," in *IEEE International Conference on Industrial Technology,* Churchill, Australia, 2009.

[146] J. M. Miller, O. C. Onar and M. Chinthavali, "Primary-Side Power Flow Control of Wireless Power Transfer for Electric Vehicle Charging," *IEEE Journal of Emerging and Selected Topics in Power Electronics,* vol. 3, no. 1, pp. 147-162, 2015.

[147] K. Hata, T. Imura and Y. Hori, "Dynamic Wireless Power Transfer System for Electric Vehicles to Simplifiy Ground Facilities - Power Control and Efficiency Maximization on the Secondary Side," in *IEEE Applied Power Electronics Conference and Exposition (APEC),* Long Beach, USA, 2016.

[148] F. Gürbüz, T. Sürgevil and M. Boztepe, "Analysis and Design of a Secondary-Side Controlled Active Rectifier for Wireless Battery Charging Application," in *10th International Conference on Electrical and Electronics Engineering (ELECO)*, Bursa, Turkey, 2017.

[149] U. K. Madawala, M. Neath and D. J. Thrimawithana, “A Power-Frequency Controller for Bidrectional Inductive Power Transfer Systems,” *IEEE Transactions on Industrial Electronics,* vol. 60, no. 1, pp. 310-317, 2013.

[150] Y.-H. Chao, J.-J. Shieh, C.-T. Pan, W.-C. Shen and M.-P. Chen, "A Primary-Side Control Strategy for Series Parallel Loosely Coupled Inductive Power Transfer Systems," in *IEEE Conference on Industrial Electronics and Applications*, Harbin, China, 2007.

[151] G. A. Covic and J. T. Boys, “Modern Trends in Inductive Power Transfer for Transportation

Applications,” *IEEE Journal of Emerging and Selected Topics in Power Electronics,* vol. 1, no. 1, pp. 28-41, 2013.

[152] R. Bosshard, U. Badstübner, J. Kolar and I. Stevanovic, "Comparative Evaluation of Control Methods for Inductive Power Transfer," in *International Conference on Renewable Energy Research and Applications (ICRERA),* Nagasaki, Japan, 2012.

[153] W. Choi, W. Ho, X. Liu and S. Hui, "Comparative Study on Power Conversion Methods for Wireless Battery Charging Platform," in *14th International Power Electronics and Motion Control Conference*, Ohrid, Macedonia, 2010.

[154] R. Bosshard, J. Kolar and B. Wunsch, "Control Method for Inductive Power Tnrafer with High Partial-Load Efficiency and Resonance Tracking," in *International Power Electronics Conference*, Hiroshima, Japan, 2014.

[155] J. T. Boys, G. A. Covic and A. W. Green, "Stability and control of inductively coupled power transfer systems," *IEE Proceedings - Electric Power Applications,* vol. 147, no. 1, pp. 37-43, 2000.

[156] H. H. Wu, A. Gilchrist, K. D. Sealy and D. Bronson, “A High Efficiency 5 kW Inductive Charger for EVs Using Dual Side Control,” *IEEE Transaction on Industrial Informatics,* vol. 8, no. 3, pp. 585-595, 2012.

[157] T. Diekhans and R. W. De Doncker, "A Dual-Side Controlled Inductive Power Trnasfer System Optimized for Large Coupling Factor Variations and Partial Load," *IEEE Transactions on Power Electronics,* vol. 30, no. 11, pp. 6320-6328, 2015.

[158] Y. Tang, Y. Chen, U. K. Madawala, D. J. Thrimawithana and H. Ma, "A New Controller for Bi-directional Wireless Power Transfer Systems," *IEEE Transactions on Power Electronics,* vol. 33, no. 10, pp. 9076-9087, 2018.

[159] A. Esser, "Contactless Charging and Communication for Electric Vehicles," *IEEE Industry Applications Magazine,* pp. 4-11, 1995.

[160] Z. Yuan, H. Xu, H. Han and Y. Zhao, "Research of Smart Charging Management System for Electric Vehicles Based on Wireless Communication Networks," in *IEEE 6th International Conference on Information and Automation for Sustainability*, Beijing, China, 2012.

[161] Y. Zhao, H. Xu, Y. Shen, H. Han and Z. Yuan, "Research of Orderly Charging Control System for Electrical Vehicles Based on Zigbee and GPRS Networks," in *IEEE Conference and Expo Transportation Electrification Asia-Pacific (ITEC Asia-Pacific),* Beijing, China, 2014.

[162] UNPLUGGED, "Deliverable 2.4.Data analysis and conclusions," UNPLUGGED, 2015.

[163] B. R. Long, "A Near Field Communication System for Wireless Charging," in *IEEE PELS Workshop on Emerging Technologies: Wireless Power Transfer (WoW),* Knoxville, USA, 2016.

[164] A. Gil, Sauras-Perez and J. Taiber, "Communication Requirements for Dynamic Wireless Power Transfer for Battery Electric Vehicles," in *IEEE International Electric Vehicle Conference (IEVC),* Florence, Italy, 2014.

[165] G. R. Nagendra, L. Chen, G. A. Covic and J. T. Boys , "Detection of EVs on IPT Highways," *IEEE Journal of Emerging and Selected Topics in Power Electronics,* vol. 2, no. 3, pp. 584-597, 2014.

[166] F. Bai and H. Krishnan, "Reliability Analysis of DSRC Wireless Communication for Vehicle Safety Applications," in *IEEE Intelligent Transportation Systems Conference,* Toronto, Canada, 2006.

[167] A. Echols, S. Mukherjee, M. Mickelsen and Z. Pantic, “Communication Infrastructure for Dynamic Wireless Charging of Electric Vehicles,” in *IEEE Wireless Communications and Networking Conference (WCNC),* San Francisco, USA, 2017.

[168] A. Gil Batres, A. Moghe and J. Taiber, "A Communication Architecture for Wireless Power Transfer Services based on DSRC Technology," in *IEEE Transportation Electrification Conference and Expo (ITEC),* Dearborn, USA, 2016.

[169] M. Sinaie, P.-H. Lin, A. Zappone, P. Azmi and E. A. Jorswieck, "Delay-Aware Resource

Allocation for 5G Wireless Networks With Wireless Power Transfer," *IEEE Transactions on Vehicular Technology,* vol. 67, no. 7, pp. 5841-5855, 2018.

[170] GSMA Intelligence, "Understanding 5G: Perspectives on future technological advancements in mobile," GSMA Intelligence, 2014.

[171] R. I. Ansari, C. Chrysostomos, S. A. Hassan, M. Guizani, S. Mumtaz, J. Rodriguez and J. J. Rodrigues, "5G D2D Networks: Techniques, Challenges, and Future Prospects," *IEEE Systems Journal,* pp. 1-15, 2018.

[172] C. T. Rim and C. Mi, "Foreign Object Detection," in *Wireless Power Transfer for Electric Vehicles and Mobile Devices*, Hoboken, USA, John Wiley & Sons Ltd, 2017, pp. 457-469.

[173] N. Kuyvenhoven, C. Dean, J. Melton, J. Schwannecke and A. E. Umenei, "Development of a Foreign Object Detection and Analysis Method for Wireless Power Systems," in *IEEE Symposium on Product Compliance Engineering Proceedings*, San Diego, USA, 2011.

[174] S. Fukuda, H. Nakano, Y. Murayama, T. Murakami, O. Kozakai and K. Fujimaki, "A Novel Metal Detector using the Quality Factor of the Secondary Coil for Wireless Power Transfer Systems," in *IEEE MTT-S International Microwave Workshop Series on Innovative Wireless Power Transmission: Technologies, Systems, and Applications,* Kyoto, Japan, 2012.

[175] G. C. Jang, S. Y. Jeong, H. G. Kwak and C. T. Rim, "Metal Object Detection Circuit with Non-overlapped Coils for Wireless EV Chargers," in *IEEE 2nd Annual Southern Power Electronics Conference (SPEC),* Auckland, New Zealand, 2016.

[176] S. Y. Jeong, H. G. Kwak, G. C. Jang and C. T. Rim, "Living Object Detection System Based on Comb Pattern Capacitive Sensor for Wireless EV Chargers," in *IEEE 2nd Annual Southern Power Electronics Conference (SPEC),* Auckland, New Zealand, 2016.

[177] S. Y. Jeong, H. G. Kwak, G. C. Jang, S. Y. Choi and C. T. Rim, "Dual-Purpose Nonoverlapping Coil Sets as Metal Object and Vehicle Position Detections for Wireless Stationary EV Chargers," *IEEE Transactions on Power Electronics,* vol. 33, no. 9, pp. 7387-7397, 2018.

[178] A. Kamineni, M. J. Neath, A. Zaheer, G. A. Covic and J. T. Boys, "Interoperable EV Detection for Dynamic Wireless Charging With Existing Hardware and Free Resonance," *IEEE Transactions on Transportation Electrification,* vol. 3, no. 2, pp. 370-379, 2017.

[179] Q. Deng, J. Liu, D. Czarkowski, M. Bojarski, J. Chen, W. Hu and H. Zhou, "Edge Position Detection of On-line Charged Vehicles With Segmental Wireless Power Supply," *IEEE Transactions on Vehicular Technology,* vol. 66, no. 5, pp. 3610-3621, 2017.

[180] L. Lisboa Cardoso, J. Afonso, M. Comesaña Martinez and A. Nogueiras Meléndez, "RFID-Triggered Power Activation for Smart Dynamic Inductive Wireless Power Transfer," in *IECON 2017 - 43rd Annual Conference of the IEEE Industrial Electronics Society,* Beijing, China, 2017.

[181] S. Y. Choi, B. W. Gu, S. Y. Jeong and C. T. Rim, “Advances in Wireless Power Transfer Systems for Roadway-Powered Electric Vehicles,” *IEEE Journal of Emerging and Selected Topics in Power Electronics,* vol. 3, no. 1, pp. 18-36, 2015.

[182] C. T. Rim and C. Mi, “History of RPEVs,” in *Wireless Power Transfer for Electric Vehicles and Mobile Devices,* First ed., Chichester, United Kingdom, John Wiley & Sons Ltd, 2017, pp. 161-208.

[183] S. Lee, J. Huh, C. Park, N.-S. Choi, G.-H. Cho and C.-T. Rim, “On-Line Electric Vehicle using Inductive Power Transfer System,” in *IEEE Energy Conversion Congress and Exposition,* Atlanta, Georgia, USA, 2010.

[184] J. Huh, C. Park, C.-T. Rim, S. Lee and G.-H. Cho, “High Performance Inductive Power Transfer System with Narrow Rail Width for On-Line Electric Vehicles,” in *IEEE Energy Conversion Congress and Exposition,* Atlanta, USA, 2010.

[185] N. P. Suh, D. H. Cho, G. H. Cho, J. G. Cho, C. T. Rim and S. H. Jang, "Ultra slim power supply and collector device for electric vehicle". Korean Republic Patent KR 1010406620000, 2011.

[186] J. Huh, S. W. Lee, W. Y. Lee, G. H. Cho and C. T. Rim, "Narrow-Width Inductive Power

Transfer System for Online Electrical Vehicles," *IEEE Transactions on Power Electronics,* vol. 26, no. 12, pp. 3666-3679, 2011.

[187] J. Huh, G.-H. Cho, B. Lee and C.-T. Rim, “Characterization of Novel Inductive Power Transfer Systems for On-Line Electric Vehicles,” in *Twenty-Sixth Annual IEEE Applied Power Electronics Conference and Exposition (APEC),* Fort Worth, USA, 2011.

[188] S. Y. Choi and C. T. Rim, "Recent Progress in Developments of On-line Electric Vehicles," in *6th International Conference on Power Electronics Systems and Applications (PESA),* Hong Kong, China, 2015.

[189] S. Y. Choi, S. Y. Jeong, B. W. Gu, G. C. Lim and C. T. Rim, “Ultraslim S-Type Power Supply Rails for Roadway-Powered Electric Vehicles,” *IEEE Transactions on Power Electronics,* vol. 30, no. 11, pp. 6456-6468, 2015.

[190] C. C. Mi, G. Buja, S. Y. Choi and C. T. Rim, "Modern Advances in Wireless Power Transfer Systems for Roadway Powered Electric Vehicles," *IEEE Transactions on Industrial Electronics,* vol. 63, no. 10, pp. 6533-6545, 2016.

[191] V. X. Thai, S. Y. Choi, B. H. Choi, J. H. Kim and C. T. Rim, "Coreless Power Supply Rails Compatible with Both Stationary and Dynamic Charging of Electric Vehicles," in *IEEE 2nd International Future Energy Electronics Conference (IFEEC),* Taipei, Republic of China, 2015.

[192] O. C. Onar, J. M. Miller, S. L. Campbell, C. Coomer, C. P. White and L. E. Seiber, "A Novel Wireless Power Transfer for In-Motion EV/PHEV Charging," in *Twenty-Eighth Annual IEEE Applied Power Electronics Conference and Exposition (APEC),* Long Beach, USA, 2013.

[193] J. M. Miller, O. C. Onar, C. White, S. Campbell, C. Coomer, L. Seiber, R. J. Sepe and A. Steyerl, "Demonstrating Dynamic Wireless Charging of an Electric Vehicle - The benefit of electrochemical capacitor smoothing," *IEEE Power Electronics Magazine,* pp. 12-24, 2014.

[194] J. M. Miller, P. Jones, J.-M. Li and O. C. Onar, “ORNL Experience and Challenges Facing Dynamic Wireless Power Charging of EV's,” *IEEE Circuits and Systems Magazine,* vol. 15, no. 2, pp. 40-53, 2015.

[195] J. M. Miller, C. P. White, O. C. Onar and P. M. Ryan, “Grid Side Regulation of Wireless Power Charging of Plug-In Electric Vehicles,” in *IEEE Energy Conversion Congress and Exposition (ECCE),* Rayleigh, USA, 2012.

[196] P. Jones and O. Onar, “Impact of Wireless Power Transfer in transportation: Future transportation enablerm or near term distraction,” in *IEEE International Electric Vehicle Conference (IEVC),* Florence, Italy, 2014.

[197] O. C. Onar, J. M. Miller, S. L. Campbell, C. Coomer, C. P. White and L. E. Seiber, "Oak Ridge National Laboratory Wireless Power Transfer Development for Sustainable Campus Initiative," in *IEEE Transportation Electrification Conference and Expo (ITEC),* Metro Detroit, USA, 2013.

[198] O. C. Onar, S. L. Campbell, L. E. Seiber, C. P. White and M. Chinthavali, "A High-Power Wireless Charging System Development and Intergration for a Toyota RAV4 Electric Vehicle," in *IEEE Transportation Electrification Conference and Expo (ITEC),* Dearborn, USA, 2016.

[199] J. M. Miller and A. Daga, “Elements of Wireless Power Transfer Essential to High Power Charging of Heavy Duty Vehicles,” *IEEE Transactions on Transportation Electrification,* vol. 1, no. 1, pp. 26-39, 2015.

[200] O. C. Onar, M. Chinthavali, S. L. Compbell, L. E. Seiber, C. P. White and V. P. Galigekere, "Mdeling, Simulation, and Experimental Verification of a 20-kW Series-Series Wireless Power Transfer System for a Toyota RAV4 Electric Vehicle," in *IEEE Transpotation Electrification Conference and Expo (ITEC),* Long Beach, USA, 2018.

[201] A. Green and J. T. Boys, "10kHz Inductively Coupled Power Transfer - Concept and Control," in *Fifth International Conference on Power Electronics and Variable-Speed Drives,* London, United Kingdom, 1994.

[202] M. Budhia, J. T. Boys, G. A. Covic and C.-Y. Huang, "Development of a Single-Sided Flux Magnetic Coupler for Electric Vehicle IPT Charging Systems," *IEEE Transactions on*

Industrial Electronics, vol. 40, no. 1, pp. 318-328, 2013.

[203] J. T. Boys and G. A. Covic, "The Inductive Power Transfer Story at the University of Auckland," *IEEE Circuits and Systems Magazine,* vol. 15, no. 2, pp. 6-27, 2015.

[204] G. A. Covic, J. T. Boys, M. L. Kissin and H. G. Lu, "A Three-Phase Inductive Power Transfer System for Roadway-Powered Vehicles," *IEEE Transactions on Industrial Electronics,* vol. 54, no. 6, pp. 3370-3378, 2007.

[205] G. A. Covic, J. Boys , A. Tam and J.-H. Peng, "Self Tuning Pick-ups for Inductive Power Transfer," in *IEEE Power Electronics Specialists Conference*, Rhodes, Greece, 2008.

[206] S. E. Shladover, "PATH at 20 - History and Major Milestones," *IEEE Transactions on Intelligent Transportation Systems,* vol. 8, no. 4, pp. 584-592, 2007.

[207] D. M. Empey, E. H. Lechner, G. Wyess, M. Vincent, J. Garbarino, R. Moore, G. J. Bailie, J. V. Josselyn, J. Frenster, C. R. Klein and S. E. Shladover, "Roadway Powered Electric Vehicle Project Track Construction and Testing Program Phase 3D," PATH, Richmond, USA, 1994.

[208] FABRIC, "FABRIC Feasibility analysis and development of on-road charging solutions for future electric vehicles," 2017. [Online]. Available: http://www.fabric-project.eu/. [Accessed 08 11 2017].

[209] FABRIC, "Review of existing power transfer solutions - Deliverable No. D3.3.1," FABRIC, 2014.

[210] FABRIC, "Assessment of the technical feasibility of ICT and charging solutions - Deliverable No. D4.2.1," FABRIC, 2014.

[211] G. Frémont, "Dynamic electric charging on motorways," in *Albertis Pavement Management Workshop*, Barcelona, Spain, 2017.

[212] A. Amditis, T. Theodoropoulos, G. Brusaglino, R. Rizzo, L. Di Noia, G. Rodella and A. Oceano, "Energy management optimization within the Electro Mobility system," in *6th International Conference on Clean Electrical Power (ICCEP),* Santa Margherita Ligure, Italy, 2017.

[213] UNPLUGGED, "Wireless charging for Electric Vehicles - Final Report," UNPLUGGED, 2015.

[214] UNPLUGGED, "FP7 UNPLUGGED project - inductive charging for electric vehicles," 2017. [Online]. Available: http://unplugged-project.eu/. [Accessed 08 11 2017].

[215] Unplugged, "Deliverable D3.1 – Technical feasibility of en-rout charging technical report," Unplugged, 2013.

[216] Unplugged, "Deliverable D3.3 - Economic feasibility of en-route charging technical report," Unplugged, 2015.

[217] Transport Research Laboratory, “Feasibility study: Power electric vehicles on England's major roads,” Highways England, 2015.

[218] Highways England, "Highways England Delivery Plan 2017-2018," Highways England, 2017.

[219] WiTricity Corporation, "WiTricity - Drive: Electric Vehicles," 2017. [Online]. Available: http://witricity.com/wp-content/uploads/2017/01/DRIVE_11_20170104-1.pdf. [Accessed 08 11 2017].

[220] Qualcomm, “Qualcomm Halo Features,” 2017. [Online]. Available: https://www.qualcomm.com/products/halo/features. [Accessed 08 11 2017].

[221] H. Jiang, P. Brazis, M. Tabaddor and J. Bablo, "Safety Considerations of Wireless Charger For Electric Vehicles - A Review Paper," in *IEEE Symposium on Product Compliance Engineering Proceedings*, Portland, USA, 2012.

[222] P. C. Schrafel, B. R. Long, J. M. Miller and A. Daga, "The Reality of Safety Concerns Relative to WPT Systems for Automotive Applications," in *IEEE PELS Workshop on Emerging Technologies: Wireless Power Transfer (WoW)*, Knoxville, USA, 2016.

[223] International Commission on Non-Ionizing Radiation Protection (ICNIRP), “ICNIRP Guidlines - For Limiting Exposure to Time-varying Electric and Magnetic Fields (1Hz-100kHz),” *Health*

Physics, vol. 99, no. 6, pp. 818-836, 2010.

[224] International Commission on Non-Ionizing Radiation Protection (ICNIRP), “ICNIRP Guidlines - For Limiting Exposure to Time-varying Electric, Magnetic Fields and Electromagnetic Fields (up to 300GHz),” *Health Physics*, vol. 74, no. 4, pp. 494-522, 1998.

[225] World Health Organization (WHO), "Extremely Low Frequency Fields. Environmental Health Criteria No.238," WHO Press, Geneva, Switzerland, 2007.

[226] K. Wada, K. Matsubara, H. Yoshino, Y. Suzuki, A. Ushiyama, S. Ohtani, K. Hattori and K. Ishii, "Development of an Exposure System for 85 kHz Magnetic Field for the Evaluation Biological Effects," in *IEEE PELS Workshop on Emerging Technologies: Wireless Power Transfer (WoW)*, Knoxville, USA, 2016.

[227] I. Nishimura, A. Oshima, K. Shibuya, T. Mitani and T. Negishi, "Absence of reproductive and developmental toxicity in rats following exposure to a 20-kHz or 60-kHz magnetic field," *Regulatory Toxicology and Pharmacology*, vol. 64, pp. 394-401, 2012.

[228] J. Chakarothai, K. Wake, T. Arima, S. Watanabe and T. Uno, "Exposure Evaluation of an Actual Wireless Power Transfer System for an Electric Vehicle With Near-Field Measurement," *IEEE Transactions on Microwave Theory and Techniques*, vol. 66, no. 3, pp. 1543-1552, 2018.

[229] A. Christ, M. G. Douglas, J. M. Roman, E. B. Cooper, A. P. Sample, B. H. Waters, J. R. Smith and N. Kuster, "Evaluation of Wireless Resonant Power Transfer Systems With Human Electromagnetic Exposure Limits," *IEEE Transactions on Electromagnetic Compatibility*, vol. 55, no. 2, pp. 265-274, 2013.

[230] S. W. Park, K. Wake and S. Watanabe, "Incident Electric Field Effect and Numerical Dosimetry for a Wireless Power Transfer System Using Magnetically Coupled Resonances," *IEEE Transactions on Microwave Theory and Techniques*, vol. 61, no. 9, pp. 3461-3469, 2013.

[231] I. Laakso and A. Hirata, "Evaluation of the induced electric field and compliance procedure for a wireless power transfer system in an electrical vehicle," *Physics in Medicine & Biology*, vol. 58, no. 21, pp. 7583-7593, 2013.

[232] T. Campi, S. Cruciani, V. De Santis, F. Maradei and M. Feliziani, "EMC and EMF Safety Issues in Wireless Charging System for an Electric Vehicle (EV)," in *International Conference of Electrical and Electronic Technologies for Automotive*, Turin, Italy, 2017.

[233] T. Shimamoto, I. Laakso and A. Hirata, "In-situ electric field in human body model in different postures for wireless power transfer system in an electrical vehicle," *Physics in Medicine & Biology*, vol. 60, no. 1, pp. 163-173, 2015.

[234] S. W. Park, "Evaluation of Electromagnetic Exposure during 85kHz Wireless Power Transfer for Electric Vehicles," *IEEE Transactions on Magnetics*, vol. 54, no. 1, 2018.

[235] M. Kim, S. Park and H.-K. Jung, "Numerical Method for Exposure Assessment of Wireless Power Transmission under Low-Frequency Band," *Journal of Magnetics*, vol. 21, no. 3, pp. 442-449, 2016.

[236] T. Campi, S. Cruciani, M. Feliziani and F. Maradei, "Magnetic Field Generated by a 22 kW-85 kHz Wireless Power Transfer System for an EV," in *AEIT International Annual Conference*, Cagliaria, Italy, 2017.

[237] Z. Chen, W. Liu and Y. Yin, "Deployment of stationary and dynamic charging infrastructure for electric vehicles along traffic corridors," *Transportation Research Part C*, vol. 77, pp. 185-206, 2017.

[238] R. Tell, R. Kavet, J. Bailey and J. Halliwell, “Very-low-frequency and low-frequency electric and magnetic fields associated with electric shuttle bus wireless charging,” *Radiation Proctection Dosimetry*, vol. 158, no. 2, pp. 123-134, 2014.

[239] A. Kyriakou, A. Christ, E. Neufeld and N. Kuster, "Local Tissue Temperature Increase of a Generic Implant Compared to the Basic Restrictions Defined in Safety Guidlines," *Bioelectromagnetics*, vol. 33, pp. 366-374, 2012.

[240] T. Campi, S. Cruciani, V. De Santis and M. Feliziani, “EMF Safety and Thermal Aspects in a

Pacemaker Equipped With a Wireless Power Transfer System Working at Low Frequency," *IEEE Transactions on Microwave Theory and Techniques,* vol. 64, no. 2, pp. 375-382, 2016.

[241] International Organization for Standardization (ISO), "ISO 14117:2012 Active implantable medical devices -- Electromagnetic compatibility -- EMC test protocols for implantable cardiac pacemakers, implantable cardioverter defibrillators and cardiac resynchronization devices," ISO, Geneva, Switzerland, 2012.

[242] Y. Gao, K. B. Farley, A. Ginart and Z. T. H. Tse, "Safety and efficiency of the wireless charging of electric vehicles," *Proceedings of the Institution of Mechanical Engineers, Part D: Journal of Automobile Engineering,* vol. 230, no. 9, pp. 1196-1207, 2015.

[243] S. Ahn and J. Kim, "Magnetic Field Design for High Efficient and Low EMF Wireless Power Transfer in On-Line Electric Vehicle," in *Proceedings of the 5th European Conference on Antennas and Propagation (EUCAP),* Rome, Italy, 2011.

[244] M. Feliziani, S. Cruciani, T. Campi and F. Maradei, "Near Field Shielding of a Wireless Power Transfer (WPT) Current Coil," *Progress In Electromagnetics Research C,* vol. 77, pp. 39-48, 2017.

[245] J. Kim, J. Kim, S. Kong, H. Kim, I.-S. Suh, N. P. Suh, D.-H. Cho, J. Kim and S. Ahn, "Coil Design and Shielding Methods for a Magnetic Resonant Wireless Power Transfer System," *Proceedings of the IEEE,* vol. 101, no. 6, pp. 1332-1342, 2013.

[246] P. R. Bannister, "New Theoretical Expressions for Predicting Shielding Effectiveness for the Plane Shield Case," *IEEE Transactions on Electromagnetic Compatibility,* vol. 10, no. 1, pp. 2-7, 1968.

[247] P. Moreno and R. G. Olsen, "A Simple Theory for Optimizing Finite Width ELF Magnetic Field Shields for Minimum Dependence on Source Orientation," *IEEE Transactions on Electromagnetic Compatibility,* vol. 39, no. 4, pp. 340-348, 1997.

[248] S. Lee, W. Lee, J. Huh, H.-J. Kim, C. Park, G.-H. Cho and C.-T. Rim, "Active EMF cancellation method for I-type pickup of On-Line Electric Vehicles," in *Twenty-Sixth Annual IEEE Applied Power Electronics Conference and Exposition (APEC),* Fort Worth, USA, 2011.

[249] S. Kim, H.-H. Park, J. Kim, J. Kim and S. Ahn, "Design and Analysis of a Resonant Reactive Shield for a Wireless Power Electric Vehicle," *IEEE Transactions on Microwave Theory and Techniques,* vol. 62, no. 4, pp. 1057-1066, 2014.

[250] H. Moon, S. Kim, H. H. Park and S. Ahn, "Design of a Resonant Reactive Shield With Double Coils and a Phase Shifter for Wireless Charging of Electric Vehicles," *IEEE Transactions on Magnetics,* vol. 51, no. 3, 2015.

[251] C. T. Rim and C. Mi, "Electromagnetic Field (EMF) Cancel," in *Wireless Power Transfer for Electric Vehicles and Mobile Devices,* Hoboken, USA, John Wiley & Sons Ltd, 2017, pp. 313-335.

[252] Q. Zhu, Y. Zhang, Y. Guo, C. Liao, L. Wang and L. Wang, "Null-Coupled Electromagnetic Field Canceling Coil for Wireless Power Transfer System," *IEEE Transactions on Transportation Electrification,* vol. 3, no. 2, pp. 464-473, 2017.

[253] C. Song, H. Kim, D. H. Jung, J. J. Kim, S. Kong, J. Kim, S. Ahn, J. Kim and J. Kim, "Low EMF and EMI Design of a Tightly Coupled Handheld Resonant Magnetic Field (HH-RMF) Charger for Automotive Battery Charging," *IEEE Transactions on Electromagnetic Compatibility,* vol. 58, no. 4, pp. 1194-1206, 2016.

[254] Wireless Power Consortium (WPC), "The QI Wireless Power Transfer System Power Class 0 Specification Parts 1 and 2: Interface Definitions Version 1.2.2," WPC, 2016.

[255] Alliance for Wireless Power (A4WP), "A4WP Wireless Power Transfer System Baseline System Specification (BSS)," A4WP, Fremont, USA, 2014.

[256] International Organization for Standardization (ISO), "ISO/PAS 19363:2017 - Electrically propelled road vehicles -- Magnetic field wireless Power transfer -- Safety and interoperability requirements," ISO, Geneva, Switzerland, 2017.

[257] Society of Automotive Engineers (SAE), "J2894/1 - Power Quality Requirements for Plug-In Electric Vehicle Chargers," SAE International, Warrendale, USA, 2011.

[258] Society of Automotive Engineers (SAE), "J2847/6 - Communication between Wireless Charged Vehicles and Wireless EV Chargers," SAE International, Warrendale, USA, 2015.

[259] Society of Automotive Engineers (SAE), "J2931/6 - Signaling Communication for Wirelessly Charged Electric Vehicles," SAE International, Warrendale, USA, 2015.

[260] International Organization for Standardization (ISO), "15118:2013 Road vehicles -- Vehicle to grid communication interface," ISO, Geneva, Switzerland, 2013.

[261] International Electrotechnical Commission (IEC), "IEC 61980:2015 Electric vehicle wireless power transfer (WPT) systems - Part 1: General requirements," IEC, Geneva, Switzerland, 2015.

[262] Y. Ma, B. Zhang and X. Zhou, "An Overview on Impacts of Electric Vehicles Integration into Distribution Network," in *IEEE International Conference on Mechatronics and Automation (ICMA)*, Beijing, China, 2015.

[263] R. C. Green II, L. Wang and M. Alam, "The impact of plug-in hybrid electric vehicles on distribution networks: A review and outlook," *Renewable and Sustainable Energy Reviews,* vol. 15, pp. 544-553, 2011.

[264] M. Kintner-Meyer, K. Schneider and R. Pratt, "Impacts assessment of plug-in hybrid electric vehicles on electric utilities and regional U.S. power grids - part 1: technical assessment," 2007.

[265] P. Olivella-Rosell, R. Villafafila-Robles and A. Sumper, "Impact Evaluation of Plug-in Elecetric Vehicles on Power Systems," in *Plug In Electric Vehicles in Smart Grids*, S. Rajakaruna, A. Ghosh and F. Shahnia, Eds., Singapore, Republic of Singapore, Springer Science+Business Media Singapore 2015, 2015, pp. 149-179.

[266] S. Zhang, X. Ai, W. Liang and R. Dong, "The influence of the electric vehicle charging on the distribution network and the solution," in *IEEE Conference and Expo Transportation Electrification Asia-Pacific (ITEC Asia-Pacific)*, Beijing, China, 2014.

[267] T. Ma and O. Mohammed, "Real-Time Plug-In Electric Vehicles Charging Control for V2G Frequency Regulation," in *39th Annual Conference of the IEEE Industrial Electronics Society (IECON)*, Vienna, Austria, 2013.

[268] F. Deflorio and L. Castello, "Dynamic charging-while-driving systems for freight delivery services with electric vehicles: Traffic and energy modelling," *Transportation Research Part C,* vol. 81, pp. 342-362, 2017.

[269] S. D. Manshadi, M. E. Khodayar, K. Abdelghany and H. Uster, "Wireless Charging of Electric Vehicles in Electricity and Transportation Networks," *IEEE Transaction on Smart Grid,* 2017.

[270] I. Karakitsios, E. Karfopoulos and N. Hatziargyriou, “Impact of dynamic and static fast inductive charging of electric vehicles on the distribution network,” *Electric Power Systems Research,* vol. 140, pp. 107-115, 2016.

[271] C. A. Garcia-Vazquez, F. LLoren-Iborra, L. M. Fernandez-Ramirez, H. Sanchez-Sainz and F. Jurado, "Comparative study of dynamic wireless charging of electric vehicles in motorway, highway and urban stretches," *Energy,* vol. 137, pp. 42-57, 2017.

[272] J. H. Park and Y. H. Jeong, "The Economics of Wireless Charging on the Road," in *The On-line Electric Vehicle - Wireless Electric Ground Transportation Systems*, Cham, Switzerland, Springer International Publishing, 2017, pp. 329-347.

[273] M. Yilmaz and P. T. Krein, "Review of Battery Charger Topologies, Charging Power Levels, and Infrastructure for Plug-In Electric and Hybrid Vehicles," *IEEE Transactions on Power Electronics,* vol. 28, no. 5, pp. 2151-2169, 2013.

[274] S. Lukic and Z. Pantic , "Cutting the Cord - Static and dynamic inductive wireless charging of electric vehicles," *IEEE Electrification Magazine,* vol. September, pp. 57-64, 2013.

[275] S. Jeong, Y. J. Jang, D. Kum and M. S. Lee, "Charging Automation for Electric Vehicles: Is a Smaller Battery Good for the Wireless Charging Electric Vehicles?," *IEEE Transactions on*

Automation Science and Engineering, pp. 1-12, 2018.

[276] Department for Transport, "Provisional Road Traffic Estimates Great Britain July 2016- June 2017," Department of Transport, 2017.

[277] Y. J. Jang, S. Jeong and M. S. Lee, "Initial Energy Logistics Cost Analysis for Stationary, Quasi-Dynamic, and Dynamic Wirless Charging Public Transportation Systems," *Energies,* vol. 9, no. 483, 2016.

[278] J. Shin, S. Shin, Y. Kim, S. Ahn, S. Lee, G. Jung, S.-J. Jeon and D.-H. Cho, "Design and Implementation of Shaped Magnetic-Resonance-Based Wireless Power Transfer System for Roadway-Powered Moving Electric Vehicles," *IEEE Transactions on Industrial Electronics,* vol. 61, no. 3, pp. 1179-1192, 2014.

[279] A. Shekhar, V. Prasanth, P. Bauer and M. Bolech, "Economic Viability Study of an On-Road Wireless Charging System with a Generic Driving Range Estimation Method," *Energies,* vol. 9, no. 76, 2016.

[280] S. Jeong, Y. J. Jang and D. Kum, "Economic Analysis of the Dynamic Charging Electric Vehicle," *IEEE Transactions on Power Electronics,* vol. 30, no. 11, pp. 6368-6377, 2015.

[281] N. Omar, M. A. Monem, Y. Firouz, J. Salminen, J. Smekens, O. Hegazy, H. Gaulous, G. Mulder, P. Van den Bossche, T. Cossemans and J. Van Mierlo, "Lithium iron phosphate based battery - Assessment of the aging parameters and development of cycle life model," *Applied Energy,* vol. 113, pp. 175-1585, 2014.

[282] Z. Bi, R. De Kleine and G. A. Keoleian, "Integrated Life Cycle Assessment and Life Cycle Cost Model for Comparin Plug-in Versus Wireless Charging for an Electric Bus System," *Journal of Industrial Ecology,* vol. 21, no. 2, pp. 344-355, 2017.

[283] Y. Wang, W. Ding, L. Huang, Z. Wei, H. Liu and J. A. Stankovic, "Toward Urban Electric Taxi Systems in Smart Cities: The Battery Swapping Challenge," *IEEE Transactions on Vehicular Technology,* vol. 67, no. 3, pp. 1946-1960, 2018.

[284] Z. Chen, Y. Yin and Z. Song, "A cost-competitiveness analysis of charging infrastructure for electric bus operations," *Transportation Research Part C,* vol. 93, pp. 351-366, 2018.

[285] B. J. Limb, T. H. Bradley, B. Crabb, R. Zane, C. McGinty and J. C. Quinn, "Economic and Environmental Feasibility, Architecture Optimization, and Grid Impact of Dynamic Charging of Electric Vehicles using Wireless Power Transfer," in *6th Hybrid and Electric Vehicles Conference (HEVC 2016)*, London, United Kingdom, 2016.

[286] B. J. Limb, R. Zane and J. C. Quinn, "Infrastructure Optimization and Economic Feasibility of In-Motion Wireless Power Transfer," in *IEEE Transportation Electrification Conference and Expo (ITEC)*, Metro Deroit, USA, 2016.

[287] J. C. Quinn, B. J. Limb, Z. Pantic, P. Barr, R. Zane and T. H. Bradley, "Feasibility of Wireless Power Transfer for Electrification of Transportation: Techno-economics and Life Cycle Assessment," in *IEEE Conference on Technologies for Sustainability (SusTech)*, Ogden, USA, 2015.

[288] M. Fuller, "Wireless charging in California: Range, recharge, and vehicle electrification," *Transportation Research Part C,* vol. 67, pp. 343-356, 2016.